UNCOVERING THE ROLE OF MUTANT RAC1 IN CUTANEOUS MELANOMA

Xuan Tien Steven Nguyen

Department of Biochemistry
Goodman Cancer Research Centre
McGill University, Montreal

December 2017

A thesis submitted to McGill University in partial fulfillment of the requirements of the degree of Master of Science

Table of Contents

Abstract

RAC1 is a member of the Rho family of small GTPases. Next-generation sequencing studies discovered that 5-10% of cutaneous melanoma possess an activating hotspot p.P29S mutation [1, 2]. Previous studies have shown that RAC1-P29S promotes proliferation of melanocytes and modulates response to mitogen-activated protein kinase (MAPK)-targeted therapy [3, 4]. However, the mechanism of action of RAC1-P29S remains unknown. To gain a better understanding of the role of RAC1-P29S in melanoma, we performed unbiased transcriptomic and proteomic analyses to elucidate signaling pathways affected by the p.P29S mutation. We performed RNA-sequencing (RNA-seq) on melanocytes engineered to overexpress RAC1-P29S. We integrated our analysis with human melanoma data available from The Cancer Genome Atlas (TCGA). Gene set enrichment analysis (GSEA) revealed that the most significant pathways deregulated in RAC1-P29S mutant melanomas were related to immune response and mitochondrial respiration. In addition, to gain insight into signaling mechanisms responsible for expression signatures and oncogenic functions of the P29S mutant, we identified several interacting proteins with RAC1-P29S in human melanocytes by utilizing proximity-dependent biotin identification (BioID) and complex purification assays. From our preliminary analysis, we identified a scaffolding protein, IQGAP1, as a preferential interactor of RAC1-P29S. In future works, we will perform more in-depth mechanistic studies from our unbiased proteomic and transcriptomic analyses presented here with the goal to devise novel therapeutic strategies to treat RAC1-mutant cancers.

Key words: Cutaneous Melanoma, RAC1 GTPase, Transcriptomics, Proteomics, Integrative analysis, Mechanistic Characterization.

Résumé

RAC1 est un membre de la famille de petits RHO GTPases. Les études de séquençage de nouvelle génération ont découvert que 5-10% des cas de mélanomes cutanés possèdent la mutation de point chaud et activatrice p.P29S [1, 2]. Des études antécédentes ont démontré que RAC1-P29S promeut la progression du mélanome, tout en modulant les réponses aux thérapies ciblées vers la voie *mitogen-activated protein kinase* (MAPK) [3, 4]. Pourtant, le mécanisme d'action de RAC1-P29S demeure inconnu. Afin de mieux comprendre le rôle de RAC1-P29S dans le mélanome, nous avons exécuté des analyses transcriptomiques et protéomiques non-biaisées pour élucider les voies de signalisations affectées par la mutation p.P29S. Après avoir effectué le séquençage de l'ARN (RNA-seq) sur des mélanocytes conçus à surexprimer RAC1-P29S, nous avons intégré nos résultats avec les données de mélanome humain disponibles dans *The Cancer Genome Atlas* (TCGA). *Gene set enrichment analysis* (GSEA) démontre que la plupart des voies significatives dérégulées dans le mélanome avec RAC1-P29S sont reliées aux réponses immunitaires et à la respiration mitochondriale. De plus, afin d'acquérir une meilleure compréhension des mécanismes de signalisations qui sont responsables des signatures d'expression et des fonctions oncogéniques de la mutation P29S, nous avons identifié des protéines qui interagissent avec RAC1-P29S dans des mélanocytes humains en utilisant l'identification biotine-à-proximité (BioID) et la purification des complexes de protéines. D'après notre analyse préliminaire, nous avons identifié la protéine d'échafaudage, IQGAP1, comme un des principaux interacteurs de RAC1-P29S. Dans des études ultérieures, nous performerons des travaux mécanistiques approfondis basés sur nos analyses protéomiques et transcriptomiques non-biaisées présentées ici, afin de mettre au point de nouvelles méthodes de traitement pour les cancers avec RAC1 muté.

Mots clés: Mélanome cutané, RAC1 GTPase, Études Transcriptomiques et Protéomiques, Analyse Intégrative, Caractérisation Mécanistique.

Acknowledgements

I would like to thank my supervisor, Dr. Ian Watson, for offering me this project, as well as mentoring me throughout my graduate studies. His guidance, insight and training were very helpful in the completion of this research project. I would also like to thank the entire Watson lab team, present and past members, for their support and feedback. They have made my graduate studies a fulfilling experience. This includes Dr. Nehme El-Hachem, Dr. Mathieu Lajoie and Miss LeeAnn Chau Ramsay for their bioinformatic expertise, Mrs. Mozhdeh Ahanfeshar-Adams for the mouse xenografts and material purchases, and my fellow graduate students, Karen Vo Hoang, Shivshankari Rajkumar, Rached Alkallas and Dr. Dan Moldeavanu. I would like to thank my Research Advisory Committee (RAC) members, Dr. Sidong Huang, Dr. David Dankort and Dr. Nathalie Lamarche-Vane, for their great suggestions on my research work. I also thank the Center for Advanced Proteomic Analyses (CAPA) facility at the Université de Montréal for their proteomics services, as well as Li-Ting Wang from Dr. Luke McCaffrey's lab, who provided me with the plasmids needed for my BioID experiments. I also acknowledge the funding grants that supported me financially throughout, such as the Graduate Excellence Fellowship (GEF) and McGill Integrated Cancer Research Training Program (MICRTP) awards. Finally, I would like to thank my family for their love, comfort and support. They have always given me sound advice throughout my undergraduate and graduate studies and I thank them for all that they have done for me.

Preface and Contributions of Authors

In this thesis, the purpose of the work done is to uncover the biological role of RAC1-P29S in cutaneous melanoma. The comprehensive background review states what is known about RAC1 and its regulation, while laying out ongoing challenges in the cutaneous melanoma field. All research elements in this thesis should be considered original content. Furthermore, the novel scholarly data presented here augments the current knowledge of cutaneous melanoma and the role of mutant RAC1 in cancer.

I would like to declare the contributions of Dr. Nehme El-Hachem and Dr. Mathieu Lajoie who helped me perform the DEG and GSEA studies. The generation of a subset of isogenic melanoma cell lines and partially transformed melanocytes overexpressing RAC1-P29S, the creation of plasmids with tagged-RAC1 mutants and the mouse xenograft studies were performed by Dr. Ian Watson and Mrs. Mozhdeh Ahanfeshar-Adams. I also state the contributions of my fellow graduate student, Miss Karen Vo Hoang, in designing the Seahorse analysis experiment for my melanoma cell lines. In terms of facilities, I declare the contributions of the CAPA facility at the Université de Montréal in setting my samples for the Mass Spectrometer. In addition to my involvement in the techniques performed above, I declare my contributions to the rest of the experimental elements of this research project. This includes the generation of the majority of the RAC1 plasmids used here and the stably expressing cell lines with BioID- and CapTEV-tagged RAC1, the pulldown assays, the Mass Spectrometry and GSEA data analysis and all the Western blots performed.

List of Tables and Figures

Abbreviations

ACR: A BCR-related protein

AID: Autoinhibitory domain

AKT: Protein Kinase B

ALS: Amyotrophic lateral sclerosis

ARHGAP22: RHO GTPase Activating Protein 22

ARP2/3: Actin-related proteins 2/3

BCR: Breakpoint cluster region

BioID: Proximity-dependent biotin identification

BirA*: *E. coli* biotin protein ligase

β-Pix: p21-activated kinase interacting exchange factor

BRAF: Serine/threonine-protein-kinase B-raf

CALML3/5: Calmodulin-like protein 3/5

CDC42: Cell division control protein 42 homolog

CHD: Calponin-homology domain

COSMIC: Catalogue of Somatic Mutations in Cancer

CPD : Cyclobutane pyrimidine dimers

CYBA : $p22^{phox}$

DEG: Differentially expressed genes

DH: Dbl-homology

DHR1/2: DOCK-homology regions 1/2

DOCK1: Dedicator of cytokinesis 1

ECAR: Extracellular acidification rate

ECM: Extracellular matrix

EGF: Epidermal growth factor

EGFR: Epidermal growth factor receptor

EMT: Epithelial mesenchymal transition

ERBB2: Erb-B2 receptor tyrosine kinase 2

ETC: Electron transport chain

FAK: Focal adhesion kinase

FDR: False Discovery Rate

FLII: Flightless-1 homolog

GAP: GTPase activating protein

GDP: Guanine-diphosphate

GEF: Guanine exchange factor

GFP: Green Fluorescent Protein

GLUT4: Glucose transporter type-4

GoF: Gain of function

GPCR: G-protein coupled receptor

GRD: GAP-related domain

GSEA: Gene set enrichment analysis

GTP: Guanine-triphosphate

GTPase: Guanine-triphosphatase

HIF-1α: Hypoxia inducible factor 1-α

HMGA2: High mobility group AT-hook 2

HNSCC: Head and neck squamous cell carcinoma

IBD: Inflammatory bowel diseases

ICMT: Protein-S-isoprenylcysteine O-methyltransferase

IFNAR: IFN-α/β receptors

IFNGR: IFN-γ receptor

IFN-α: Interferon-α

IFN-β: Interferon-β

IFN-γ: Interferon-γ

IKK: Inhibitors of IκB

INM: Inner nuclear membrane

IQ motifs: Isoleucine/glutamine-containing motifs

IQGAP1-3: IQ motif containing GTPase activating protein 1-3

ISG: IFN-stimulated genes

IκB: Inhibitors of NF-κB

JAK1: Janus kinase 1

JNK/SAPK: Jun N-terminal kinase/stress-activated protein kinase

KPNA2: Importin/karyopherin α2

KPNB1: Karyopherin β1

Lamin-A: A-type lamins

LAP2α: Lamina-associated polypeptide 2 isoform α

LIMK1/2: LIM kinases 1/2

LoF: Loss of function

LRRK2: Leucine-rich repeat kinase 2

MAPK: Mitogen-activated protein kinase

MDCK: Madin-Darby canine kidney

MITF: Microphthalmia-associated transcription factor

MLC: Myosin light chain

MMP: Matrix metallopeptidase

MS: Mass Spectrometry

mTORC1/2: Mammalian target rapamycin complex 1/2

NCF1: $p47^{phox}$

NCF2: $p67^{phox}$

NCF4: $p40^{phox}$

NCI: National Cancer Institute

NCK: Non-catalytic region of tyrosine kinase adaptor protein 1

NEDD9: Neural precursor cell expressed developmentally down-regulated protein 9

NES: Normalized enrichment score

NF-κB: Nuclear factor κ-light-chain-enhancer of activated B cells

NHGRI: National Human Genome Research Institute

NLS: Nuclear localization signal

NOX1-4: NADPH oxidase 1-4

NRAS: Neuroblastoma RAS viral oncogene homolog

NSCLC: Non-small cell lung carcinoma

OCR: Oxygen consumption rate

p53DD: Dominant-negative p53

PAK1-6: p21-activated kinase 1-6

PBD: p21-binding domain

PBR: C-terminal polybasic region

PD1: Programmed death protein 1

PDGF: Platelet-derived growth factor

PD-L1: Programmed death-ligand 1

PH: Pleckstrin homology

PI3K: Phosphoinositide (PI) 3-kinase

PIP2: Phosphatidylinositol-4-5-biphosphate

PIP3: Phosphatidylinositol-3-4-5-triphosphate

PKC: Protein Kinase C

PREX1/2: Phosphatidylinositol 3-4-5-triphosphate-dependent RAC exchanger 1/2

PTM: Post-translational modifications

RAC1: Ras-related C3 botulinum toxin substrate 1

RCE1: CAAX prenyl protease 2

RGCT: Ras-GAP C-terminus domain

RHOA: Ras homolog gene family member A

RHOGDI: Rho protein GDP dissociation inhibitor

ROCK: Rho-associated protein kinase

ROS: Reactive oxidative species

RPPA: Reverse-phase protein array

RTK: Receptor tyrosine kinase

SCNA: Somatic copy number alterations

SFN: 14-3-3 σ/Stratifin

SH2-3: Src Homology 2-3

SMC: Smooth muscle cells

SMG: Significantly mutated gene

SOD: Superoxide dismutase

SOS1: Son of sevenless 1

STAT1-3: Signal transducer and activator of transcription 1-3

TCA: Tricarboxylic acid

TCGA: The Cancer Genome Atlas

TCR: T-Cell receptor

TGF-β: Transforming growth factor β1

TIAM1: T-cell lymphoma invasion and metastasis-1

TIMP: Tissue-specific inhibitors of MMPs

TMPO: Thymopoietin

TNF-α: Tumor necrosis factor-α

TRIO: Triple functional domain protein

UVR: Ultraviolet radiation

VCP: Valosin-containing protein

VEGF: Vascular endothelial growth factor

WAVE1: WASP-family verprolin homologous protein 1

WHO: World Health Organization

WT: Wild-type

WW: Polyproline binding domain

ZNF750: Zinc finger protein 750

1. Comprehensive Literature Review

1.1 RAC1 is Significantly Mutated in Cutaneous Melanoma

1.1.1 Introduction to Cutaneous Melanoma

***Excerpts from the book chapter that I co-authored with Dr. Ian R. Watson, "*Melanomics: Comprehensive Molecular Analysis of Normal and Neoplastic Melanocytes*" from "*Melanoma*" (Editors: David E. Fischer & Boris C. Bastian), are used in this part of this comprehensive review**

Cutaneous melanoma is the deadliest form of skin cancer, where the cell of origin is the melanocyte. Melanocytes are derived from the neural crest lineage. Melanocytes reside primarily in the basal layer of the epidermis; however, they are found in various anatomical sites. Their primary function is to produce melanin and provide pigmentation for the skin, eyes and hair. There are different types of melanocytic neoplasms that differ in clinical features, histopathological appearance and biological behaviour (reviewed in [5]). Benign melanocytic neoplasms are termed nevi, while malignant neoplasms are defined as melanomas. When detected in its earliest stages (stage I, II and resectable stage III), melanoma is generally curable with early detection and surgery. Unfortunately, once the melanoma metastasizes (unresectable stage III and stage IV), patient prognosis significantly decreases [6]. The World Health Organization (WHO) estimates about 2-3 million non-melanomas and 132,000 melanoma skin cancers are diagnosed worldwide each year, and unlike the majority of cancers, the rate of melanoma has been increasing significantly in both men and women [7].

Ultraviolet radiation (UVR) is a major environmental risk factor for cutaneous melanoma development, and is composed of three components, each with differing wavelengths: UVA (320-400 nm), UVB (290-320 nm), and UVC (200-290 nm) (reviewed in [8]). Although, only UVA and UVB contribute to skin damage (almost all UVC is absorbed by the atmosphere and ozone layer). Most cutaneous damage are due to UVB exposure, which induce formation of cyclobutane pyrimidine dimers (CPD) and pyrimidine 6-4 pyrimidone photoproducts [8]. UV signature mutations are mechanistically characterized by the deamination process of cytosine or 5-methyl-cytosine in the CPDs into uracils or thymidines, which are subsequently replicated in an error-free process, thus generating C>T transitions at dipyrimidine sites [9]. Meta-analyses from

experimental sequencing data with defined UV exposure established that C>T transitions at dipyrimidines in more than 60% of the total mutational burden or CC>TT mutations in more than 5% define the presence of a UV signature [10]. Melanomas from different anatomical sites are also subject to various degrees of UVR exposure, where they are categorized as either chronically sun-damaged (CSD) or non-CSD melanomas [5]. CSD melanomas are generally diagnosed in older patients (>55 years old) on the head, neck, and dorsal surfaces of extremities, while non-CSD melanomas are commonly found on the trunk and proximal extremities of younger patients [11].

1.1.2 Genomic Studies Discover RAC1-P29S as a Hotspot Mutation in Cutaneous Melanoma

First generation sequencing analyses identified driver mutations in frequently mutated melanoma oncogenes and tumor suppressors, which consists of mutually exclusive hotspot mutations in the MAPK regulators. These include serine/threonine-protein-kinase B-raf (BRAF) (p.V600) and neuroblastoma RAS viral oncogene homolog (NRAS) (p.G12, G13 and Q61L), found in approximately 50% and 20% of patients, respectively. Interestingly, the vast majority of hotspot mutations in *BRAF* and *NRAS* are not caused by the characteristic UV-induced C>T transitions at dipyrimidines. The development of BRAF inhibitors (*e.g.* vemurafenib and dabrafenib) and MEK kinase inhibitors (*e.g.* trametinib) has led to more effective treatment options for melanoma patients when compared to chemotherapy (*e.g.* dacarbazine), where targeted therapy elicits dramatic anti-tumor responses in the clinic. However, drug resistance still remains problematic to this day (reviewed in [12]).

To identify novel significantly mutated genes (SMGs) in melanoma, research groups needed to sequence larger sample cohorts (*i.e.* sequencing >100 samples), and developed novel algorithms to address the high and heterogeneous mutation burden in melanoma that made the identification of driver mutations difficult [13, 14]. Hodis *et al.* developed InVEx, a statistical tool that uses sequencing data from intronic and untranslated regions to infer a gene-specific mutation burden that allows for the identification of SMGs. They identified established melanoma tumor suppressors and oncogenes as significantly mutated, (*BRAF, NRAS*, *MAP2K1*, *TP53*, *PTEN* and *CDKN2A*), along with novel SMGs possessing recurrent hotspot or loss of function (LoF) mutations caused by UV signature mutations [13]. *RAC1* (p.P29S) was identified as one of

those novel SMGs, along with *PPP6C* (p.R301C), and *STK19* (p.D89N) and the LoF mutations in *ARID2* [13, 14]. These SMGs were concurrently discovered by Krauthammer *et al.*, who used exome sequencing on 147 cutaneous melanoma samples, taking into account gene expression instead to identify SMGs [14]. In 2015, The Cancer Genome Atlas (TCGA), which is a collaboration between the National Cancer Institute (NCI) and National Human Genome Research Institute (NHGRI) with the goal to characterize approximately 40 cancer types across multiple data platforms, published the largest integrative multi-platform analysis of cutaneous melanoma through systematic characterization at the DNA, RNA and protein levels in a relatively large sample cohort (n=333 patients). This project used 67 (20%) primary cutaneous melanomas, which all originated from non-glabrous skin, and 266 (80%) metastases. To identify SMGs, the TCGA used InVEx and identified *RAC1* (p.P29S) once more as an SMG, along with other well-established melanoma oncogenes and tumor suppressors (*BRAF*, *NRAS*, *PTEN* and *CDKN2A)*, recently identified SMGs (*PPP6C*, *MAP2K1*, *ARID2*) and novel ones (*NF1*, *RB1*, and *IDH1*).

These genomic studies clearly demonstrated that *RAC1* (p.P29S) mutations were important in in cutaneous melanoma based on frequency, which is found in 5-10% of sun-exposed cutaneous cases [1, 2]. This mutation is shown to be the 3rd most commonly mutated proto-oncogene in the coding region in melanoma after *BRAF* and *NRAS* [1, 2]. Furthermore, RAC1-P29S is the most common cancer-associated recurrent missense mutation among the family of small RHO GTPase. Other RHO GTPase members also harbor mutations in homologous residues (<1% incidence), such as *RAC2* (P29L) and *RHOT* (P30L) [1]. Overexpression of RAC1-P29S in human immortalized melanocytes with either BRAF-V600E or NRAS-G12D oncogenic mutations maintains the guanine-triphosphate (GTP) active state [1, 2]. Furthermore, RAC1-P29S promoted membrane ruffling at the edges of COS-7 and NIH3T3 cells [15]. In light of the discovery of targeted therapy resistance seen in the clinic, Watson *et al.* demonstrated that overexpression of RAC1-P29S confers resistance to BRAF inhibitors, vemurafenib and dabrafenib [3]. These studies suggest that RAC1 is an important therapeutic target in melanoma. Unfortunately, the majority of guanine-triphosphatases (GTPases) are thought to be undruggable, which makes targeting RAC1-P29S in melanoma a challenge.

1.2 Protein Structure of RAC1

The RHO family of small GTPases is a branch of the large RAS superfamily, where its members act as molecular switches that cycle between active GTP and inactive guanine-diphosphate (GDP) states (Fig.1A). This subfamily is further classified into three categories that overlap in biological function and cellular processes: Ras homolog gene family member A (RHOA), cell division control protein 42 homolog (CDC42) and Ras-related C3 botulinum toxin substrate 1 (RAC1). RAC1 is a prominent GTPase that is ubiquitously expressed. RAC1 is best known for its role in spatial rearrangement of the cytoskeleton, by specifically remodelling actin filaments. Furthermore, there are two other RAC family members, RAC2 and RAC3, which share 89-93% amino acid homology with RAC1 [16, 17]. RAC2 is expressed in hematopoietic cells, such as human neutrophils and phagocytes, regulating oxidation. RAC3, which was initially discovered in the breast cancer cell line DU4475, is ubiquitously expressed and regulates cell proliferation and migration, much like RAC1 [17, 18]. Biochemically, RAC1 and RAC3 behave almost identically. Due to the different conformational flexibilities of its the nucleotide binding domain, RAC2 has decreased nucleotide association rate and a higher binding affinity to the downstream effector p21-activated kinase (PAK) family [19, 20].

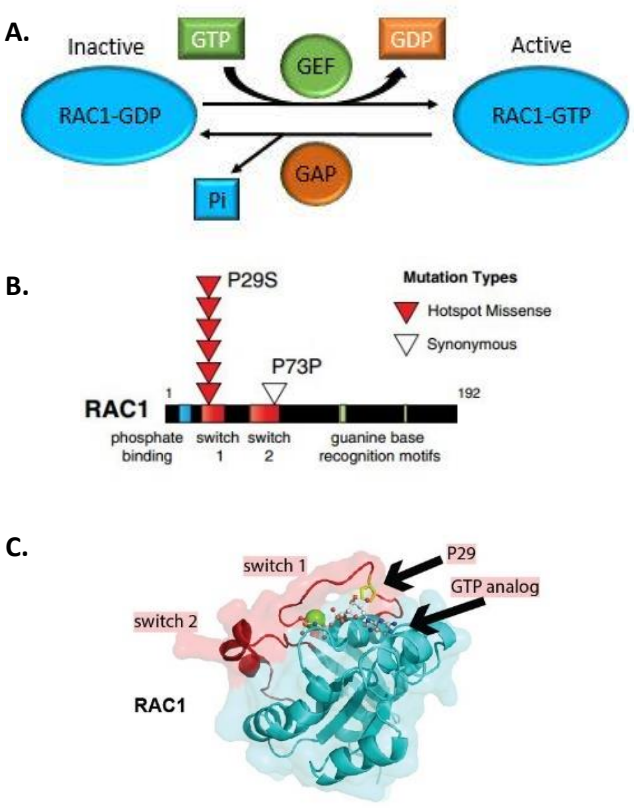

Figure 1: The Biochemistry of RAC1-P29S. **A.** Schematic of the mechanism of action of RAC1 GTPase. **B.** Schematic of the protein domains in RAC1 along with the position of the P29S hotspot missense mutation. The figure is taken from *Hodis et al*. [1]. **C.** Schematic of the 3D protein structure model of RAC1-P29S with a GTP analog. The figure is taken from *Hodis et al.* [1].

Structurally, RAC1 possesses a guanine nucleotide-binding domain (G-domain) that is comprised of a central β-sheet made up of six stands, surrounded by six α-helices and two short 3_{10} helices. Structural regions,

which are mostly conserved in RHO GTPase family members, consists of an insert region, a hypervariable region, and a G-domain that is divided into two Switch regions (Switch I and II) near the N-terminus. The flexible Switch loop regions are involved in forming the nucleotide binding pocket, where guanine nucleotide and other molecular interactors bind. The Switch I loop primarily interacts with downstream effectors, while Switch II loop interacts with guanine exchange factors (GEFs) [21, 22]. Switch I and II regions have several conserved binding motifs. The phosphate binding motif, also known as the P-loop, are found at amino acids 10-17 and 57-61. The guanine base recognition motifs are present at amino acids 116-119 and 158-160. Finally, the effector loop, which interacts with the ribose structure and a free Magnesium (Mg^{2+}) ion, are found between amino acids 28-38 [22]. Under normal conditions, Mg^{2+} as a cofactor coordinates RHO GTPase activity, by binding to residues in the Switch I, Switch II regions and the P-loop (T35, D57 and T17 respectively) to maintain GDP in the binding pocket [23, 24]. Mg^{2+} thus inhibits the spontaneous exchange between guanine nucleotides in GTPases. The 13-residue insertion region (residues 123-135) is unique to the RHO GTPase family and it consists of two exposed α-helices separated by an extended loop, providing additional charged surfaces for hydrophobic interactions [22]. The hypervariable region is located near the C-terminus and is involved in subcellular localization of the RHO GTPase. It is characterized by the highly variable polybasic domain, upstream to a four amino-acid sequence, the CAAX motif, at the end of the C-terminus. The CAAX motif is open to many post-translational modifications (PTM), such as prenylation (geranylgeranyl or, less frequently, farnesyl), AAX tripeptide proteolysis and carboxymethylation [21, 25, 26]. When RAC1 is activated, it is prenylated at the cysteine residue of the CAAX motif, and localizes to the endoplasmic reticulum for the proteolytic cleavage of the AAX tripeptide tail by CAAX prenyl protease 2 (RCE1). The exposed C-terminal isoprenylated cysteine residue is then methylesterified by protein-S-isoprenylcysteine O-methyltransferase (ICMT) (reviewed in [27]). RAC1 then anchors to the plasma membrane where downstream signaling occurs following PTMs [26]. Furthermore, RAC1 has a proline-rich domain near its CAAX motif that helps it translocate to focal adhesion complexes by interacting with proteins containing Src homology 3 (SH3) domains (*e.g.* p21-activated kinase interacting exchange factor (β-PIX)) [28].

RAC1b is an alternatively spliced isoform of RAC1 that carries out different biological functions compared to the wild-type (WT) form [29]. This constitutively active variant is formed when the exon 3b is included during translation, adding a 19-amino acid insert next to the Switch II region [30]. It is considered a self-activating GTPase, since the insert leaves Switch I in a more open conformation and renders Switch II more mobile. Ultimately, this leads to a GEF-independent GDP/GTP exchange and impairs GTP hydrolysis [31]. Furthermore, RAC1b is not regulated by Rho protein GDP dissociation inhibitors (RHOGDIs) and it fails to stimulate known RAC1-WT signaling effectors, such as the PAK proteins [32, 33].

Examination of the RAC1 protein structure observed that the P29S mutation is in the hydrophobic pocket of the Switch I domain, where it is energetically less favourable for RAC1 to be in a GDP-bound inactive state (Fig.1B & C) [1]. The change from proline to serine causes a lack of shape complementarity, reduces hydrophobicity and forms unfavorable proximity between the serine hydroxyl oxygen and the adjacent hydrophobic residues. For GTP binding, the packing of the Switch I loop is less compact and its flexibility is more restricted, showing higher hydrogen bonding with the polar and main sides of the E31 residue, thus stabilizing the GTP-bound form. So P29S likely destabilizes RAC1's inactive GDP-bound state and favors its GTP-bound state [1]. Biochemically, when overexpressed in HEK293FT cells, RAC1-P29S is shown to have a higher affinity to GTP active state when compared to the WT form utilizing a PAK-PBD pulldown. Furthermore, in the presence of exogenous GDP, RAC1-P29S shows an attenuated shift towards its inactive form, in accordance to its structural prediction [1]. Davies *et al.* demonstrates that RAC1-P29S maintains intrinsic GTP hydrolysis and that RAC1 is spontaneously activated by substantially increasing inherent GDP to GTP nucleotide exchange, allowing it to have increased binding affinity to downstream effectors [15]. This fast cycling event is similar to what is observed with the F28L amino acid change, another previously known spontaneously activating and fast recycling mutation, also associated with several other cancer cases [15, 34]. However, the fast cycling induced by F28L is a result of reduced affinity for the bound nucleotide, as opposed to the P29S mutation, which just destabilizes the GDP-loaded inactive state [34].

1.3 Regulation of RAC1 Signaling

RHO GTPase signaling is a highly regulated process, where its activation depends on interactions with various regulatory factors, such as the aforementioned RHOGDIs, the GEFs and the GTPase activating proteins (GAPs). Binding of the GAPs helps increase the hydrolysis rate of GTP to GDP and inorganic phosphate. All RHO GTPases have weak intrinsic GTPase function, so they require GAPs to promote GTP hydrolysis. GEFs promote the exchange between GDP to ambient GTP in the cytoplasm. Most of the GAP proteins share a highly conserved ~170 amino acid homology region, termed the RhoGAP domain, which is necessary for the GTP hydrolysis activity [35, 36]. Crystal structures show that RhoGAPs mostly regulate RHO GTPases by interacting with the Switch I, Switch II and the P-loop regions through a unique shallow pocket in the RhoGAP domain [37]. Similarly to RasGAPs, they stabilize the glutamine residue Glu61 of RAC1, which coordinates the attacking water molecule needed for hydrolysis to occur (reviewed in [38]). Furthermore, the arginine residue Arg85, also known as the arginine finger, interacts with the P-loop by entering the phosphate binding site during the catalytic cycle, where it promotes the transition state of the GTP-hydrolysis reaction by stabilizing the γ-phosphate [37]. Many GAPs have a strong affinity for RAC1, such as p50RhoGAP, p190, BCR/ACR and 3BP-1 [39].

GEFs are responsible for the GDP to GTP exchange in the nucleotide binding pocket of many GTPases. To destabilize the interaction between the GTPase and GDP, GEFs override the effect of Mg^{2+} on the GDP stability and catalyze the release of nucleotides, allowing GTP to bind instead. All GEFs are directed to RHO GTPase via various upstream stimuli, which includes activated receptor tyrosine kinases (RTK), G-protein coupled receptors (GPCR) and integrin receptor signaling. Of the 80 members of the GEF family, 20 of them interact with RAC1 directly (reviewed [40]). Among these GEFs, they are categorized in either the dedicator of cytokinesis (DOCK) or the Dbl protein families. All 11 members of the DOCK GEF family possess two highly conserved regions, DOCK-homology regions 1 and 2 (DHR1 and DHR2 respectively). The DHR1 domain regulates their recruitment to the plasma membrane following Phosphoinositide 3-kinase (PI3K) activation, while DHR2 is responsible for GEF activity (reviewed in [41]). Members of the larger Dbl GEF family share a sequence homology that contains the Dbl-homology (DH) domain, that encodes for catalytic activity, and the adjacent C-terminal pleckstrin homology (PH) domain,

which mediates membrane localization through lipid binding and protein-protein interactions (reviewed in [42]). Liu *et al.* examined the crystal structure of Triple functional domain protein (TRIO), a known RAC1 GEF, showing that the functional important residues of the DH domain are highly conserved. Furthermore, the PH domain directly enhances DH domain nucleotide exchange activity. Liu *et al.* also demonstrated that the DH-PH domains have a higher GEF activity (100 fold) than DH domain only [43]. Both domains are thus required to catalyze the nucleotide exchange and can be oncogenic, since constitutive activation of GEFs can induce tumorigenic transformation (reviewed in [42]). Upon binding to RAC1, GEFs induce stable conformational changes to the Switch I (residues 25-39) and Switch II (residues 57-75) regions. This sterically hinders the binding sites for the Mg^{2+} ion and disrupts the interaction between the P-loop and the β-phosphate group on GDP, altering the cleft to release the nucleotide [44]. Interestingly, only the DH domain contacts with RAC1, while the orientation of the PH domain changes relative to the initial GTPase-free structure.

Due to the variety of additional protein domains specific to each Dbl GEF, they play different biological roles depending on the cellular contexts. Dbl GEFs can also have varying subcellular localization signals or scaffolding functions for protein complex formations, while simultaneously regulating various RAC1-mediated signaling pathways. For example, TRIO GEF has two DH-PH modules, one specifically for RAC GTPases near the N-terminus and the another for other RHO GTPases [43]. Interestingly, in metastatic breast carcinoma, a TRIO-RAC1-PAK signaling axis can disassemble invadopodia formation in favour of a much more coordinated cell invasion through cortactin signaling [45]. In addition to the DH and PH domains, VAV proteins (VAV1 and VAV2) have cysteine-rich domains that act similarly to a zinc finger lipid-binding domain in Protein Kinase C (PKC), as well as SH2-SH2-SH3 domains for protein-protein interactions [46]. In T-cells development, VAV has been shown to interact with the T-Cell receptor (TCR) and induce activation of RAC1 or CDC42. This leads to activation of the c-Jun N-terminal kinase (JNK) signaling pathway [47]. Furthermore, PI3K substrates can regulate VAV activity. For example, phosphatidylinositol-4-5-biphosphate (PIP2) can inhibit VAV activity, while phosphatidylinositol-3-4-5-triphosphate (PIP3) enhances phosphorylation and activation of VAV, suggesting crosstalk between PI3K and RAC signaling [48]. β-PIX is a RAC1-specific GEF that interacts directly to the

hypervariable region of RAC1 and helps RAC1 bind to its effector protein PAK1 [49]. RAC1 itself binds to the SH3 domain of β-PIX, allowing it to localize towards focal adhesions sites and mediate cell spreading [28].

Different GEFs can also have opposing effects for the same GTPase. For example, T-cell lymphoma invasion and metastasis-1 (TIAM1) and Phosphatidylinositol 3,4,5-triphosphate-dependent RAC exchanger 1 (PREX1) GEFs directly regulate RAC1 downstream signaling and modulate its interactome, allowing them to influence RAC1 anti- and pro- migratory signaling, respectively [50]. TIAM1 helps maintain the integrity of cadherin-mediated cell-cell adhesion, while PREX1 is associated with cell-cell contact dissolution, leading to increased cell migration [50, 51] PREX1 is shown to stimulate RAC1-mediated migration through the interaction between RAC1 and flightless-1 homolog (FLII) protein, which has not been seen with TIAM1-RAC1 activation [52]. Furthermore, breakpoint cluster region (BCR) and a BCR-related protein (ACR) are both Dbl proteins that stimulate nucleotide exchange for RAC1 and RAC2. However, they can also function as both positive (GEF) and negative (GAP) regulators of RHO GTPase, since they harbour DH and RhoGAP domains [53]. The discovery that regulatory proteins can possess both GEF and GAP-specific domains highlights the complex relationship of RAC1 regulatory pathways.

The hypervariable region determines the subcellular localization of RHO GTPase. However, the localization, as well as the interaction between RHO GTPases and their regulatory factors, are regulated by RHOGDI. RHOGDIs binds mostly to the N-terminus, interacting directly with the effector binding sites (Switch I and II regions). They restrict the spatial flexibility needed for GDP to GTP exchange and lock the GTPase in an inactive state by recruiting Mg^{2+} ion, thus stabilizing the GDP [21]. They also prevent interactions with GEFs by sequestering the RHO GTPases in the cytosol or in different organelles [21, 26]. This also acts as a means of removing RHO GTPases from the plasma membrane when its signaling needs to be terminated. To be dissociated from RAC1, RHOGDIs are phosphorylated by PKC upon various upstream signaling cues, which alters its affinity for the GTPase [54]. Phosphorylation of RAC1 by Protein kinase B (AKT) on Ser71 leads to RAC1 inactivation, since the PTM inhibits the GTP binding [55]. Another regulatory event that RAC1 may use to sustain its activity is its cooperation with other signaling pathways that prevent it from being internalized and maintain its anchoring to the plasma membrane [56].

1.4 Biological Functions of RAC1

1.4.1 RAC1 Downstream Signaling

When in its inactive form, RAC1 is localized in the cytoplasm, where it binds to RHOGDI that sequesters it to different cytoplasmic compartments. When in its GTP-bound state, RAC1 is linked to a lipid moiety that allows it to localize to the plasma membrane [21]. Once at the plasma membrane, RAC1 can interact with a number of effector and adaptor proteins. Its main cellular role is to organize the cytoskeleton, where it controls the assembly of actin stress fibers and focal adhesion complexes for various cellular processes. RAC1 activates the PAK family of proteins (*e.g.* PAK1-6), which are serine-threonine kinases that phosphorylate and activate further downstream effectors. PAK proteins have 3 main domains: a p21-binding domain (PBD) at the N-terminus, the autoinhibitory domain (AID) and a kinase domain at the C-terminus. For group I PAKs (PAK1-3), they normally form a dimer when inactive, but dissociate once a GTP-bound RAC1 binds to the PBD, where they are activated by trans-autophosphorylation. For group II PAKs (PAK4-6), their kinase activity is constitutive. Active group I and II PAK proteins act as monomers and the phosphorylation stabilizes their activated form (reviewed in [57]).

PAKs activate actin-binding LIM kinases (*e.g.* LIMK1/2), which then inactivates cofilin through phosphorylation [58]. Cofilin normally binds to F-actin filaments, preventing their polymerization by converting the filaments into G-monomers. Inactivation of cofilin thus allows the actin filament assembly [59]. In addition, active RAC1 binds to the non-catalytic region of tyrosine kinase adaptor protein 1 (NCK) to dissociate WASP-family verprolin homologous protein 1 (WAVE1) from its regulatory complex. WAVE1 then associates with and stimulates the actin-related proteins 2/3 (ARP2/3) complex, which upregulates actin polymerization [60]. Active RAC1 also interacts directly with numerous adaptor proteins, such as the IQ motif containing GTPase activating protein 1-3 (IQGAP1-3), which are scaffolding proteins ubiquitously expressed in all human tissue [39]. IQGAPs possess evolutionary conserved multi-structured domains: a calponin-homology domain (CHD) at its N-terminus, a polyproline binding domain (WW), 4 isoleucine/glutamine-containing (IQ) motifs, a GAP-related domain (GRD) and a Ras-GAP C-terminus domain (RGCT) (reviewed in [61, 62]). IQGAPs bind to GTP-bound RHO GTPases via their

GRD, which contain similar structure homology to those found in traditional GAPs. RAC1 and CDC42 are specific substrates of IQGAP1, which stabilizes their active state by inhibiting their intrinsic GTPase activity [63]. By binding to Rho-GTPases, IQGAPs have been implicated with various cellular processes through actin cytoskeleton reorganization, such as cell adhesion, migration and morphology (reviewed in [64]). Furthermore, as scaffolding proteins, IQGAPs interact with numerous proteins and depending on cellular contexts, mediate a large network of signaling pathways. These interacting proteins bind to various domains and motifs on IQGAP, including the IQ motifs (*e.g.* S100B, MEK1/2 and Ca2+/calmodulin), the CHD (*e.g.* F-actin), the WW domain (*e.g.* ERK1/2) and the RGCT domain (*e.g.* E-cadherin, β-catenin, CLIP-170, Dia1 and APC) (reviewed in [61]). Through IQGAP adaptor proteins, RAC1 can modulate its signaling for cytoskeletal rearrangement, as well as influence other signaling pathways.

1.4.2 RAC1 Mediates Several Biological Processes

The actin remodelling plays a crucial part in regulating cell motility and cell migration, where both biological processes require the formation of membrane protrusions that allow cells to contract and attach to their extracellular surroundings. Through the reorganization of the cytoskeleton, RAC proteins regulate the formation of membrane ruffling and lamellipodia, an actin projection that protrudes on the leading edge of the cell surface and is typical of mesenchymal movements. In melanoma cells, studies have shown that in addition to the control of cell migration, RAC1 also inhibits RHOA activity to promote mesenchymal movements. While RHO and Rho-associated protein kinase (ROCK) mediate amoeboid migration that requires RAC1 inactivation [65]. In smooth muscle cells, RAC1 plays a role in mediating migration and maintains cell-cell contacts [66]. Furthermore, Braga *et al.* shows that in keratinocytes, in order for RAC1 to act on actin accumulation at the cell periphery, it requires cadherin-dependent contacts, implying a complex relationship between RAC1 signaling and cell adhesion regulation [67]. Interestingly, in endothelial cells, the RAC1-PAK1 signaling cascade mediates their permeability by regulating adherens junctions and cell contractility through myosin light chain (MLC) phosphorylation [68].

In addition to the PAK effector proteins, RAC1 can interact directly with other signaling pathways that promote other biological processes. Olson *et al.* demonstrated that RAC1 can

stimulate cell proliferation pathways, such as the MAPK-like JNK/SAPK (Jun NH2-terminal kinase or stress-activated protein kinase) pathway [69]. RAC1 stimulates JNK/SAPK activity by promoting the phosphorylation of the c-Jun transcription factor, which binds to AP-1 promoter sequences, leading to increased expression of many oncogenes required for cell proliferation, growth and differentiation [69, 70]. Through the JNK pathway, RAC1 also activates canonical Wnt signaling, where β-catenin accumulates in the nucleus [71]. RAC1 contributes to cell survival by crosstalk with the PI3K/AKT and the nuclear factor κ-light-chain-enhancer of activated B cells (NF-κB) pathways [72-74]. Furthermore, in the fibroblast-like COS-7 cell line, overexpression of constitutively active RAC1 provides protection from death cues by initiating AKT-dependent survival mechanisms [72]. Olson *et al.* and Klein *et al.* also demonstrate that RHO GTPases stimulate cell cycle progression by promoting the G1-S state transition and DNA synthesis by increasing the amount of cyclin D1 through the NF-κB signaling pathway [69, 75]. Furthermore, Moore *et al.* demonstrates that RAC1 GTPase plays an essential role in G2/M progression, where the RAC1-T17N dominant negative mutant inhibited cell growth [76]. However, the exact molecular mechanisms that link RAC1 signaling with cell cycle progression are still unclear. Furthermore, RAC1 function is cell type- and cellular context- dependent.

1.4.3 RAC1 and Reactive Oxidative Species

RAC1 is also a crucial factor in mediating inflammatory responses to pathological events (reviewed in [77]). For example, RAC1 plays a role in inflammatory processes important in cardiovascular diseases and arthritis. RAC1 regulates many inflammatory responses due to its role in cytokine release and production of reactive oxidative species (ROS) [78, 79]. Aside from its role in cytoskeletal rearrangement and signal transduction, RAC1 is also a cytoplasmic component of the NADPH oxidase complex, where active RAC1 is recruited for superoxide production, which affects metabolism, promotes inflammation and causes cell damage [79]. NADPH oxidase complex is a membrane-bound enzyme complex mainly formed when active RAC1, $p47^{phox}$ (NCF1), $p67^{phox}$ (NCF2) and $p40^{phox}$ (NCF4) all translocate to the membrane to bind to NADPH oxidase 1-4 (NOX1-4) and $p22^{phox}$ (CYBA) subunits. This complex is normally found in phagocytic cells, but can also be found at the plasma membrane of non-phagocytic cells (reviewed in [80]). In response to growth factors or cytokines that signal through RAC1 or RAC2,

superoxide is produced by transferring electrons from NADPH to oxygen molecules. Depending on the dosage and the amount of superoxide dismutase (SOD) enzyme present in a cell, superoxide can be genotoxic, promoting DNA damage [81]. Superoxide generation in endothelial cells is required for the expression of adhesion molecules that are induced by tumor necrosis factor-α (TNF-α) and NF-κB signaling [82]. Moldovan *et al.* also demonstrated that superoxide has a role in actin cytoskeleton reorganization, where they overexpressed human SOD in endothelial cells overexpressing constitutively activated RAC1-G12V, which reduced superoxide concentration and decreased the amount of actin filaments and ruffle formation [83].

RAC1 activity and ROS production have been shown to be involved with NF-κB activation, a known pro-survival and pro-inflammatory response pathway that induces transcription of many anti-apoptotic genes (*e.g. BCL2L1*, *TRAF1/2* and *BIRC2/3*) [84, 85]. The family NF-κB transcription factors is composed of p50, p52, RelA/p65, c-rel, and RelB; although, NF-κB1/p105 and NF-κB2/p100 are the inactive precursors of p50 and p52, respectively. When activated, these transcription factors dimerize and co-localize to the nucleus, but are normally sequestered in the cytoplasm by inhibitors of NF-κB (IκB) (*e.g.* IκBα, IκBβ and IκBε). Dissociation between the transcription factors and the IκB proteins depends on the Inhibitors of IκB (IKK) (*e.g.* IKKα, IKKβ, IKKγ/NEMO), which phosphorylate the IκBs to mark them for proteasomal degradation [85]. Crosstalk between RAC1-mediated ROS production and the NF-κB pathway is demonstrated by the NF-κB pathway prevention of ROS-mediated cell killing [86]. Furthermore, NF-κB regulates NOX2 expression and other ROS-producing enzymes, further emphasizing the relationship between these two pathways in promoting cell survival [87, 88].

1.4.4 Nuclear Function of RAC1

RAC1 is also found in the nucleus; however, the role of nuclear RAC1 remains poorly understood. Many RAS and RHO GTPases family members possess a C-terminal polybasic region (PBR), which is composed of a series of lysine and arginine, preceding the CAAX sequence of the C-terminus. Among the RAC family members, this PBR is unique to RAC1. It is thought that the PBR promotes nucleocytoplasmic shuttling, where the GTPase interacts with nuclear shuttling proteins. This is possible through the nuclear localization signal (NLS) sequence (K(K/R)X(K/R)) in

the PBR. Upon activation, RAC1 can accumulate in the nucleus, although the degree of its translocation to the nucleus vary between cell types [89]. Sandrock *et al.* demonstrated that RAC1 binds directly with importin/karyopherin α2 (KPNA2) [90]. KPNA2 is an adaptor protein that recognizes cargo protein with an NLS sequence, such as RAC1, that binds to the karyopherin β1 (KPNB1) receptor on the nuclear membrane for nuclear translocation [91]. Many studies have speculated that RAC1 may regulate transcription by interacting with signal transducer and activator of transcription (STAT) proteins [92, 93]. Michaelson *et al.* demonstrated that activated RAC1 localized to the nucleus depending on the cell cycle phase, and that the late G2 phase was the most enriched for nuclear RAC1, suggesting a role in cell division [94].

1.5 RAC1 is Deregulated in Various Diseases

Deregulation of RAC1 signaling leading to aberrant RAC1-mediated cellular processes, such as cell migration/invasion, plasticity, adhesion, growth, proliferation, apoptosis and ROS overproduction has been found in many pathological conditions. RAC1 and RAC1-regulated GEF overexpression, and/or loss of GAP function, contribute to aberrant RAC1 signaling. Based on the role of RAC1 and its effectors in various pathological conditions, RAC1 has historically been studied as a potential therapeutic target. However, similar to RAS GTPases, RHO GTPases that include RAC1 are considered “undruggable” due to their biochemical structure. Targeting downstream factors, such as PAK signaling, is possible; however, PAK inhibitors have not demonstrated efficacy in any oncology clinical trial to date (reviewed in [95]). Efforts to pharmacologically target RAC1 by developing small molecule inhibitors that can interfere with its GTP binding domain have been attempted, but no such drug has progressed past the pre-clinical stage [96].

1.5.1 Cardiovascular Diseases

Deregulated RAC1 has been shown to play important roles in many cardiovascular diseases, where *in vivo* mouse studies reported that aberrant RAC1 activation upregulates focal adhesions in cardiomyocytes, leading to spontaneous development of cardiac hypertrophy [97]. Transgenic mice are also susceptible to ischemic injury with increased myocardial infarctions [98]. Many phenotypes observed in cardiovascular system are also correlated with increased levels of NOX2,

superoxide and PAK proteins [98]. Overexpression of RAC1 in smooth muscle cells (SMCs) resulted in increased vascular levels of superoxide, which contribute to hypertension and cardiomyocyte hypertrophy [98]. Despite administration of angiotensin-II, which induces hypertensive stress, dominant negative *Rac1* as well as *Rac1* deletions in transgenic mouse models demonstrate reduced NADPH oxidase activation, ultimately decreasing myocardial oxidative stress [99, 100]. This provides insight into how RAC1-mediated ROS production worsens cardiovascular conditions. In addition, NADPH oxidase activity has been involved with the development of atherosclerosis, implying a role for RAC1 in this disease [101, 102]. RAC1 impacts the permeability and cell adhesion of endothelial cells, by affecting their adherens junctions. Downstream PAK inhibition reduced endothelial cell permeability in many areas affected by atherosclerosis, which emphasizes the importance of RAC1-PAK signaling in SMC migration and lipoprotein deposition leading to cardiovascular diseases [68, 103]. Upon TNF-α stimulation, dominant negative expression of RAC1 prevented the migration of aortic SMCs to the inner layers of arteries, which also suggests cytokine involvement [104]. RAC1 coordinates leukocyte trans-endothelial migration and accumulation in the arterial walls when vascular injuries occur [105]. Thus, RAC1 contributes to cardiovascular diseases by regulating endothelial permeability, ROS production and migration of SMCs and leukocytes.

1.5.2 Neurodegenerative Diseases

In the nervous system, RAC1 and other RHO GTPases are essential for neuronal development, morphology, migration and plasticity (reviewed in [106]). Due to the important protective function RAC1 has in maintaining the integrity of several neuronal aspects, various neurodegenerative diseases exhibit loss of RAC1 signaling. This is prevalent in Parkinson's disease, a neurodegenerative disease characterized by locomotive, cognitive and behavioral inhibitions mainly caused by the degeneration of dopaminergic neurons in the midbrain. *In vitro* studies have demonstrated that familial mutations in leucine-rich repeat kinase 2 (LRRK2) that lead to neuronal cell death can be rescued by RAC1 overexpression [107, 108]. Conversely, despite the seemingly protective role of RAC1 in neurodegenerative diseases, many proinflammatory cytokines (*e.g.* TNF-α and IL-1β) stimulate RAC1-mediated activation of NADPH oxidase and ROS production to promote inflammation that degrade neuron cells. This is

prominently found in neuron microglia that harbour mutations in SOD1, which is affiliated with amyotrophic lateral sclerosis (ALS) [109, 110]. Another major neurodegenerative disease implicated with deregulated RAC1 signaling is Alzheimer's disease, where there is neuronal loss in the hippocampus and cerebral cortex. Studies have suggested that Alzheimer's disease is attributed to aberrant accumulation of extracellular amyloid-β plaques [111]. RAC1 has been shown to regulate the transcription and expression of these plaques' proteolytic cleavage precursor, amyloid precursor protein (APP) [112, 113]. Therefore, studies have reported both RAC1 protective and neural degenerative promoting effects.

1.5.3 Glucose-related Diseases

In skeletal muscle and fat cells, abnormalities in glucose uptake through insulin receptor signaling leads to type 2 diabetes. Studies have shown that RAC1 plays an important role in glucose uptake, where it regulates the translocation of glucose transporter type-4 (GLUT4)-containing vesicles from the intracellular compartments to the plasma membrane upon insulin stimulation [114, 115]. Once these skeletal muscle cells were stimulated by insulin, RAC1 and PAK1 expression levels increased. Furthermore, PAK phosphorylation is decreased in insulin-resistant conditions, such as intralipid infusion in healthy volunteers [115]. Through RAC1 signaling, actin filament remodelling complex Arp2/3 facilitates GLUT4-vesicles translocation in muscle cells, where GLUT4 interacts with actin via actinin-4 [116, 117]. In addition, RAC1 signaling cooperates with PI3K/AKT signaling for GLUT4 translocation and it has been suggested that both signaling pathways are required for downregulating insulin resistance [114]. These studies are indicative of the involvement of RAC1 in glucose-related diseases, such as diabetes.

1.5.4 Inflammatory Diseases

Aberrant RAC1 expression has also been implicated with various mechanisms of inflammation (*e.g.* NF-κB activation, cytokine release, phagocytosis and invasiveness of pathogens) that lead to many pathological and autoimmune disorders (reviewed in [77]). RAC1-mediated inflammatory responses have also been observed in many forms of arthritis, which is an agglomeration of diseases that affect the joints. RAC1 was detected in many osteoarthritis cartilages, where it is shown to promote accumulation of matrix fragments such as fibronectin by inducing the

expression of many matrix metallopeptidases (MMP) (*e.g.* MMP-13 and ADAMTS-5) [118-120]. Through cartilage matrix degradation, RAC1 activation contributes to the advancement of osteoarthritis. Furthermore, RAC1 has important functions in the development of inflammatory arthritis, such as rheumatoid arthritis that is characterized by an increased population of activated T-cells and antibodies that induce localized inflammation and swelling in the synovial membranes. Moreover, RAC1 promotes the proliferative and invasive properties of fibroblast-like synovial cells, making them behave similarly to tumor cells [121]. Along with inflammatory responses, many inflammatory disorders show deregulated RAC1 signaling, such as chronic inflammatory bowel diseases (IBD), which includes ulcerative colitis and Crohn's disease [122]. In these disorders, RAC1 harbours single nucleotide polymorphisms that increase its expression, leading to aberrant innate immunity, increased neutrophil/macrophage recruitment, and subsequent pro-inflammatory cytokine expression in the colon [122]. Winge *et al.* also revealed that RAC1 is a crucial player in the psoriasis pathogenesis, a disease that exhibits deregulated keratinocyte proliferation, inflammation and immune cell infiltration [123]. Using a Rac1 G12V transgenic mouse model, constitutively activated Rac1 in keratinocytes produced psoriatic lesions similar to what is observed in humans by modulating inflammatory pathways, such as STAT3, NF-κB, and zinc finger protein 750 (ZNF750). This highlights the relationship between hyperactive RAC1 that promotes innate immunity and the surrounding immune cells that stimulate inflammatory responses.

1.6 The Role of RAC1 in Cancer Development

In this thesis, we focused on understanding the role of mutant RAC1 in melanoma development and metastasis. Metastasis is a multi-step process, through which cancerous epithelial cells become invasive towards their surrounding microenvironment, intravasate into blood and lymph vessels and extravasate into distant tissue sites to colonize new sites, which will impact a patient's morbidity and mortality (reviewed in [124, 125]). At the molecular level, metastatic cancer cells are mainly characterized by abnormal cytoskeletal remodelling that affect cell migration as well as their ability to cross tissue boundaries. Many cancers types display deregulated RAC1 expression and signaling. Studies have shown *in vitro* that RAC1 is a crucial downstream effector required for Ras-induced transformation in NIH3T3 cells [126, 127]. *In vivo*

studies have also demonstrated the requirement for RAC1 in KRAS-induced lung cancer and HRAS-induced skin cancer development [128, 129]. Suppression of RAC1 has even been shown to induce cell death in glioma cells, while introduction of the constitutively activating G12V mutation induces oncogenic transformation, where tumors formed similar to the human Kaposi's sarcoma [127, 130].

1.6.1 RAC1 Mutations Discovered in Various Cancer Types

Since the first discoveries of the hotspot mutations in RAC1 in 2012, RAC1 mutations have been found in additional human cancers [1, 2]. When examining the Catalogue of Somatic Mutations in Cancer (COSMIC) database of cancer genomes, RAC1 mutations have been reported in low frequency in numerous cancer types. The vast majority are missense substitutions (87%) [131]. Furthermore, the base substitutions that are observed are predominantly C>T transitions (78%), followed by G>A (~6%) and G>T/A>G (~3%) as the second and third next frequent nucleotide substitution, respectively. The most frequent missense mutation is the c.85C>T, which encodes for the P29S amino acid change, as described above in the melanoma studies.

The role of RAC1-P29S in cancer is poorly understood, with only a few publications that have attempted to characterize its function. Kawazu *et al.*, reported that other RAC1 mutants identified from sequencing cell lines, RAC1-C157Y and RAC1-N92I, have transforming capabilities from pre-clinical studies in sarcoma [4]. Activating mutations have also been identified in other RAC family members, such as RAC2-P29L and RAC2-P29Q [4]. The COSMIC database show that more than one RAC1 mutation can occur in different cancers types, which includes the large intestine, cervix, liver, endometrium, stomach, oesophagus, lung, upper aerodigestive tract, haematopoietic/lymphoid and breast [131]. The MSK-IMPACT Clinical Sequencing Cohort, which is the most recent large-scale genomic study by the Memorial Sloan-Kettering Cancer Centre that sequenced tumors from more than 10,000 patients, identified many hotspot mutations involving the P29 residue (*e.g.* P29S, P29F, P29L and P29T) in melanoma, Merkel cell carcinoma, squamous cell carcinoma, anaplastic thyroid cancer and breast invasive ductal carcinoma [132-134]. However, RAC1 mutations occur at very low frequency in these other cancers (<1%) compared to melanoma (5-10%).

1.6.2 RAC1 Effectors and Regulators are Deregulated in Cancer

PAK family members are shown to be upregulated and hyperactivated in various cancer types, where its kinase activity contributes to tumor progression, invasion aggressiveness and metastasis (reviewed in [135, 136]). Furthermore, they are the best understood downstream effectors for RAC GTPases, with PAK1 and PAK4 being the most studied PAK family members (reviewed in [135]). Through RHO GTPases-dependent and -independent activation, PAK1 can integrate with multiple signaling pathways by phosphorylating downstream effectors or by acting as a scaffold, which allows RAC1 signaling to crosstalk with other signaling cascades to promote cancer cell invasion. Initial gain of function (GoF) and LoF studies focused on PAK1 activation by Erb-B2 receptor tyrosine kinase 2 (ERBB2) signaling in invasive breast cancer cell lines, where overexpression and hyperactivation of PAK1 signaling led to enhanced cell attachment and anchorage-independent growth [137-139]. Furthermore, in invasive tumor cells, PAK1 signaling mediates actin-rich extensions needed for extracellular matrix (ECM) degradation through LIMK activity [45, 58, 140]. *PAK1* gene amplification at Chromosome 11q13-14 has been observed in various cancer types (*e.g.* breast cancer, ovarian carcinoma, colorectal carcinoma and uveal melanoma) and its expression correlates with clinicopathologic features in human cancers (reviewed in [135]). PAK2 and PAK4 are also widely overexpressed in various human cancers. PAK1 overexpression has been observed in ovarian and breast cancer, PAK2 in esophageal and lung cancer, and PAK4 in uterine, pancreatic and ovarian cancers [133]. Furthermore, overexpression of PAK4 drives AKT- and ERK-related signaling, suggesting PAK4-driven pathways in different human cancers [141]. For the other lesser known PAK proteins, further studies are required to understand how RAC1 signals through them. Although recent studies have demonstrated their upregulation in certain cancers. For example, Gong *et al.* reported that PAK5 is overexpressed during colorectal cancer development [142].

In addition to RAC1 downstream effectors, a large number of GEF are deregulated in numerous cancers, where their hyperactivation is associated high active RAC1 levels that contribute to tumor progression and poor patient outcome [143]. For example, many invasive squamous head and neck cancers have high levels of GTP-bound RAC1 due to epidermal growth factor receptor (EGFR) activation of VAV2 GEF [144]. Furthermore, many glioblastomas and

breast cancer cells express high levels of TRIO, ECT2 and VAV3 GEF levels, where their depletion affects cell migration and invasion [145]. GEFs also link RAC1 activation with other signaling pathways. For example, PREX1, a PI3K-dependent GEF, activates RAC1 for spontaneous prostate cancer metastasis *in vivo* [145]. When RTKs are activated in fibroblasts, they recruit several downstream effector proteins, including son of sevenless 1 (SOS1) protein, which acts both as a RAS and RAC GEF. SOS1 acts as a bridge between RHO GTPase and MAPK pathway. When SOS1 complexes with E3B1 and EPS8, it acts exclusively as a RAC-GEF [146].

1.6.3 RAC1 Promotes Epithelial Mesenchymal Transition

As mentioned above, activation of RAC1 signaling mediates malignant transformation and metastasis characterised by gain of migratory and invasive properties (reviewed in [147]). This invasive phenotype induced by deregulated RAC1 signaling is important for epithelial mesenchymal transition (EMT), where epithelial cells acquire the ability to bypass apoptosis and cell adhesion and invade the ECM. RAC1 hyperactivation has been reported to regulate cellular plasticity control, which drives cells to acquire elongated actin morphology and adopt mesenchymal-like movements [65]. For example, in A375 melanoma cells, RAC-specific GEF DOCK3 complexes with the adaptor protein NEDD9 to regulate RAC1 and WAVE2 signaling. This drives mesenchymal movement and suppresses amoeboidal movement by decreasing actomyosin contractility. Furthermore, RHOA signals through ROCK kinases to upregulate expression of a RAC-specific GAP, RHO GTPase Activating Protein 22 (ARHGAP22), to suppress mesenchymal movement [65]. This interplay between RHO GTPases is crucial for the cell movement determination, where upregulation of RAC1 favours a more invasive phenotype.

RAC1 can at the same time promotes the assembly and disassembly of E-cadherin coordinating cell-cell contacts. Through PAK1 signaling, constitutively active RAC1, as well as RAC3 and RAC1b, can disrupt cadherin-mediated junction sites in keratinocyte, while in Madin-Darby canine kidney (MDCK) cells, RAC1 and CDC42 are required for spatio-temporal regulation of cell-cell adhesion [33, 148, 149]. During EMT, RAC1 utilizes actin extensions for cell-cell contacts with the surrounding stromal cells (reviewed in [150]). Upon RAC1-mediated upregulation of lamellipodia, new focal adhesions complexes form in these actin extensions.

When the extending lamellipodia of tumor cells contacts the ECM, integrin receptors (*e.g.* integrin β1) on the plasma membrane bind to ECM ligands and cluster together, where downstream signaling involving focal adhesion kinase (FAK), α-actinin, talin, vinculin and paxillin form the focal adhesion complex [151]. RAC1 influences the development of focal complex through its induction of ruffling lamellipodia and coordinate their formation to further an invasive pathway in the ECM [152]. In EMT, tumor cells gain the ability to form invadopodia, which are actin-rich protrusions of the plasma membrane that are indicative of cellular invasiveness and that also help in localizing MMPs for proteolytic digestion of the ECM (reviewed in [153]). Through the TRIO-RAC1-PAK1 signaling axis, RAC1 mediates cortactin phosphorylation, which promotes invadopodia dissolution [45]. This mechanism allows tumor cells to better maximize invasive coordination by properly using the necessary morphological cell structures. For tumor invasion to initiate, the basement membrane that separates epithelial cells from stromal cells needs to be degraded. RAC1 activation facilitates the invasion process by upregulating the expression and release of several MMPs needed for ECM proteolytic degradation, such as collagenase-1 and matrix metalloproteinase through the JNK signaling pathway [154, 155]. However, TIAM1-RAC1 signaling can upregulate the expression of the tissue-specific inhibitors of MMPs (TIMPs), such as TIMP-1 and TIMP-2 [156]. While it is unclear how RAC1 signaling upregulates TIMP expression, RAC1 coordinates tumor invasion by regulating the expression of both MMPs and TIMPs.

In addition, by regulating ECM degradation, RAC1 also plays an important role in tumor angiogenesis, which is the process through which tumor cells promote the creation of new blood vessels from pre-existing vessels for nutrient supply and waste disposal that will ensure its growth and survival. Neoangiogenesis requires highly coordinated cell migration, making it a RAC1-dependent process (reviewed in [157]). As mentioned previously, RAC1 coordinates cell-cell adhesions between tumor cells and the ECM, which also includes assembly and maturation of endothelial cells into new vasculature structures. Vader *et al.* knocked-down RAC1, showing that vascular endothelial growth factor (VEGF)-mediated vessel formation, endothelial cell migration, invasion and proliferation were inhibited *in vitro* and *in vivo* [158]. VEGF signaling seems to be dependent on RAC1 signaling for tumor angiogenesis to occur.

1.6.4 Various Signaling Pathways Crosstalk with RAC1 in Cancer

Overproduction of other growth factors (*e.g.* platelet-derived growth factor (PDGF), epidermal growth factor (EGF) and insulin) is also responsible for stimulating different cellular processes can induce the formation of lamellipodia and membrane ruffling, implying crosstalk with RAC1 signaling to promote deregulation of cell proliferation, survival and growth [159]. RAC1 regulates cell proliferation through the MAPK-like JNK and p38 pathways, but can cooperate with the NF-κB pathway to affect anchorage-independent proliferation in non-small cell lung carcinoma (NSCLC) [84, 160]. Furthermore, RAC1-mediated cell proliferation is also attributed with progression through the G1/S cell cycle checkpoint and promotes the G2 phase [69, 76]. This indicates that cooperation between RAC1 and the NF-κB signaling is needed for enhanced cell proliferation in tumor cells. RAC1 also promotes cell survival independently of NF-κB stimulation by interacting directly and activating PI3K to stimulate AKT [72]. Upon growth factor stimulation, RAC1 and PI3K/AKT signaling can induce cell growth and migration in the MDA-MB-231 breast cancer cell line through PAK1 activation [161]. The RAC1-mediated ROS production also contributes to VEGF/PDGF-induced activation of the PI3K/AKT pathway in many cell types [162, 163]. Other RAC1 crosstalks with cancer-related pathways include mammalian target rapamycin complex 1/2 (mTORC1/2) subcellular localization for cell growth, increased canonical Wnt signaling, and transforming growth factor β1 (TGF-β) upregulation to modify cells from the tumor microenvironment [164-166]. Thus, RAC1 cooperates with different signaling pathways to promote the metastatic tumor formation.

Moreover, the constitutively active splice isoform Rac1b, which is predominantly identified in skin and epithelial tissues from the intestinal tract, is required for K-Ras induced lung cancer in transgenic mouse models [167]. Furthermore, RAC1b was shown to promote transformation of NIH3T3 cells and is overexpressed in several cancers, including colorectal, lung, breast and pancreatic cancers [30, 168-171]. Expression of RAC1b in colorectal cancer cells promoted their survival, while in lung epithelial cells, RAC1b has been implicated in enhanced spontaneous tumor formation and MMP-induced EMT [169, 170, 172]. Faria *et al.* shows that RAC1b is also overexpressed in thyroid carcinomas and is associated with distant metastases and poor clinical

outcome [173]. This further adds emphasis on RAC1 and its isoforms being important regulators in tumor progression and therapeutic strategies to target them need to be addressed.

2. Objectives

RAC1 is a well-studied RHO GTPase that regulates many signaling pathways and has numerous reported functions. Work from our group and others have recently discovered the P29S hotspot mutation in RAC1 in approximately 5-10% of cutaneous melanomas. However, its function and the signaling pathways that are important for its role in melanoma are poorly understood. The objective of this thesis was to utilize an unbiased transcriptomic and proteomic approach to elucidate the role and mechanism of RAC1-P29S in cutaneous melanoma.

Aim 1: To identify mRNA expression changes and significant pathways deregulated in the RAC1-P29S melanomas through unbiased transcriptomic analysis.

Aim 2: To gain mechanistic insight into possible signaling pathways deregulated by RAC1 mutations by characterizing RAC1-P29S interacting proteins.

3. Aim1: Transcriptomic analysis of RAC1-P29S in melanoma

3.1 Mutations in the Switch 1 Region lead to Higher RAC1 Activity

As shown in Table 1, RAC1 hotspot mutants co-occur with the two most frequently mutated genes in melanoma, *BRAF* and *NRAS*, as determined from the melanoma TCGA data. However, a higher percentage *BRAF/NRAS* WT melanomas possess the *RAC1* (p.P29S) mutation [174]. Next, we investigated the role of RAC1-P29S on tumor progression. We used two primary immortalized human melanocyte lines that constitutively express TERT, dominant-negative p53 (p53DD), CDK4-R24C [175]. The melanocytes either stably express BRAF-V600E (HMEL melanocytes) or NRAS-G12D (PMEL-NRAS melanocytes) hotspot mutations. We define both these lines as partially transformed melanocytes, since HMEL melanocytes don't form tumors in immunocompromised mice compared to PMEL-NRAS melanocytes, which has a 50% tumor penetrance (data not shown). HMEL and PMEL-NRAS melanocytes with stable overexpression of GFP, RAC1-WT and RAC1-P29S were injected into NCR-nude immunocompromised mice (Suppl.Fig.1 A-B). The HMEL partially transformed melanocytes rarely form melanomas when injected in NCR-nude mice, as was observed in the GFP control group (Suppl. Fig.1A, C & E). The PMEL-NRAS partially transformed cell line is more tumorigenic (Suppl. Fig.1B, D & F), and approximately 50% of GFP overexpressing controls formed tumors. However, in both the HMEL and PMEL-NRAS cells, overexpression of the RAC1-P29S mutant promoted tumor progression (Suppl. Fig.1C-F). HMEL infected with RAC1-P29S mutant had a significant increase in tumor burden measured at week 2 (Mann-Whitney $p<0.0001$) and decreased survival with 100% penetrance (Log-rank (Mantel-Cox) test: $p<0.0001$) at week 4.5 (Suppl. Fig.1C & E). PMEL-NRAS infected with the RAC1-P29S mutant had a significant increase in tumor burden measured at week 3 (Mann-Whitney $p<0.0001$) and decreased survival with approximately 80% penetrance (Log-rank (Mantel-Cox) test: $p<0.0001$) at week 10 (Suppl. Fig.1D & F). It should be noted that that RAC1-P29S had a greater effect on tumor burden and survival than overexpression of RAC1-WT. Furthermore, overexpression of RAC1-WT had an intermediate phenotype when compared to GFP-overexpressing tumors in HMEL partially transformed melanocytes (p value<0.0001), but had no effect in the PMEL-NRAS cell line (Suppl. Fig.1C-F).

Table 1. Co-Occurrence of the Significantly Mutated Genes with *BRAF* and *NRAS* Hotspot Mutations

SMG	BRAF (hotspot)	NRAS (hotspot)	BRAF/NRAS wild-type
BRAF	100%	5%	0%
NRAS	1%	100%	0%
NF1	2%	15%	27%
MAP2K1	4%	3%	2%
RAC1	2%	5%	12%
CDKN2A	11%	17%	12%
TP53	13%	17%	8%
PTEN	13%	7%	4%
STK19	2%	5%	4%
SERPINB3	3%	0%	4%
PPP6C	5%	15%	2%
DDX3X	6%	12%	2%
CASP8	5%	2%	2%
IDH1	5%	5%	4%
WBP2NL	3%	0%	6%
CTNNB1	7%	2%	4%

TCGA-SKCM data, N=255 whole exome sequences

Next, we wanted to determine whether other non-P29S RAC1 somatic mutations identified in the Cutaneous Melanoma TCGA dataset (TCGA-SKCM-provisional; N=478) also affect RAC1 GTPase activity. A total of 9 somatic mutations, including the P29S mutation, were identified and are shown in in Figure 2A [133, 134]. We utilized a common p21-activated kinase-binding domain (PBD) pull-down assay to assess the activity status of the various RAC1 mutants. One of the downstream effectors of RAC1 are the family of PAK proteins, where each member shares a PBD domain that binds specifically to RAC1 in its GTP active state. For this assay, we use beads that were conjugated to recombinant PBD domain, from which we can isolate GTP-bound RAC1.Equal amounts of plasmids were transfected in HEK293FT cells for RAC1 p. V14E, E31D, S71F, P87L, N92K and P140L expressing plasmids. We pulldown equal amount lysate and performed Western blots where we observed that only RAC1-V14E, RAC1-P29S and RAC1-P29L were found in a higher fraction of the RAC1-GTP active form compared to wild-type (Fig.2C & D). This experiment was

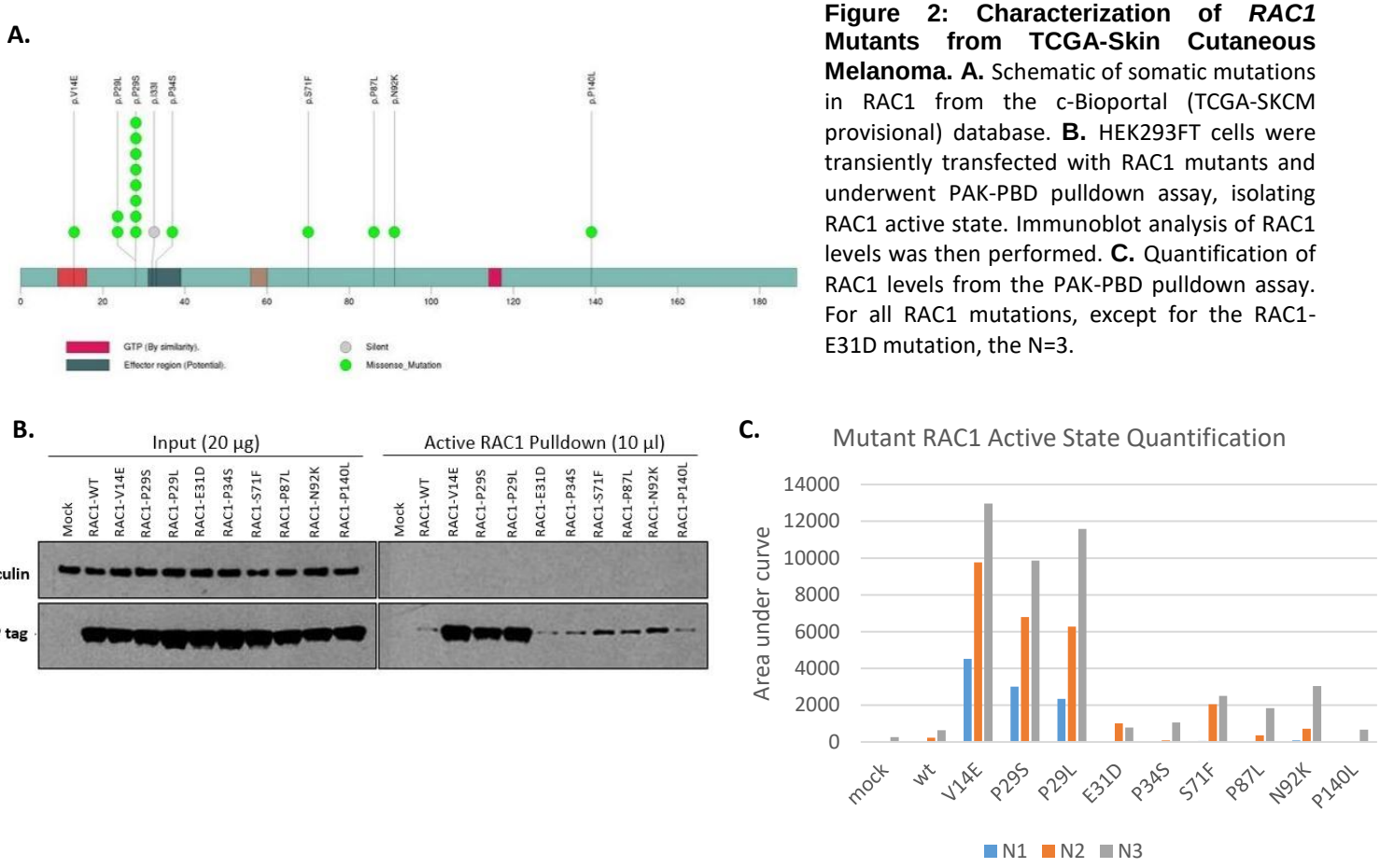

Figure 2: Characterization of *RAC1* Mutants from TCGA-Skin Cutaneous Melanoma. A. Schematic of somatic mutations in RAC1 from the c-Bioportal (TCGA-SKCM provisional) database. **B.** HEK293FT cells were transiently transfected with RAC1 mutants and underwent PAK-PBD pulldown assay, isolating RAC1 active state. Immunoblot analysis of RAC1 levels was then performed. **C.** Quantification of RAC1 levels from the PAK-PBD pulldown assay. For all RAC1 mutations, except for the RAC1-E31D mutation, the N=3.

performed in triplicates, yielding the similar trends. Thus, the three mutations found in the Switch I domain (V14E, P29S, P29SL) are activating and were included in our transcriptomic analysis from the TCGA dataset.

3.2 Unbiased Transcriptomic Analysis Identifies Patient-Relevant Signaling Pathways

Our preliminary results in section 3.1 demonstrated that RAC1-P29S promotes melanoma progression in partially transformed melanocytes possessing *BRAF* and *NRAS* hotspot mutations, and that overexpression of RAC1-WT had an intermediated phenotype. In addition to RAC1-P29S, V14E and P29L were found in biochemical experiments to be activating. Interestingly, we identified from TCGA-SKCM database that *RAC1* is also a significantly amplified gene in cutaneous melanoma. We utilized GISTIC 2.0, which is a statistical tool used to identify significantly deleted and amplified genes on the TCGA-SKCM dataset that identified *RAC1* among one of the 94 significantly amplified genes at the minimal common region (Chr.7p22.3) (Fig.3A) [176].

Next, to gain a better understanding of the mRNA expression changes found in RAC1-P29S mutant melanomas we excised xenograft tumors from the HMEL and PMEL-NRAS *in vivo* experiment, and performed RNA-seq on a subset of tumors. Specifically, we compared mRNA expression changes between HMEL-GFP control and P29S xenografts (n=3 per group), and between PMEL-NRAS-GFP control and P29S xenografts (n=5 per group). We utilized the Illumina HiSeq 2000 platform to determine mRNA expression changes. From the expression data, a list of ranked differentially expressed genes (DEGs) with an False Discovery Rate (FDR) <5% were generated for each sample group. For the HMELs (BRAF-mutant group), 108 DEGs were upregulated and 43 were downregulated, while in the PMEL-NRAS-mutant group, 817 upregulated and 700 downregulated genes were observed (Suppl.Fig.2A & B).

To identify patient-relevant genes differentially expressed in our analysis, we intersected our xenograft mRNA expression analysis with TCGA (Fig.3B). Subsequently, a DEG analysis was performed on the TCGA-SKCM dataset. In the TCGA data, a total of 23 patients harboured either a RAC1-P29S, P29L or V14E mutation. Considering we observed that the P29S mutation was more active compared to WT in our biochemical PBD assays and *in vivo* tumorigenesis experiment, we performed DEG analysis of these 23 RAC1 mutant patient samples (P29S, P29L, and V14E) with 15 samples harbouring RAC1-WT amplifications. A total of 81 DEGs were downregulated and 50 were upregulated for samples with RAC1 mutants (FDR<5%, Suppl.Fig.2C). For all three DEG studies, gene set enrichment analysis (GSEA) was performed to determine significant pathways that are deregulated upon RAC1-P29S overexpression. A total of 497 reactome and hallmark gene sets were used for this study and the normalized enrichment score (NES) was calculated. Upon filtering for FDR<5%, 258 pathways were identified for NRAS & RAC1 mutant samples, 278 pathways for BRAF & RAC1 mutant samples, and 323 pathways for TCGA samples with mutant RAC1 (Suppl.Fig.3-5). Among the significantly altered signaling pathways, which were common between all three cohorts (RNA-seq data + TCGA), the three most upregulated common pathways (positive NES values) were linked to immune response, specifically interferon signaling. The three most common downregulated pathways (negative NES values) are involved in mitochondrial respiration. All pathways identified by the Hallmark gene sets (Interferon-α, Interferon-γ and oxidative phosphorylation) follow the same trend in all three respective sample cohorts, as

shown in the pathway enrichment plots (Fig.3C-E). Notably, RAC1 is known to regulate these biological processes. Thus, our unbiased transcriptomic analysis suggests that RAC1-P29S modulates immune and mitochondrial respiration processes in cutaneous melanoma. Interestingly, we also observed EMT to be an upregulated signaling pathway. However, it was only deemed significant in xenograft tumors formed by PMEL-NRAS melanocytes and in the TCGA-SKCM cohort (Suppl.Fig.3 & 5). Further investigation is required to determine expression levels of EMT markers in melanoma cell lines with RAC1-P29S overexpression, as well as characterize the mesenchymal phenotype induced by RAC1-P29S.

The common specific significant pathways identified in the GSEA analysis were oxidative phosphorylation, respiratory electron transport chain (ETC) and the tricarboxylic acid (TCA) cycle. To validate whether the RAC1-P29S mutation affects oxidative phosphorylation, we performed preliminary Seahorse Mitochondrial Respiration assays on isogenic BRAF-V600E mutant melanoma cells lines (451Lu, A375 and MALME-3M) stably overexpressing GFP, RAC1 WT and P29S. We measured oxygen consumption rate (OCR-pmol/min/μg), which is a general measurement for oxidative phosphorylation status in a cell, along with extracellular acidification rate (ECAR-mpH/min/μg), which measures the glycolysis rate. Compared to GFP controls, overexpression of both RAC1-WT and P29S in the MALME-3M and A375 melanoma cells lines led to decreased mitochondrial respiration (Suppl.Fig.6B & C). However, no significant difference was observed between RAC1 WT and the P29S mutant. In addition, when examining at ECAR levels, for two of the isogenic melanoma cell lines, 451Lu and A375, acidification levels were lower in the P29S overexpressing cells (Suppl.Fig.6D & E). However, there was no difference in the ECAR values between the WT and P29S mutant in the MALME-3M cell line (Suppl.Fig. 6F). We should note these were preliminary studies that demonstrate some trends that suggest that both overexpression of WT and the P29S mutant in melanoma cell lines affect mitochondrial respiration by decreasing oxidative phosphorylation. However, experimental replicates and consistent statistics are required, and complementary knockdown experiments of cell lines with endogenous RAC1-P29S mutants are needed to draw any conclusions.

The specific pathways elucidated from the GSEA analysis involving immune regulation were specific to Interferon-α (IFN-α) and Interferon-γ (IFN-γ) signaling pathways. This suggests that

RAC1-P29S potentially modulates both type I and II interferon cytokines, where the type I is mostly involved in viral response and type II regulates immune and inflammatory responses [177, 178]. The Type II interferon group is solely comprised of IFN-γ, which has been known to upregulate expression of the immune checkpoint inhibitor programmed death-ligand 1 (PD-L1) in melanoma [179]. PD-1 is a co-inhibitory T-cell receptor that inhibits T-cell activation, and PD-L1 is its ligand expressed in many cell types, including tumors cells [180]. Recently, monoclonal antibodies (*e.g.* pembrolizumab and nivolumab) were developed to target both PD-1 and PD-L1, thus activating the immune system by preventing the PD-1 and PD-L1 interaction. Together with ipilimumab, which is an anti-CTLA-4 monoclonal antibody, immunotherapy treatments produced durable responses and increased overall survival in melanoma patients and are now the standard of care for melanoma treatment (reviewed in [181]). Vu *et al.* has reported that RAC1-P29S upregulates PD-L1 expression in melanoma [182]. We speculated that RAC1-P29S regulates PD-L1 expression through IFN-γ signaling. When treating 451Lu and A375 melanoma cell lines overexpressing GFP, RAC1 WT and P29S mutant cell lines with IFN-γ, we observed an increase in PD-L1 expression (Fig.4) [179].

In summary, through unbiased integrative transcriptomic analysis, we identified significant pathways that provide some insight into the mechanism and signaling pathways altered by the RAC1-P29S mutant in cutaneous melanoma. RAC1-P29S may deregulate metabolism and mitochondrial respiration, as well as promote immune evasion through the expression of PD-L1. Future works needs to confirm our preliminary findings, and elucidate the specific mechanisms by which RAC1-P29S modulates these downstream signaling pathways. We anticipate our proteomic analysis in aim 2 will aid to address these challenges.

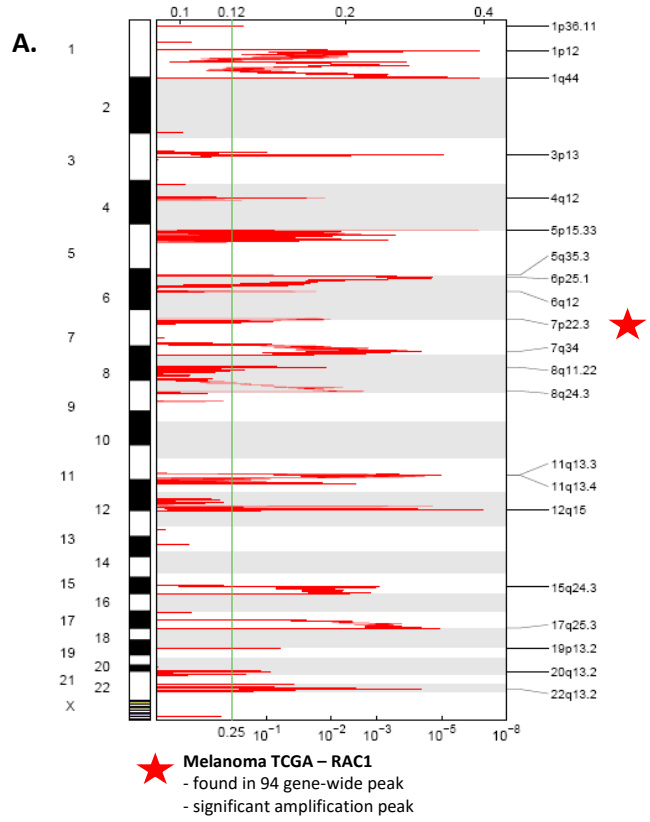

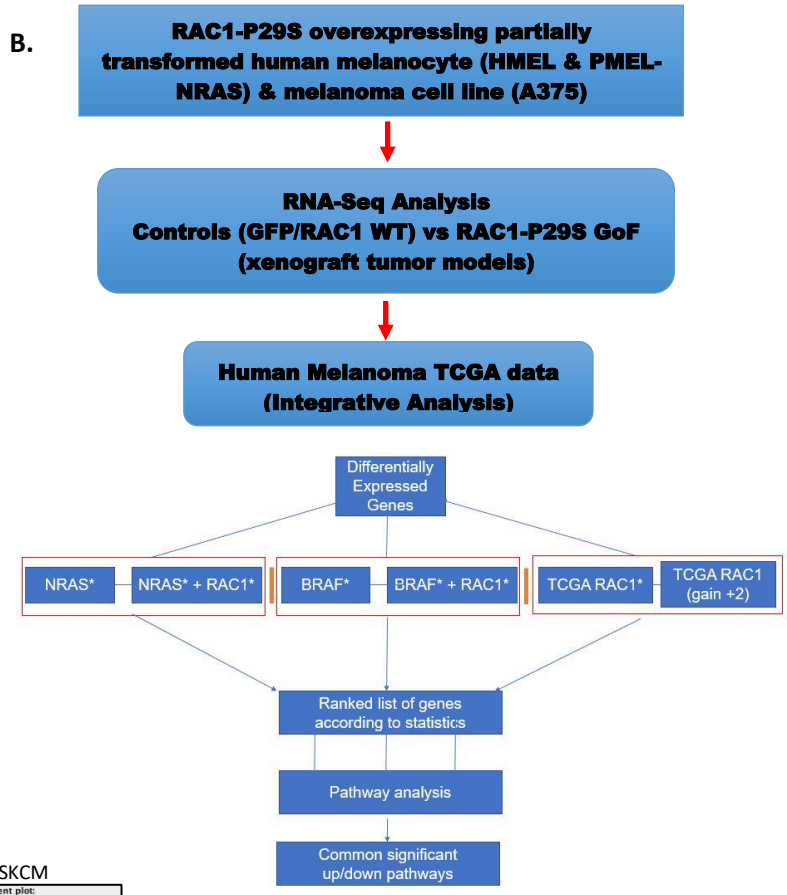

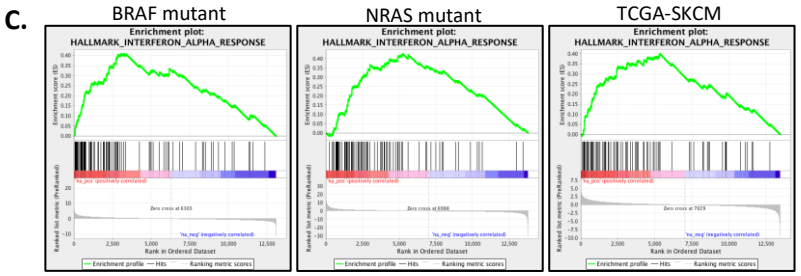

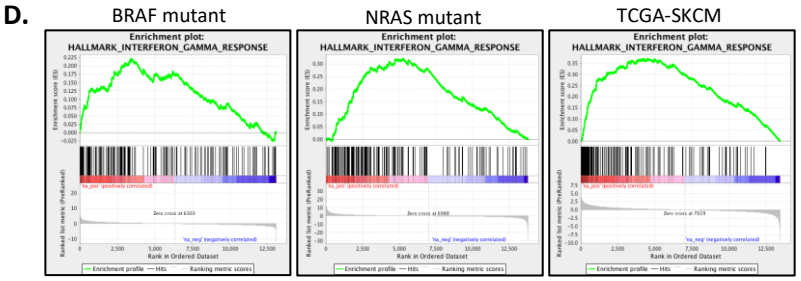

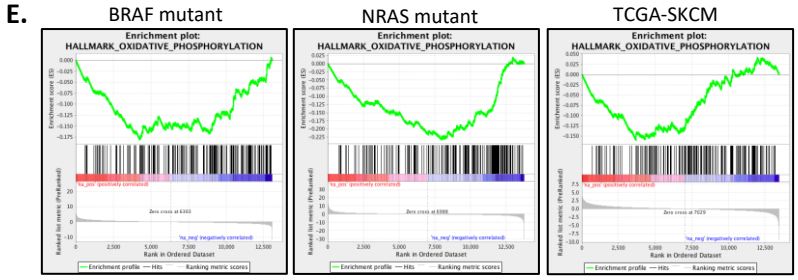

Figure 3: Bioinformatic Integrative Analysis of RAC1-P29S. A. GISTIC analysis of the TCGA-SKCM (FDR<0.25). *RAC1* is significantly amplified at the minimal common region (7p22.3) in Melanoma. **B.** Schematic of integrative analysis with the TCGA cohort and the GSEA outline through the comparison between DEG and TCGA **C.** Pathway enrichment plots showing Interferon-α Response Hallmark between TCGA and RNA-seq datasets. **D.** Pathway enrichment plots showing Interferon-γ Response Hallmark between TCGA and RNA-seq datasets. **E.** Pathway enrichment plots showing Oxidative Phosphorylation Hallmark between TCGA and RNA-seq datasets.

Table 2. List of Common Significant Pathways between RNA-Sequencing Data & TCGA-Skin Cutaneous Melanoma

GSEA pathways	Normalized Enrichment Scores (NES)		
	NRAS	BRAF	TCGA-SKCM
HALLMARK_INTERFERON_ GAMMA_RESPONSE	5.05	3.42	5.78
HALLMARK_INTERFERON_ ALPHA_RESPONSE	4.77	4.55	4.45
REACTOME_INTERFERON_SIGNALING	3.40	2.03	3.39
HALLMARK_OXIDATIVE_ PHOSPHORYLATION	-3.94	-2.90	-2.63
REACTOME_RESPIRATORY_ ELECTRON_TRANSPORT	-2.17	-3.07	-2.02
REACTOME_TCA_CYCLE_AND_RESPIRATORY_ ELECTRON_TRANSPORT	-2.14	-2.93	-2.06

4. Aim2: Delineating the Interactome of RAC1-P29S in Human Melanocytes

4.1 Unbiased Proteomic Analysis Identifies Proteins near RAC1-P29S

We complement the unbiased transcriptomic analysis with proteomic studies in hopes of gaining mechanistic insight into how RAC1-P29S promotes of melanoma progression. We employed the proximity-dependent biotin identification (BioID) method to identify novel interactors of the RAC1-P29S mutant. This approach utilizes a mutant *E. coli* biotin protein ligase (BirA*) tag to our control and RAC1 plasmids. BirA* biotinylates any protein in close range (~ 10 nm) to the tag (Fig.5A) [183, 184]. Proteins that have been biotinylated are isolated through affinity capture (Streptavidin-agarose beads) and sent for Mass Spectrometry (MS) analysis. This proximity-labeling method allowed us to gain insight into relevant protein-protein interactors to the P29S mutant in partially transformed melanocytes. Specifically, the BirA* tag (that also includes an additional Myc-tag), was conjugated to the N-terminus of eGFP and RAC1 WT, the P29S active and the T17N dominant negative mutants. Stable cell lines were generated in HMEL and PMEL-NRAS cells described above. After lentiviral infection and Blasticidin selection (10 µg/µl), we verified stable overexpression of the recombinant proteins and biotinylation levels in HMEL-BioID and PMEL-NRAS-BioID melanocytes (Fig.5B & C). One of the major goals of this

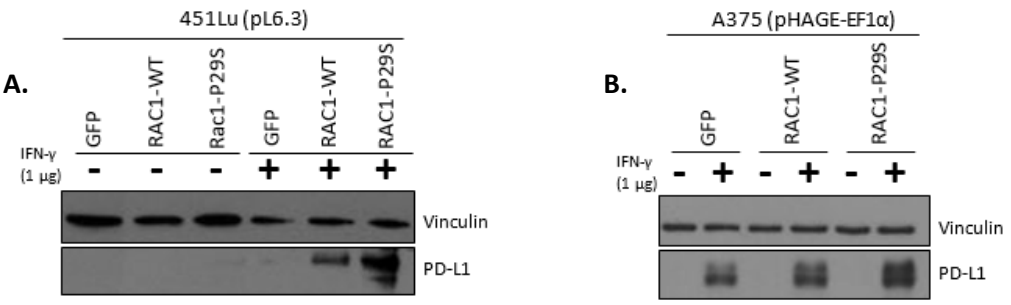

Figure 4: IFN-γ Induction Coordinates with RAC1-P29S for PD-L1 Upregulation. The immunoblots show levels of PD-L1 expression. **A.** 451Lu melanoma cell line overexpressing RAC1 (WT & P29S) and GFP were incubated with or without IFN-γ-supplemented media for 48 hours. **B.** A375 melanoma cell line overexpressing RAC1 (WT & P29S) and GFP were incubated with or without IFN-γ-supplemented media for 48 hours.

analysis is to characterize the RAC1 interactome in a disease-relevant system (*i.e.* melanocytes), and to identify P29S-specific interactors to provide mechanistic insight of this mutant.

We first focused our BioID analysis in the HMEL stable cell lines (eGFP, RAC1-WT, RAC1-P29S & RAC1-T17N) for the biotin affinity capture study [3]. For each cell line, four 15 cm plates of cells were pooled together, lysate protein concentrations were normalized to 12 μg/μl and incubated with Streptavidin-agarose beads. The beads were collected and sent for MS at the Université de Montreal MS core facility. The Scaffold 4.0 software was used to analyze our data where we elucidated a total of 362 proteins. We identified 50 biotinylated proteins that were found in RAC1-WT, P29S, or T17N mutants that were not identified in our eGFP negative control (Fig. 5D). Notably, 47 of the 50 biotinylated proteins were found in the P29S overexpressing HMEL cell line (Fig.5D & Table 3). Next, we performed GO term analysis to help categorize the interacting proteins that we observed, identifying a total of 18 Biological Processes (Fig.5E).

Notably, significant pathways identified in this analysis include proteins involved in the "Metabolic Process" (*e.g. TUFM* [185]), "Viral process" (*e.g. RUVBL1/2* [186]) and "Immune Process" (*e.g. CD99* [187]), which intersects with significant pathways identified in our unbiased transcriptomic analysis (Table 2). Importantly, as shown in Table 3, a total of 12 proteins were uniquely biotinylated by our BioID-RAC1-P29S construct. Furthermore, we observed 13 proteins that were biotinylated by both RAC1-WT and RAC1-P29S, and a total of 5 proteins by RAC1-P29S and the dominant negative RAC1-T17N.

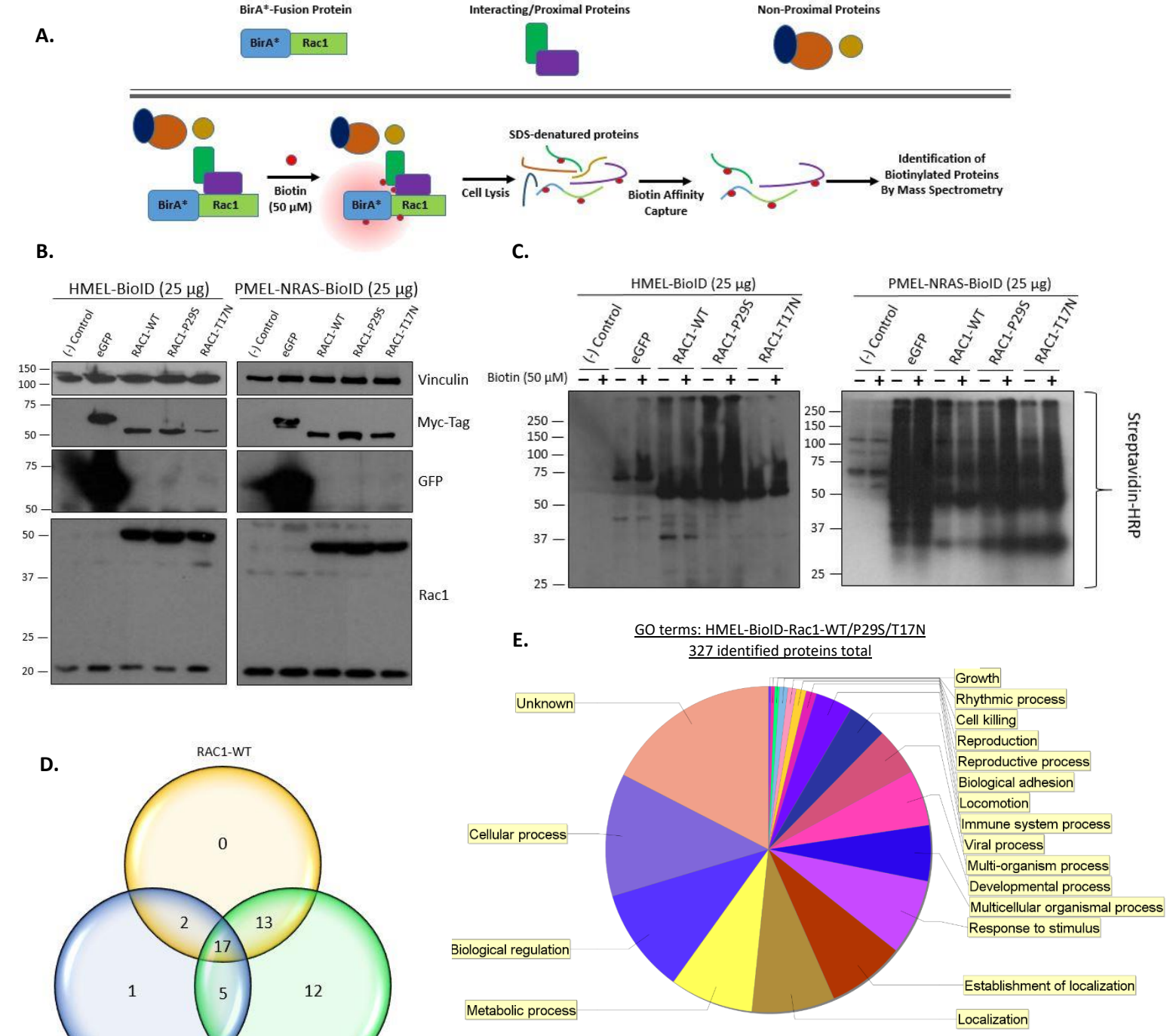

Figure 5: BioID Analysis of HMEL Melanocytes with RAC1-P29S Overexpression. A. Schematic diagram of the BioID system. **B.** Immunoblot of overexpressed constructs levels (eGFP, RAC1 WT, P29S, T17N) in stable HMEL-BioID and PMEL-NRAS-BioID cell lines. **C.** Validation of the biotinylation in the BioID system by immunoblotting with Streptavidin-HRP. **D.** A total of 362 proteins were identified. Venn diagram shows the number of proteins identified by Mass Spectrometry, excluding proteins affiliated with the BioID-eGFP sample**.** Scaffold 4.0 software was used for the identification analysis (exclusive unique peptide counts). Protein threshold (99%); Min. # peptide count (n=2); Peptide threshold (95%). **E.** GO terms (Biological process) for HMEL-BioID-RAC1-WT/P29S/T17N samples only, as determined from Mass Spec. data on the Scaffold 4.0 software.

Table 3. List of Proteins Identified by BioID/Mass Spectrometry Affiliated with RAC1-P29S

P29S only		WT-P29S		P29S-T17N		WT-P29S-T17N	
Identified Proteins (12)	**Gene ID**	**Identified Proteins (13)**	**Gene ID**	**Identified Proteins (5)**	**Gene ID**	**Identified Proteins (17)**	**Gene ID**
High mobility group protein HMGI-C	HMGA2	Thymopoietin, isoform CRA_c	TMPO	Emerin	EMD	Ras-related C3 botulinum toxin substrate 1	RAC1
cDNA FLJ61587, highly similar to Integrin α-1 (Fragment)	ITGA1	Catenin δ-1	CTNND1	Actin-related protein 2	ACTR2	Nucleolin, isoform CRA_b	NCL
Transitional endoplasmic reticulum ATPase	VCP	Vesicle-associated membrane protein 3	VAMP3	RuvB-like helicase	RUVBL1/2	Vacuolar protein sorting-associated protein 13C	VPS13C
Testicular secretory protein Li 63	UBE1	Torsin-1A-interacting protein 1	TOR1AIP1	Calpain small subunit 1 (Fragment)	CAPNS1	cDNA FLJ61290, highly similar to Neutral α-glucosidase AB	GANAB
cDNA, FLJ95650, highly similar to Homo sapiens karyopherin (importin) β 1 (KPNB1), mRNA	KPNB1	CD99 antigen	CD99	Rab GDP dissociation inhibitor	-	MHC class I antigen (Fragment)	HLA-A
Na+/ K+-transporting ATPase subunit α (Fragment)	-	SNARE protein Ykt6	YKT6			Integrin β	ITGB5
Solute carrier family 3 (Activators of dibasic and neutral amino acid transport), member 2, isoform CRA_e	SLC3A2	Synaptosomal-associated protein 23	SNAP23			Ribosomal protein S5, isoform CRA_a	RPS5
Methylenetetrahydrofolate dehydrogenase (NADP+ dependent) 1, methenyltetrahydrofolate cyclohydrolase, formyltetrahydrofolate synthetase, isoform CRA_a	MTHFD1	Receptor protein-tyrosine kinase	-			Testicular tissue protein Li 96	ITGA3
α-Adducin	ADD1	Synaptosomal-associated protein 29	SNAP29			Elongation factor Tu, mitochondrial	TUFM
Thrombospondin 1, isoform CRA_a	THBS1	MHC class I antigen (Fragment)	HLA-B			Vesicle amine transport protein 1 homolog (T californica), isoform CRA_a	VAT1
Guanine nucleotide binding protein (G protein), beta polypeptide 1, isoform CRA_a	GNB1	Signal recognition particle 9 kDa protein	SRP9			cDNA FLJ61188, highly similar to Basigin	BSG
cDNA, FLJ92825, highly similar to Homo sapiens SAR1a gene homolog 1 (S. cerevisiae) (SARA1), mRNA	SAR1A	Testis secretory sperm-binding protein Li 233m	ST13			Far upstream element-binding protein 2	KHSRP
		cDNA FLJ41945 fis, clone PLACE6019676, highly similar to Coatomer subunit γ	COPG			Splicing factor, arginine/serine-rich 2, isoform CRA_a	SFRS2
						Insulin-like growth factor 2 mRNA-binding protein 2	IGF2BP2
						Serine/arginine-rich-splicing factor 3	SRSF3
						60S ribosomal protein L9 (Fragment)	RPL9
						Leucine-rich repeat-containing protein 59	LRRC59

- Scaffold 4.0 software – Protein threshold (99%); Min.# peptide count (n=2); Peptide threshold (95%).

4.2 Identifying Direct Protein Interactors to RAC1-P29S

As a complementary approach to the BioID method, we utilized the NativePure Affinity Purification technique from Invitrogen to isolate native protein complexes, in hopes of identifying direct interactors of RAC1-P29S. First, we subcloned the CapTEV tag into the N-terminus of RAC1-WT, P29S and T17N and eGFP control expressing plasmids. This CapTEV portion includes a BioEase tag that only biotinylates our insert (e.g. RAC1 inserts or eGFP control), a 6XHis tag, and TEV cleavage sites (Fig.6A). For this experiment, only HMEL partially transformed melanocytes were used for lentiviral infection. After Blasticidin (10 µg/µl) selection, expression levels and biotinylation of recombinant protein were determined through immunoblotting (Fig.6B). Similar to the BioID method, four 15 cm plates for each cell line were pooled together, lysed through freeze-thaw cycles in order to preserve native protein complexes and normalized to 5 µg/µl. Once the beads were conjugated to biotinylated RAC1 (WT, P29S, T17N) or the eGFP control, they were washed several times, AcTEV protease was added to cleave the TEV cleavage sites, from which protein complexes were extracted and concentrated.

During the biotin affinity capture process using Streptavidin-agarose beads, several aliquots (50 µl) per sample were taken during the experiment in order to validate whether pulldown and cleavage of protein complexes occurred (Fig.6C). The first aliquot represents the lysate sample before being added to the column; the second aliquot is the eluate that hasn't bound to the Streptavidin-agarose beads after an incubation period; the third aliquot is the bead solution before adding the AcTEV protease; and the fourth aliquot is the bead solution after overnight cleavage by the AcTEV enzyme. Blotting for the His-tag was performed to validate the cleavage step, where protein complexes can only be detected when its CapTEV tag has been cleaved by AcTEV protease. Bands at 75 kDa in the first and second lanes represent impurities that didn't bind to the beads. In the last lane, the band at 50 kDa is most likely the AcTEV protease, which also contains a polyhistadine tag at its N-terminus. On the same lane, the band at 25 kDa band is the cleaved recombinant protein (eGFP or RAC1) (Fig.6C).

After concentrating the isolated protein complexes, 5 µl aliquots per sample were added to Bis-Tris 4-12% Criterion pre-cast gel. We silver-stained the gel to identify bands of interest, and

unique bands present in the P29S sample were excised and sent for MS for protein identification (Fig.6D). The same gel regions from the eGFP lane were also excised as a negative control for the MS analysis. Through the Scaffold software, MS identified a list of 55 proteins. For the selection process, several criteria were placed for precise identification to the corresponding excised gel bands. First, from the list of protein, any keratin-based or unknown/unidentified proteins were eliminated. Second, only proteins that were not present in the eGFP lane were selected. Third, proteins with or above 2 exclusive unique peptide counts were considered. Fourth, for more stringent selection, the identified protein's molecular weight must correspond to the gel piece's position in the gel and match with the molecular weight ladder used for the silver staining process. With this affinity purification method, we identified with 100% confidence two proteins that were found specifically in complex with RAC1-P29S: IQGAP1 (MW=189 kDa) and LAP2α (MW=75 kDa). These proteins are shown by the arrows in the silver staining gel (Fig.6D). Table 4 shows the list of ranked identified proteins that have at least passed the first 3 selection criteria, along with the different levels of confidence.

In summary, our proteomic interactome analysis has provided us with insight into possible mechanisms of action of the RAC1-P29S on observed oncogenic phenotypes in melanoma (*i.e. in vivo* melanoma growth). Specifically, our preliminary affinity capture experiment identified with 100% confidence two unique P29S interactors in IQGAP1 and LAP2α in HMEL partially transformed melanocytes. However, validation studies are needed to confirm the observed interactions from our proteomic studies presented here, and functional studies are needed establish the link between mutant RAC1 and our observed oncogenic phenotypes.

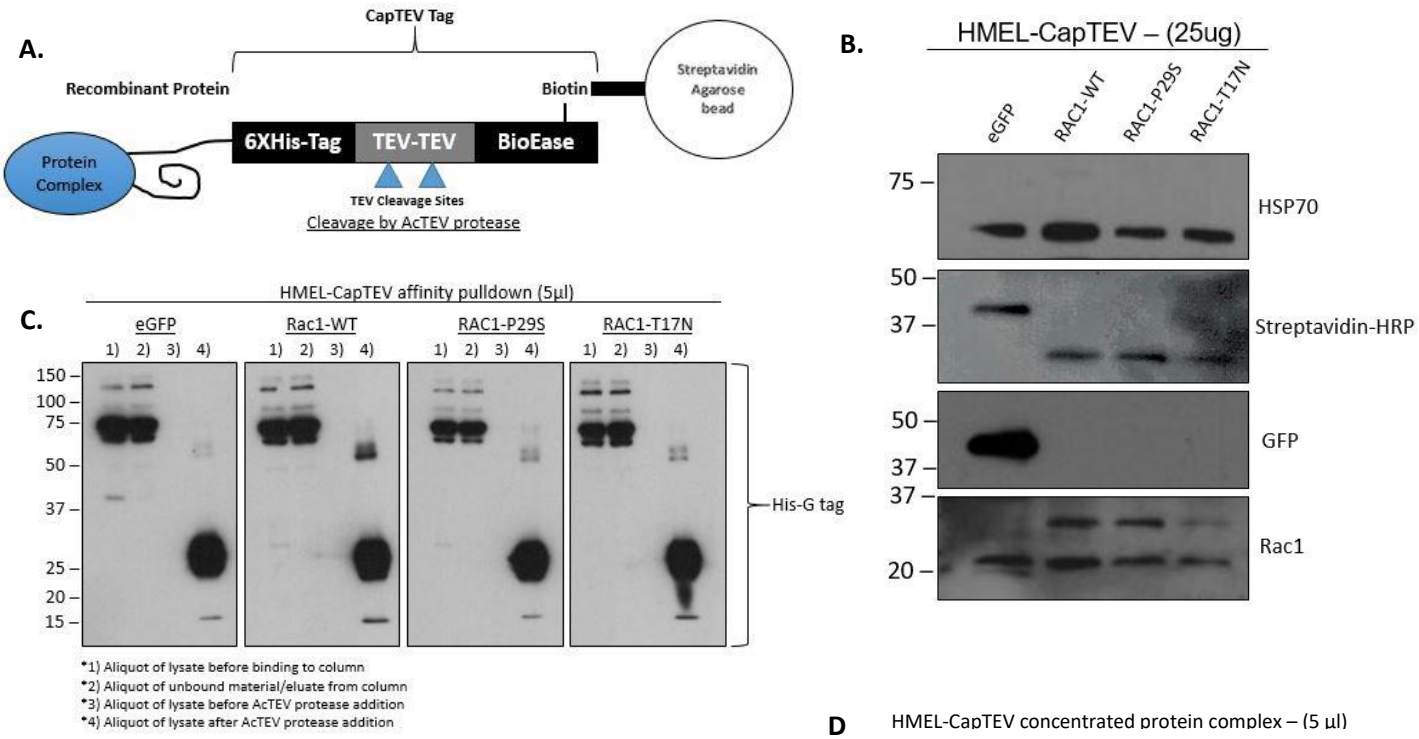

Figure 6: NativePure Affinity Complex Purification of HMEL Melanocytes with RAC1-P29S Overexpression. A. Schematic diagram of the Native Pure CapTEV system. **B.** Immunoblot of overexpressed constructs levels (eGFP, RAC1 WT, P29S, T17N) in generated stable HMEL-CapTEV cell lines. **C.** Validation of the protein complex affinity pulldown. Aliquots were taken before adding lysate to column, after elution of column, before and after addition of AcTEV protease. **D.** Silver staining of affinity purified protein complexes (5 µl) on a 4-12% Bis-Tris gradient gel. Arrows indicate protein bands identified with 100% confidence by Mass Spectrometry.

Table 4. List of RAC1-P29S Interactors Identified by Mass Spectrometry

Ranking	Identified Proteins	Alternate ID	MW (kDa)	# Exclusive unique peptide counts	Probability Rate	Commentary
1	Ras GTPase-activating-like protein IQGAP1	IQGAP1	189 kDa	7	> 95%	100% confidence - aligns to DNA ladder (above 150 kDa)
2	Lamina-associated polypeptide 2, isoform α	TMPO	75 kDa	7	> 95%	100% confidence - aligns to DNA ladder (right at 75 kDa)
3	14-3-3 protein σ	SFN	28 kDa	5	> 95%	Identified in band below 75 kDa
4	Calmodulin-like protein 5	CALML5	16 kDa	4	> 95%	Identified in band below 75 kDa
5	Protein S100	-	13 kDa	14	> 95%	Identified in band below 75 kDa
6	Protein S100-A8	S100A8	11 kDa	8	> 95%	Identified in band below 75 kDa
7	Bleomycin hydrolase	BLMH	53 kDa	3	80-94%	Identified in band below 75 kDa
8	Retroviral-like aspartic protease 1	ASPRV1	37 kDa	4	80-94%	Identified in band below 75 kDa
9	Fructose-bisphosphate aldolase (Fragment)	ALDOA	32 kDa	3	80-94%	Identified in band below 75 kDa
10	14-3-3 protein ζ/δ	YWHAZ	28 kDa	2	80-94%	Identified in band below 75 kDa
11	Insulin-degrading enzyme	IDE	118 kDa	3	80-94%	Identified in band below 75 kDa. Lower confidence due protein size
12	Enolase 1, (α), isoform CRA_a	ENO1	47 kDa	2	50-79%	Identified in band below 75 kDa
13	Glutamine synthetase	PIG59	42 kDa	2	50-79%	Identified in band below 75 kDa
14	Glyceraldehyde-3-phosphate dehydrogenase	GAPDH	36 kDa	2	50-79%	Identified in band below 75 kDa
15	cDNA FLJ57123, highly similar to Histidine ammonia-lyase (EC 4.3.1.3)	HAL	24 kDa	2	50-79%	Identified in band below 75 kDa
16	Filaggrin	FLG	435 kDa	2	50-79%	Identified in band below 75 kDa. Lower confidence due protein size
17	Triosephosphate isomerase (Fragment)	TPI1	27 kDa	2	20-49%	Very low confidence due to low probability percentage
18	L-lactate dehydrogenase A chain (Fragment)	LDHA	17 kDa	2	20-49%	Very low confidence due to low probability percentage

- Scaffold 4.0 software – Protein threshold (99%); Min.# peptide count (n=2); Peptide threshold (95%).

5. Summary of Results

The RAC1-P29S (c.85C>T) driver mutation is found in 5-10% of sun-exposed cases. It co-occurs with both *BRAF* and *NRAS* hotspot mutations. However, it is found at a higher frequency in BRAF/NRAS WT melanomas (Table 1). This activating mutation accelerates the GDP to GTP transition state. In addition to the P29S mutation, the TCGA-SKCM provisional study found 29 cases out of 287 patient samples that had *RAC1* alterations, where 20 samples had missense mutations [133, 134]. The P29S mutation accounted for 9 patient samples, while 4 had the P29L mutation, which wasn't previously identified in cutaneous melanoma. Alongside the confirmed activating missense P29S mutation, TCGA-provisional study identifies a total of 9 other somatic mutations in cutaneous melanoma (Fig.2A). Xenograft studies demonstrated that partially transformed melanocytes with oncogenic BRAF (HMEL cell line) or NRAS (PMEL-NRAS cell line) hotspot mutations overexpressing RAC1-P29S leads to increased melanoma progression as measured by tumor volume and shortened overall survival (endpoint of tumor burden of 1.5 cm) (Suppl.Fig.1).

This thesis focused on understanding the biological role of RAC1-P29S in melanoma by performing unbiased transcriptomic and proteomic analyses to gain insight as to how it mediates its oncogenic signaling. In our first aim, we demonstrated that other RAC1 mutants found in large sequencing studies, which included P29L and V14E, are activating, much like the P29S mutation (Fig.2B & C). Through our integrative unbiased transcriptomic and GSEA pathway analyses, we found that mitochondrial respiration and interferon signaling were deregulated in xenografts tumors formed by RAC1-P29S overexpression (Table 2). Validation experiments show that, upon IFN-γ induction, only melanoma cell lines with RAC1-P29S overexpression could express PD-L1, implying the involvement of mutant RAC1 in immune evasion (Fig.4). Overexpression of both RAC1-WT and P29S in a subset of melanoma cells lines led to decreased oxidative phosphorylation compared to controls (Suppl.Fig.6A-C). These results suggest that amplifications of RAC1 as seen in our genetic data may affect mitochondrial respiration. However, the increased pro-tumorigenic phenotype we observed with the P29S mutation in our *in vivo* studies might not be attributable to mitochondrial changes. This is based on the fact that we have observed little

difference between the WT and P29S-expressing melanoma cell lines (Suppl.Fig.6A-C). Furthermore, the GSEA pathway analysis determined EMT as a significantly altered pathway in the PMEL-NRAS xenografts tumors and TCGA-SKCM cohorts, making this a potentially relevant biological process to target (Suppl.Fig.3 & 5). These results are still preliminary, and future work will be required to clarify the role of RAC1 amplification and the P29S mutant in regulating mitochondrial respiration. Loss of function studies using either CRISPR/Cas9 or shRNAs in cell lines that have endogenous P29S mutations and amplification of RAC1 will be important in future studies.

In our second aim, our proteomic analyses identified RAC1 interacting proteins using two methods. Importantly, our preliminary analysis discovered unique RAC1-P29S-binding proteins. These included the IQGAP1 scaffolding protein and the LAP2α nuclear protein (Fig.6D). These results provide some mechanistic and biological insight into how RAC1-P29S promotes melanoma progression. This work is still preliminary and requires validation of findings presented here. Future work will include co-immunoprecipitation to validate interacting proteins. shRNA knockdown of RAC1-P29S-specific binding proteins will help elucidate which of these interactors is relevant for the oncogenic function of this hotspot RAC1 mutation. Our work will be helpful to the melanoma research community, where our findings could potentially aid in the development of novel therapeutic strategies to target melanoma and other cancer cases with mutant RAC1.

6. Discussion

6.1 Additional *RAC* Family Aberrations in Melanoma

Other amino acid changes have been reported at the proline 29 position in RAC2 that have been found in cancer cell lines. These include the RAC2-P29L and RAC2-P29Q activating mutants in the chronic myelogenous leukemia (CML) cell line KCL-22 and breast cancer cell line HCC1143, respectively. Thus, our work has the potential to be of utility in other cancers where mutations at this position in the Switch I region are found in other RAC family members [4].

GISTIC analysis of the melanoma TCGA dataset found *RAC1* amplifications along with 94 other genes that are co-amplified (*i.e.* are present in the minimal common region of amplification) (Fig.3A). Amplification of *RAC1* has been linked with resistance to chemotherapy and radiotherapy in HNSCC cell lines [188]. High-throughput screens using RNA interference (RNAi) to target commonly amplified genes in breast tumors that have acquired HER2-targeted therapy resistance also identified *RAC1* amplifications as the most important relevant mechanisms for resistance [189]. Interestingly, our mouse xenograft study has shown that in the BRAF and NRAS mutant model, overexpression of RAC1-WT displays different phenotypes (Suppl.Fig1E & F). In the xenografts models of partially transformed melanocytes with the BRAF mutation (HMEL), overexpression of RAC1 WT was oncogenic, but not to the same extent as P29S (Suppl.Fig1C & D). In the NRAS mutant partially transformed melanocytes (PMEL-NRAS), there RAC1-WT overexpression did not significantly increase tumor growth compared to the GFP control. This suggests that RAC1 may behave differentially depending on the genetic context. However, the lack of phenotype observed in the RAC1 WT overexpressing in PMEL-NRAS line may be due to the fact the PMEL-NRAS line forms tumors more readily. Thus, it is important for future studies to take into account genetic background of model systems studying RAC1, and to study co-operating affects with other known melanoma oncogenes and tumor suppressors.

6.2 Metabolic Role of RAC1 in Melanoma

Pathway analysis discovered oxidative phosphorylation to be the most downregulated pathways upon RAC1-P29S overexpression in xenograft and in the TCGA melanoma dataset (Table 2). In cutaneous melanoma, deregulation of the mitochondria has been reported. Metabolic rewiring is an established hallmark of cancer, where cancer cells have high bioenergetic demands, and thus display metabolic changes under oxygen- and nutrient-deprived conditions. The Warburg effect (*i.e.* aerobic glycolysis), is characterized by an increase in glucose uptake, low oxidative phosphorylation and increased glycolysis with higher production of lactate from glucose [190]. Melanomas express many genes that regulate cellular metabolism to generate energy and building blocks needed for tumor growth. Under normal oxygen conditions, glucose undergoes glycolysis to generate 2 ATP molecules and pyruvate, the latter of which enters the mitochondria where it is converted to Acetyl-CoA by pyruvate dehydrogenase and

further metabolized by the TCA cycle and oxidative phosphorylation, resulting in the production of 30 ATP molecules/glucose. The Warburg effect has been observed in many melanoma cell lines under hypoxic conditions, where glucose is converted to lactate [191]. Furthermore, the BRAF-V600E oncogenic mutation has been shown to decrease oxidative phosphorylation and promote glycolysis addiction [192-195]. In human melanomas resistant to vemurafenib, mitochondrial respiration levels were upregulated and mitochondrial superoxide production were increased upon drug exposure [196].

In metastatic cells, rapid proliferation into the ECM means that melanoma cells have high energetic demand and are characterized by the Warburg effect. In melanoma, in order to drive malignant transformation, mutations in MAPK pathway effectors regulate the expression of significant transcription factors that are associated with decreased oxidative phosphorylation, such as HIF1α, Myc and Microphthalmia-associated transcription factor (MITF) (reviewed in [195]). This is especially prevalent for BRAF mutant melanoma, which is important for metabolic rewiring by upregulating specific transcription factors (reviewed in [197]). Mutations in the MAPK pathway specifically mediate the expression levels of MITF, which has been associated with melanoma formation and metastasis [175, 198, 199]. MITF is a basic helix-loop-helix leucine zipper transcription factor that mainly upregulates transcription of genes involved in the regulation of lineage-specific pathway. MITF promotes the expression PCG1α, another transcription factor which in turn upregulates the expression of metabolic genes related to oxidative phosphorylation [199]. In addition, suppression of MITF is associated with invasion in cultured melanoma cells and in melanoma xenografts on immunocompromised mice [200, 201]. Bianchi-Smiraglia *et al.* has shown that MITF upregulates directly guanosine monophosphate reductase (GMPR), which partially depletes intracellular GTP pools, thus affecting the activation of GTPases [202]. Wawrzyniak *et al.* identifies GMPR as a melanoma invasion suppressor, where it is downregulated in metastatic melanoma [203]. This MITF-GMPR axis may be required for suppression of melanoma cell invasion, and could be downregulated in vemurafenib-resistant BRAF-V600E melanoma cells. We have preliminary data that suggests RAC1-WT and P29S overexpression in melanoma modulate MITF expression and activity. Thus, investigation of the mechanistic links between MITF and RAC1 remain an area of future investigation.

6.3 Immune Regulation in Melanoma

IFNs are cytokines that mediate antiviral and immunomodulatory effects in response to pathogens or tumor cells, with IFN-α classified in type I and IFN-γ in type II. Type I IFNs bind to IFN-α/β receptors (IFNAR), and are generally produced when the body detects viral infection. IFN-α is mainly produced by leukocytes and fibroblasts, and is mainly involved in innate immune response targeted against viral infection. In humans, IFN-γ is the only type II IFN, where they are released by T cells and natural killer cells and bind to IFN-γ receptor (IFNGR) complex to regulate immune and inflammatory responses. Both types of IFNs activate Janus kinase 1 (JAK1) and downstream signal transducer and activator of transcription 1 (STAT1) pathway, which leads to upregulation of IFN-stimulated genes (ISGs). These ISGs complex with one another to bind to IFN-stimulated response elements, inducing the expression of genes related to immune regulation and antiviral/antimicrobial response (reviewed in [204]).

RAC1 has known roles in regulating inflammation and the NF-κB signaling pathway, and we speculate RAC1-P29S regulation of these pathways may be important for melanoma progression [84, 85]. Studies have reported that metastatic melanomas exhibit high activation of NF-κB, which was shown to promote its progression [205]. Furthermore, constitutive NF-κB signaling was shown to upregulate the expression and release of various chemokines that act through autocrine and paracrine means (reviewed in [206]). Mouse melanoma cells that express chemokines and their receptors have demonstrated the ability to evade cytotoxic T-cells through PI3K signaling [207]. Recently, Shain *et al.* performed whole exome sequencing (WES) of 20 desmoplastic melanoma, a rare form of cutaneous melanoma with sarcomatous histology in CSD skin of elderly patients, and discovered recurrent hotspot promoter mutations in *NFKBIE* in ~15% of cases, altering the binding motif for several transcription factors (*e.g.* GABPA and ELF1) [208]. *NFKBIE* encodes for IκBε, which inhibits NF-κB signaling pathway by sequestering the NF-κB transcription factors in the cytoplasm. Immune checkpoint inhibitor proteins, such as PD-L1, were also shown to be dependent on NF-κB upon IFN-γ induction [179]. Whether RAC1 coordinates immune regulation and evasion through NF-κB or other immune checkpoint pathways is still unclear and will be investigated in future studies.

Furthermore, Park *et al.* has shown that RAC1 is required for maximal STAT protein activation in rat astrocytes stimulated by IFN-γ as overexpression of the T17N dominant negative mutation attenuated IFN-γ-mediated transcription and lowered phosphorylation of STAT1 and STAT3 [209]. This suggest that RAC1 may serve as a mediator of IFN signaling, consistent with results from our GSEA analysis. It is possible that overexpression of RAC1-P29S differentially expresses genes that are involved in IFN and STAT signaling to promote tumor growth and immunosuppression.

6.4 Mesenchymal Phenotype in Melanoma

Activated RAC1 signaling plays an essential role in EMT by promoting a migratory and invasive phenotype (*as mentioned in Section 1.6.3*). Pathway analysis found that EMT was upregulated when overexpressing RAC1-P29S in xenograft tumors and in the TCGA melanoma dataset, implying a role of RAC1-P29S in migration and invasion. However, this pathway was only significant (FDR<5%) in the xenograft tumors formed by PMEL-NRAS melanocytes and in the TCGA cohort (Suppl.Fig.3 & 5). Various studies have reported the switch from an epithelial to a mesenchymal phenotype in melanoma, where melanocytes acquire EMT-like features and metastatic properties (reviewed in [210]). Alonso *et al.* performed gene expression profiling of metastatic samples, showing that loss of E-cadherin and gain of N-cadherin and osteonectin were mainly associated with metastatic development [211]. Furthermore, this phenotype switching is characterized by the shift of many EMT transcription factors implicated in melanoma progression (reviewed [212]). For example, high expression levels of ZEB1 and TWIST1 transcription factors correspond with E-cadherin loss and metastatic progression [213]. In addition, Denecker *et al.* demonstrated that loss of ZEB2 leads to de-differentiation in melanocytes through MITF downregulation and concomitant upregulation of ZEB1 expression in melanoma cell lines [214]. MITF, which is identified as a lineage survival factor, acts as a melanoma differentiation marker in melanocytes, where it regulates melanocyte development and can promote invasiveness in melanoma [175, 200]. Studies by both Caramel *et al.* and Denecker *et al.* show that MITF downregulation is regulated by the expression of ZEB family members, which is consistent with previous work that have shown the role of MITF in phenotype switching [213, 214]. Therefore, loss of adhesion molecules, EMT transcription factor rearrangement and melanocyte

differentiation program alteration are critical steps for EMT in melanoma. Whether they are regulated by RAC1-P29S to promote the mesenchymal phenotype is still unclear. Future studies regarding the role of RAC1-P29S in metastasis include characterizing its migratory and invasive properties, looking into the histology of the xenograft tumors that overexpress either the WT or mutant form of RAC1 and determining the expression levels of EMT factors upon mutant RAC1 overexpression.

6.5 Targeting RAC1-P29S Signaling

The best characterized druggable target downstream of RAC1 are the PAK proteins. Interestingly, the PAK proteins were not identified in any of our proteomic analyses. However, aberrant PAK signaling has been implicated in various cancer types (*as mentioned in Section 1.6.2*), including melanoma. Babagana *et al.* demonstrated that in BRAF-mutant melanoma cell lines, PAK1 signaling correlated with resistance to BRAF and MEK inhibitors, while genetic and pharmacological suppression of PAK1 sensitized cells to both types of treatment [215, 216]. Furthermore, PAK1 activation in BRAF-mutant cells reactivated ERK signaling by phosphorylating CRAF and MEK for BRAF inhibitor acquired resistance. In response to BRAF/MEK inhibition, PAK1 phosphorylated the JNK and β-catenin bypassing ERK signaling [216]. Although not identified in our proteomic screens, the consensus from published studies is that targeting PAK proteins provides the best potential treatment for RAC1-mutant melanomas. For example, Araiza-Oliviera *et al.* show that use of conventional small-molecule RAC inhibitors (*e.g.* NSC23766) and PAK inhibitors (*e.g.* Frax-1036 and PF3758309) prevented aberrant embryonic development in zebrafish with RAC1-P29S expression and prevented ERK activation in melanoma cell lines, highlighting PAK signaling as an important pathway for acquired treatment resistance [217]. However, to date PAK inhibitors have all failed clinical trials due to toxicity [136]. Although, our proteomic analysis did not nominate PAK signaling as the key component for RAC1-P29S signaling in melanoma, future studies should examine new PAK inhibitors with reduced toxicity in RAC1 mutant melanomas in light of the known importance of these kinases in RAC signaling.

Furthermore, our proteomic analysis also failed to identify the GEF regulators as RAC1-P29S interactors. This finding is rather surprising, considering that both PIP3-dependent RAC

exchanger 1 & 2 (PREX1/2) have been implicated in melanoma. Ryan *et al.* show that in either BRAF- and NRAS-mutant melanomas, MAPK signaling drove aberrant PREX1 upregulation, leading to active RAC1-dependent invasion [218]. PREX2 was also found to be significantly mutated in melanoma, where it harbored either missense or truncating mutations [219]. Lissanu Deribe *et al.* demonstrated that PREX2 truncating mutations have increased RAC1 GEF activity and accelerated tumor development in NRAS-mutant melanomas [220]. While overexpression or oncogenic mutations in GEFs promote melanoma progression, it is unknown how they cooperate with RAC1-P29S. Despite not being identified by mass spectrometry, GEFs still play an essential role in RAC1-P29S melanomagenesis. Tomino *et al.* show that the DOCK1 GEF greatly accelerates the GDP/GTP exchange of RAC1-P29S [221]. In addition, both DOCK1 inactivation and pharmacological inhibition suppressed RAC1-P29S-mediated invasion and macropinocytosis, suggesting that DOCK1 is a critical regulator for RAC1-P29S-dependent malignant transformation. Future studies should investigate whether other regulators are important for RAC1-P29S activation and whether they can also be targeted for RAC1-mutant melanomas.

6.6 Mechanism of Action of RAC1-P29S in Melanoma

IQGAP1 has been shown to be upregulated in various tumors as well as amplified in several cancer cell lines (reviewed in [222]). In metastatic mouse melanoma cells selected from pulmonary metastases a ≥2.5-fold expression increase in IQGAP1 was observed [223]. Furthermore, IQGAP1 can form a complex with the RAC1-specific GEF, TIAM1, and downstream effector PAK6 [224, 225]. Interestingly, IQGAP1 is able to link RHO GTPase signaling with other cancer-related pathways, such as MAPK pathway. IQGAP1 can interact with several MAPK effectors, where ERK1/2 binds to the WW domain and MEK1/2 at the IQ motifs [226, 227]. IQGAP also interacts with BRAF through its IQ motifs, and Jameson *et al.* has shown that the IQGAP-MAPK pathway interaction contributes to vemurafenib resistance in BRAF-mutant mouse tumors [228, 229]. As mentioned previously, RAC1-P29S similarly confers resistance to BRAF inhibitors [3]. IQGAP1 has been identified as an important signaling scaffold regulating MAPK signaling in canine oral mucosal melanoma, an aggressive type of melanoma that does not harbour *BRAF* or *NRAS* mutations as seen in cutaneous melanoma [230]. Furthermore, CRISPR/Cas9 knockout of IQGAP1 significantly reduced MAPK activation and led to diminished cell proliferation. We

speculate that IQGAP1 may contribute to oncogenic transformation in melanoma by bridging RAC1-P29S and MAPK signaling. Future studies are required to validate IQGAP1 as a preferentially interacting protein of RAC1-P29S. We will also determine whether downregulation of IQGAP1 sensitizes RAC1-P29S mutant melanomas to BRAF-inhibitors.

In addition to IQGAP1, our native pure affinity complex purification and MS analysis identified LAP2α as a protein that preferentially binds RAC1-P29S. LAP2 proteins, which are also known as Thymopoietin (TMPO), exists in three alternative spliced isoforms of the *TMPO* gene (LAP2α, LAP2β and LAP2γ). These different LAP2 proteins are inner nuclear membrane (INM) proteins and are ubiquitously expressed in all cells, with LAP2α diffusely expressed across the nucleus due to the lack of a transmembrane domain, while LAP2β and LAP2γ are found on the nuclear membrane [231]. In the nucleoplasm, LAP2α binds directly during the early G1 stages of the cell cycle to intranuclear A-type lamins (Lamin-A), which is responsible for the structural outline of the nucleus [232]. However, lamins has been involved in many DNA-related cellular processes, where they anchor chromatin to the nuclear envelope for higher chromatin organization and regulate cell cycle dynamics (reviewed in [233]). While many studies show that RAC1 has a NLS sequence that allows it to bind to nuclear import proteins, it is still unknown as to what potential role RAC1 has in the nucleus of cancer cells, especially in the context of melanoma. Navarro-Lérida *et al.* demonstrated that RAC1 controls the morphology and organization of the nuclear membrane by regulating nuclear actin polymerization once it enters the nucleus [234]. Furthermore, this study suggested a balance between RHOA and RAC1, where nuclear RAC1 accumulation promotes an invasive phenotype by increasing cytoplasmic RHOA signaling [234]. Whether the LAP2α-RAC1-P29S interaction is important for RAC1 nuclear functions remains an unanswered question raised by the work presented here.

In addition to IQGAP1 and LAP2α, the native protein complex affinity purification experiment identified other proteins that may be important for oncogenic signaling of RAC1-P29S, potentially through IQGAP1 (Table 4). For example, MS identified proteins known to bind directly to IQGAP1, such as S100 proteins, which bind to the IQ motifs of IQGAP1 [235]. S100 proteins are a family of Ca^{2+} binding proteins of the EF-hand type that are expressed in a variety of cell types (reviewed in [236]). S100B is a marker for melanocytic tumors and is highly expressed in melanoma cells,

where it regulates the progression of cell cycle [237, 238]. In addition, S100 proteins can bind to other Ca^{2+} proteins, such as calmodulin, which also binds to the IQ motifs of IQGAP1 through Ca^{2+}-dependent and independent means [239, 240]. Calmodulin-like protein 5 (CALML5) is a calcium binding protein identified by MS and is the most expressed gene in the epidermis where it regulates their differentiation [241]. By comparing the DEGs between non-metastatic and metastatic cutaneous melanomas in a microarray analysis, Riker *et al.* shows that *CALML5* expression is decreased for metastatic samples [242]. In another large-scale high-throughput proteomic study, Huttlin *et al.* identified Calmodulin-like protein 3 (CALML3) as a novel binding protein to IQGAP1 [243]. Furthermore, 14-3-3σ/stratifin emerged from our MS analysis, which is encoded by *SFN* gene as another RAC1-P29S complex protein. Sun *et al.* performed MS and also identified 14-3-3σ/stratifin as a CALML5 binding protein, suggesting a CALML5-SFN epidermal differentiation axis [241]. High-pressure liquid chromatography tandem mass spectrometry identified the interaction between IQGAP1 and 14-3-3 proteins, which are mitotic proteins that are pivotal in regulating cell cycle advancements [244]. However, further validation studies are required to determine how IQGAP1 mediates these Ca^{2+}-related and cell-cycle proteins in melanomas harboring RAC1-P29S.

We utilized the Cytoscape 3.5 software that connects with public Interactome datasets, such as BioGRID and APID, to gain a better overall understanding of the putative RAC1-P29S interacting proteins identified by both the complex purification and the BioID methods (Suppl.Fig.7). This result suggested that there two hubs of interaction that centers on IQGAP1 and the valosin-containing protein (VCP) that have been reported to interact with many of the proteins identified in our RAC1-P29S proteomic studies. VCP was identified using the BioID approach, and interestingly, was also recently discovered as a novel direct interactor to IQGAP1 [245]. VCP is an ATPase enzyme that segregates proteins from larger cellular structures, where it is involved in protein quality control and has chromatin-associated functions [246, 247]. Yu *et al.* investigated the VCP interactome, and among the 288 proteins that immunoprecipitated with VCP, several were also identified through our proteomic analysis [248]. These include proteins encoded by *ADD1*, *CTNND1*, *SLC3A2*, *ST13*, *BSG*, *SRSF3* and *YWHAZ* (Table 3 & 4). Along with VCP, other nuclear proteins identified in the BioID analysis unique to RAC1-P29S were HMGA2 and

KPNB1. Transcriptome profiling performed by Raskin *et al.* found high mobility group AT-hook 2 (HMGA2) transcription factor as an important biomarker for melanoma progression, where it can localize to the nucleus via its NLS sequence by binding to importin-α2/KPNA2 [249]. RAC1 is also known to interact with KPNA2-KPNB1 to shuttle it to the nucleus. Thus, our proteomic analysis is suggestive that the nuclear role of RAC1-P29S may be worth examining in more detail [90].

We should note that there was a lack of concordance between the two proteomic approaches used here. Specifically, most of the proteins identified in the protein complex affinity capture and BioID are not found by both methods (Tables 3 & 4). As a result, validation studies of our proteomic findings will be paramount. However, many of the proteins we identified in this study are known RAC1-binding proteins giving us confidence that these methods may be complementary. Importantly, what was key to our study was identifying proteins that are found to complex preferentially with the RAC1-P29S mutant. Yet again, validation of these findings is compulsory. Whether these proteins similarly preferentially interact with other active forms of RAC1, such as the RAC1b active splice isoform, would also be of interest [167, 172, 250].

7. Methodology

1) Cell Lines:

Various cell lines were used in this project. Our lab has generated immortalized partially-transformed melanocytes of human origin, HMEL and PMEL-NRAS, that stably overexpress GFP and RAC1 (WT and P29S). Isogenic human melanoma cell lines with stable RAC1 overexpression include: A375-pHAGE (GFP, RAC1WT, RAC1-P29S), 451Lu-pL6.3 (GFP, RACWT, RAC1P29S) and MALME-3M-pHAGE (RAC1WT, RAC1P29S). Isogenic human immortalized melanocytes with BRAF-V600E mutation (HMEL) and NRAS-G12D mutation (PMEL-NRAS) were used to generate for lentiviral infection, where they would stably overexpress Myc-BioID-tagged and CapTEV-tagged constructs (eGFP, RAC1-WT, RAC1-P29S, RAC1-T17N). HEK293FT cell line (Thermo Fischer Scientific) was used for transfection experiments.

2) Plasmids and Cloning Methods:

* All plasmid constructs were sequence-verified using the McGill University and Genome Quebec Innovation Centre's sequencing services.

Obtained the pLENTI6.0/CapTEV-RAC1-WT & RAC1-P29S plasmids, which were made as described in *Watson et al. 2014* [3]. Constructed the pLENTI6.0/CapTEV-eGFP plasmid by PCR amplifying an eGFP insert sequence, DNA purifying with the GeneJet Gel Extraction Kit (Thermo Fischer Scientific) and subcloned into pDONR223 vector (Invitrogen). Using the Invitrogen NativePure Lentiviral Gateway Vector kit, subcloning into pLENTI6.0/CapTEV-NT-DEST1 (Invitrogen) was performed. The pLENTI6.0/CapTEV-RAC1-T17N plasmid was made by using the Quick-Change Lightning Site-Directed Mutagenesis (Agilent Technologies), as described in their protocol. The primers used for eGFP amplification (no start codon + attb sites) are the forward sequence (5'–GGGGACAACTTTGTACAAAAAAGTTGGCGTGAGCAAGGGCGAGGAGCTG–3') and the reverse sequence (5'–GGGGACAACTTTGTACAAGAAAGTTGGGTTACTTGTACAGCTCGTCCATGCC–3'). The primers used for of site-directed mutagenesis RAC1-T17N are the forward sequence (5'–TGGGAGACGGAGCGCCTACTGATCAG–3') and the reverse sequence (5'–CTGATCAGTAGGCGCTCCGTCTCCCA–3').

We received the pcDNA3-eGFP-RAC1-WT, along with the other pcDNA3 vectors containing mutant RAC1 (V14E, P29S, P29L, P34S, S71F, P87L, N92K and P140L) conjugated to eGFP sequence. Using the Quick-Change Lightning Site-Directed Mutagenesis (Agilent Technologies), vector with RAC1 mutations c.93A>T (E31D) was generated. Primers used are the forward sequence (5'–CCAATGCATTTCCTGGAGATTATATCCCTACTGTCTTTG–3') and the reverse sequence (5'–CAAAGACAGTAGGGATATAATCTCCAGGAAATGCATTGG–3').

XhoI and BamHI restriction enzyme sites were added to the RAC1-WT/P29S/T17N and eGFP inserts, which were later ligated into the pGEM-T-Easy Vector System (Promega) and subcloned into the pcDNA3.1-myc-BioID vector (Addgene), which was given to us by Dr. Luke McCaffrey's lab (Goodman Cancer Research Centre, Experimental Medicine Department, McGill University, Montreal, Quebec, Canada). Amplification of inserts along with Myc-BioID tags were extracted with the GeneJet Gel Extraction Kit. Subcloning was done by Invitrogen Gateway Technology to pDONR223 (Invitrogen), then into pLENTI6.3-CMV (Invitrogen). Primers used for the addition of restriction enzymes sites (XhoI and BamHI) are the forward sequences ((eGFP) 5'–GCCGAACTCGAGGTGAGCAAGGGCGAGGAGCTG–3') and ((RAC1) 5'–GCCGAACTCGAGCAGGCCATCAAGTGTGTGGTG–3'); and the reverse sequences ((eGFP) 5'–GCCGAAGGATCCTTACTTGTACAGCTCGTCCAT–3') and ((RAC1) 5'–GCCGAAGGATCCTTACAACAGCAGGCATTTTCT–3'). The primers used for the amplification of the BioID tags with the inserts (no start codon + attb sites) are the forward sequence (5'–GGGGACAAGTTTGTACAAAAAAGTTGGCGCCACCATGGAACAAAAACTCATCTCA–3') and the reverse sequences ((eGFP) 5'–GGGGACCACTTTGTACAAGAAAGTTGGGTTACTTGTACAGCTCGTCCAT–3') and ((RAC1) 5'–GGGGACCACTTTGTACAAGAAAGTTGGGTTACAACAGCAGGCATTTTCT–3').

3) Lentivirus Production and Stable Cell Line Generation:

The pL6.0/CapTEV (eGFP/RAC1-WT/RAC1-P29S/RAC1-T17N) and pL6.3-BioID eGFP/RAC1-WT/RAC1-P29S/RAC1-T17N constructs were used for lentiviral transduction. Lentiviruses were produced in 293FT cells and were used to stably infect immortalized partially-transformed human HMEL and PMEL-NRAS melanocytes at 48h and 72h after transfection in the presence of 10 µg/mL polybrene (Sigma-Aldrich). Target infected cells were selected for with 10 µg/ml

Blasticidin S HCl (Invitrogen) for 6 days. The stable cell lines generated are HMEL-CapTEV (eGFP/RAC1-WT/RAC1-P29S/RAC1-T17N), HMEL-BioID & PMEL-NRAS-BioID (eGFP/RAC1-WT/RAC1-P29S/RAC1-T17N).

4) Cell Culture and Transient transfection:

The HEK293FT cell line was maintained with DMEM (High Glucose w/L-glutamine, Na-Pyruvate) medium (Wisent Bioproducts) supplemented with 10% Fetal Bovine Serum (FBS; Wisent Bioproducts). Transient transfection was performed with linear polyethylenimine (PEI) MW 25,000 (Polyscience Inc.). The A375, 451Lu and MALME-3M melanoma cell lines, as well as HMEL and PMEL-NRAS melanocytes were maintained with RPMI1640 medium (Wisent Bioproducts) supplemented with 5% FBS (Wisent Bioproducts) and 1% Penicillin-Streptomycin (10,000 U/ml) (Gibco, Life Technologies). All cell cultures were incubated at 37°C in a humidified 5% CO_2 incubator.

5) Mouse Xenograft & Unbiased Analyses Studies

For our xenograft studies, our lab used partially transformed HMEL and PMEL-NRAS melanocytes that stably express GFP and RAC1 (WT and P29S). These cells were injected into NCR-nude mice for xenograft assays, as previously described in *Watson et al. 2014* [3]. After formation of xenograft tumors, survival end points were measured when the length reached 15mm or when there was visible evidence of ulceration and tumor volume was measured bi-weekly and calculated with the formula: $volume = 0.5 \times [length \times (width)^2]$. Mann-Whitney non-parametric tests were used for significant differences in tumor volume, while Log-rank (Mantel-Cox) tests were used for significant differences in survival. Xenograft tumors were then excised (HMEL: n=3 ; PMEL-NRAS: n=5) and sent for RNA-seq analysis using the Illumina HiSeq 2000 platform to determine all RNA expression changes [3].

6) Immunoblotting and RAC1 PBD Pulldown Assay

After growing to 80-90% confluency in 10cm plates, cells were lysed with RIPA buffer (Thermo Fischer Scientific) supplemented by 1X Halt-Protease Inhibitor Cocktail (Thermo Fischer Scientific). Cell lysates were cleared by centrifugation and protein concentrations were

determined by DC Protein Array (Bio-Rad). Denatured lysates underwent SDS-PAGE, where they were run on 10% Tris gels, which were then transferred to nitrocellulose membranes (Bio-Rad). The blots were blocked with 5% milk in PBS-T, followed by appropriate primary and secondary antibody incubation. Blots were imaged through enhanced chemiluminescence (Thermo Fischer Scientific & GE Healthcare).

For RAC1 activation assays were performed as previously described in *Hodis et al. 2012*, and according to the manufacturer's protocol (Cell Biolabs) [1]. Antibodies used for immunoblotting includes: α-Vinculin (1/10,000; Abcam – #ab18058), α-GFP (1/5000; Clontech – #632381), α-RAC1 (1/1000; Cell Biolabs – STA-401-1, Part. #240106), α-Myc Tag (1/2000; Cell Signaling Technology – #2276), Streptavidin-HRP (1/2500; Thermo Fischer Scientific – #434323), α-HSP70 (1/1000; Cell Signaling Technology – #4872), α-His-G Tag (1/5000; Invitrogen – #R940-25), α-PD-L1 (E1L3N)-XP (1/1000; Cell Signaling Technology – #13684).

7) Bioinformatic Analysis

* All figures generated for this bioinformatic analysis were used in the R package.

The GISTIC 2.0 software was used to identify and localize genes with focal somatic copy number alterations (SCNAs) in the TCGA-SKCM dataset that promote cancer development and growth. SCNA profiles were separated into underlying arm-levels and focal alterations, allowing to estimate background rates for each category and define boundaries of different SCNA regions. An FDR q-values<0.25 was set for peak region significance.

From the RNA-seq data, by comparing HMEL and PMEL-NRAS xenograft tumor samples overexpressing GFP or RAC1-P29S, differentially expressed genes (DEG) were identified with the DESeq software and ranked with an FDR<5%. Then from the GSEA software, 497 reactome and hallmark gene sets were used for pathway analysis on the list of ranked genes. Significant pathways were determined through normalized enrichment scoring (NES) with an FDR<5%, from which GSEA enrichment plots were generated. The plots also indicate the number of genes that are de-regulated per pathway through quantitative size values. Results were integrated with the TCGA-SKCM dataset (RAC1 mutant (N=23) vs RAC1-WT amplification (N=15)), which also underwent the same form of analysis (DEG & GSEA).

8) Affinity Capture of Biotinylated Proteins

Four 15cm plates per generated stably expressing HMEL-BioID melanocytes (eGFP/RAC1-WT/RAC1-P29S/RAC1-T17N) were incubated for 24h in 50µM Biotin-supplemented media. Cells were washed 3 times in PBS, pooled together per sample and lysed in RIPA buffer supplemented with 1X Halt-Protease Inhibitor Cocktail (Thermo Fischer Scientific). Lysates were sonicated on ice at 30% amplitude (3 x 10 second bursts with 2 second rest in between) and centrifuged at 20,850g. Once protein concentration was determined with the DC Protein Array (Bio-Rad) and normalized to 12 µg/µl, lysates were incubated for 3h with Streptavidin-Agarose beads (Invitrogen). Beads were collected by centrifugation (400g for 1 minute), washed 3 times with RIPA buffer, 3 times with NETN buffer and 5 times with Milli-Q water. Beads were sent for Mass Spectrometry (MS) analysis

9) Affinity Purification of Protein Complex

The generated stably expressing HMEL-CapTEV melanocytes (eGFP/RAC1-WT/RAC1-P29S/RAC1-T17N) were grown in 15cm plates. The NativePure Mammalian Affinity Purification (Invitrogen) kit was then performed, as described by the manufacturer. After determining the protein concentration with the DC protein array (Bio-Rad), lysates were normalized to 5 µg/µl. Once the eluted protein complexes were concentrated and isolated, 5 µl aliquots per sample was run on a Criterion XT Bis-Tris 4-12% gradient pre-cast gel (Bio-Rad). The gel was-stained with the Pierce Silver Stain for Mass Spectrometry Kit (Thermo Fischer Scientific). Bands of interest were excised from the gel, de-stained and sent for their MS analysis.

10) Mass Spectrometry:

Samples for the BioID and NativePure protein complex pulldown assays were sent to the *Institut de Recherche en Immunologie et en Cancérologie* (IRIC) at the University of Montreal for their Mass Spectrometry facility services. MS data was analyzed through the Scaffold 4.0 software, where exclusive peptide count and total spectrum count results were used for protein identification and abundance. GO term analysis on the Scaffold 4.0 software was also performed for BioID samples. Through the Cytoscape 3.5 software, we used the BioGRID and APID

Interactome databases to determine whether there are already known interactions that were observed between the proteins identified by MS.

11) Mitochondrial Respiration Analysis:

The isogenic A375, 451Lu and MALME-3M melanoma cell lines that stably overexpress GFP, RAC1-WT and RAC1-P29S were used for this Seahorse Mitochondrial Respiration experiment. Mitochondrial respiration was monitored in real time with the Seahorse Bioscience Extracellular Flux Analyzer (XF96; Seahorse Bioscience). Oxygen consumption rate (OCR) and extracellular acidification rate (ECAR) were measured in this study. The Wave 2.4 software was used to analyze the seahorse data.

12) Interferon-γ Induction

The isogenic melanoma cell line 451Lu & A375 that stably overexpresses RAC1 (WT and P29S) and GFP was incubated with complete media supplemented with 1 µg of human IFN-γ (Shenandoah Biotechnology) for 48h at 37°C, as described in *Gowrishankar et al. 2015* [179]. Cells were then lysed with RIPA buffer supplemented with 1X Halt-Protease Inhibitor Cocktail (Thermo Fischer Scientific) for immunoblotting.

8. Supplementary Data

1) Increased Tumorigenesis of Partially Transformed Melanocytes Overexpressing RAC1-P29S in Xenograft Assays.

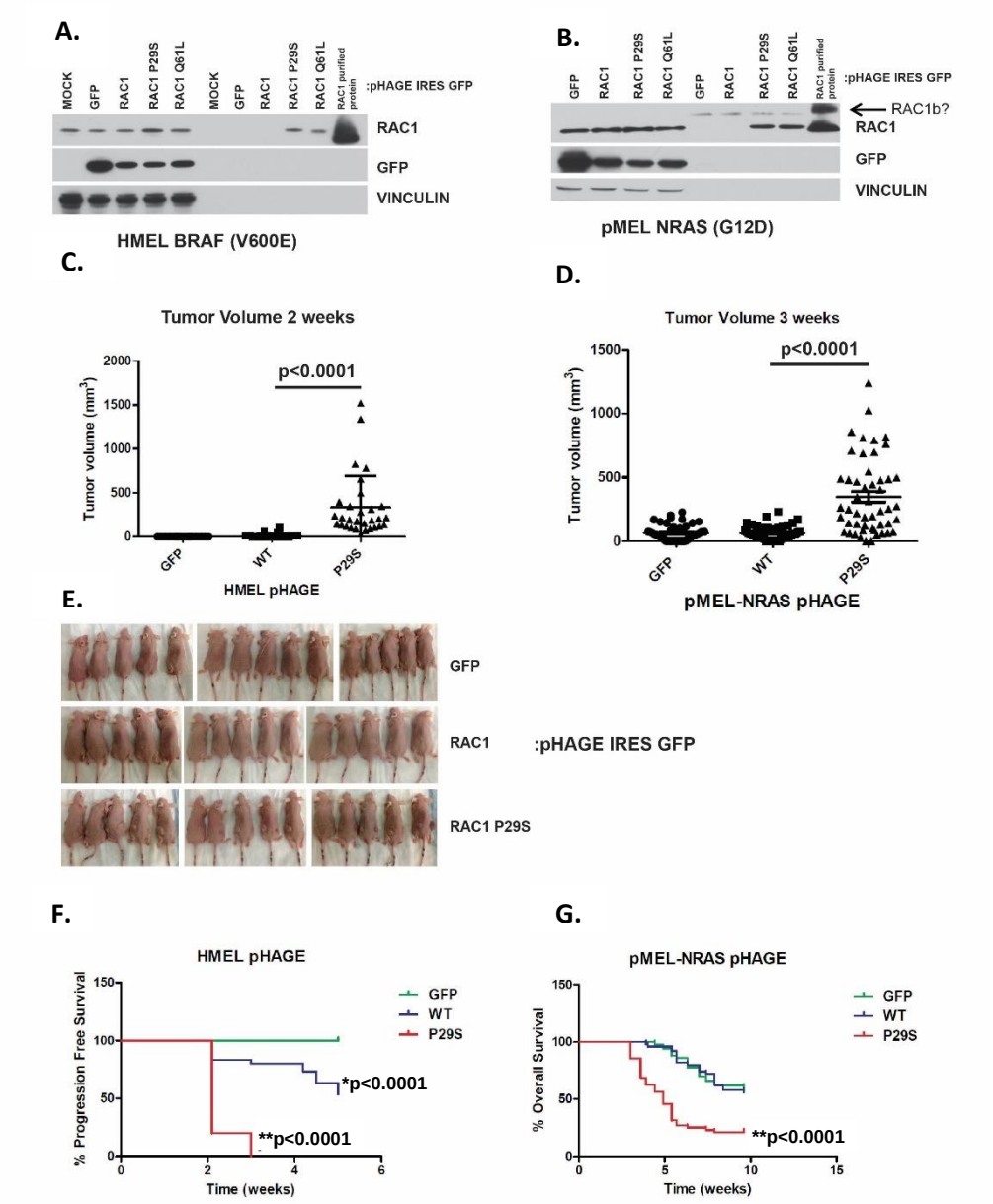

Supplementary Figure 1: A-B. Partially transformed melanocytes HMEL and PMEL-NRAS that stably overexpresses RAC1 (WT, P29S & Q61L) and GFP were lysed and underwent PAK-PBD pulldown assay, isolating RAC1 active state. Immunoblot analysis of RAC1 levels was then performed. **C-D.** Xenograft tumors formed by HMEL and PMEL-NRAS melanocytes with stably overexpressing RAC1 (WT & P29S) and GFP were excised (4.5 weeks and 3 weeks respectively) and their tumor volume was measured. Significance was determined through Mann-Whitney nonparametric tests. **E.** Images of the nude mice cohorts for each sample group used for tumor burden analysis. **F-G.** The Kaplan-Meier survival curves for mice with xenograft tumors formed by HMEL and PMEL-NRAS overexpressing RAC1 (WT & P29S) and GFP. Significance was determined through Log-rank (Mantel-Cox) tests. (*p = GFP vs RAC1-WT; **p = RAC1-WT vs RAC1-P29S)

2) Differentially Expressed Gene Analysis for *BRAF*/*NRAS*-mutant Xenograft and TCGA – Skin Cutaneous Melanoma Data.

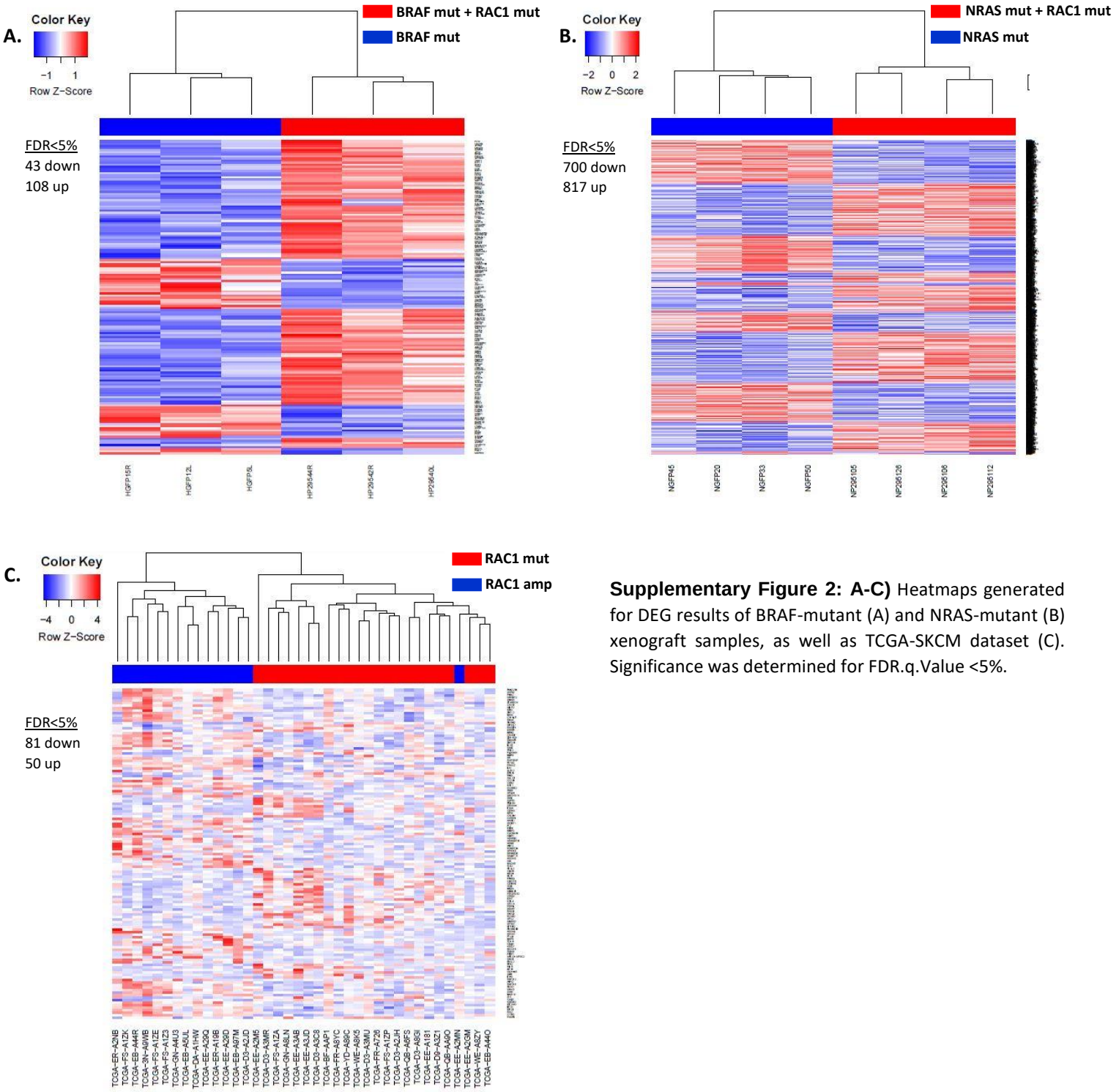

Supplementary Figure 2: A-C) Heatmaps generated for DEG results of BRAF-mutant (A) and NRAS-mutant (B) xenograft samples, as well as TCGA-SKCM dataset (C). Significance was determined for FDR.q.Value <5%.

3) GSEA Enrichment Plot for NRAS-mutant Melanocytes with RAC1-P29S Overexpression.

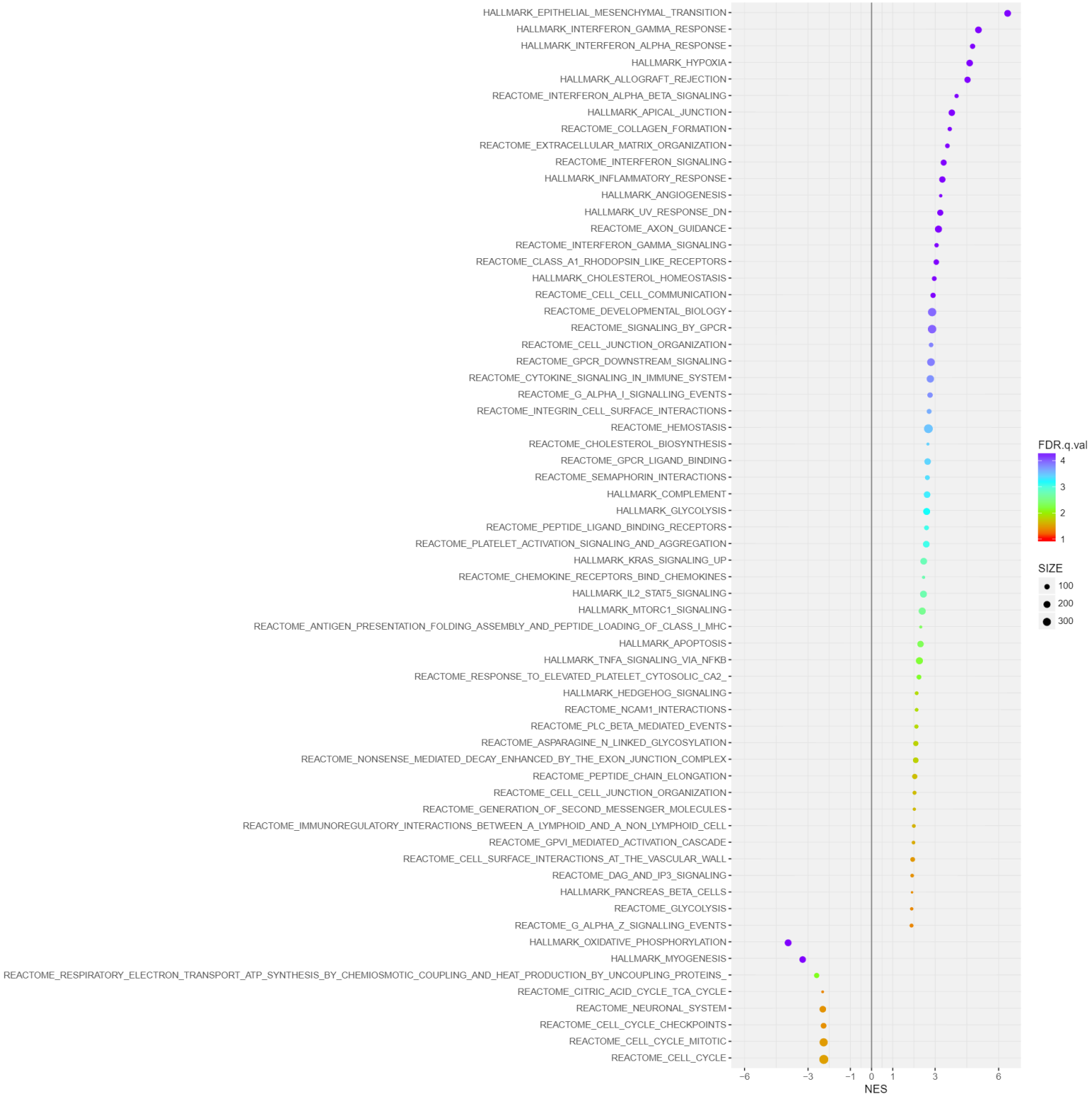

Supplementary Figure 3: GSEA enrichment plots for RAC1-WT vs RAC1-P29S in the NRAS mutant melanocyte cohort. A total of 258 Reactome and Hallmarks gene sets were identified with an FDR.q.Value <5%.

4) GSEA Enrichment Plot for BRAF-mutant Melanocytes with RAC1-P29S Overexpression.

Supplementary Figure 4: GSEA enrichment plots for RAC1-WT vs RAC1-P29S in the BRAF mutant melanocyte cohort. A total of 278 Reactome and Hallmarks gene sets were identified with an FDR.q.Value <5%.

5) GSEA Enrichment Plot for TCGA-SKCM Samples with RAC1-P29S Overexpression.

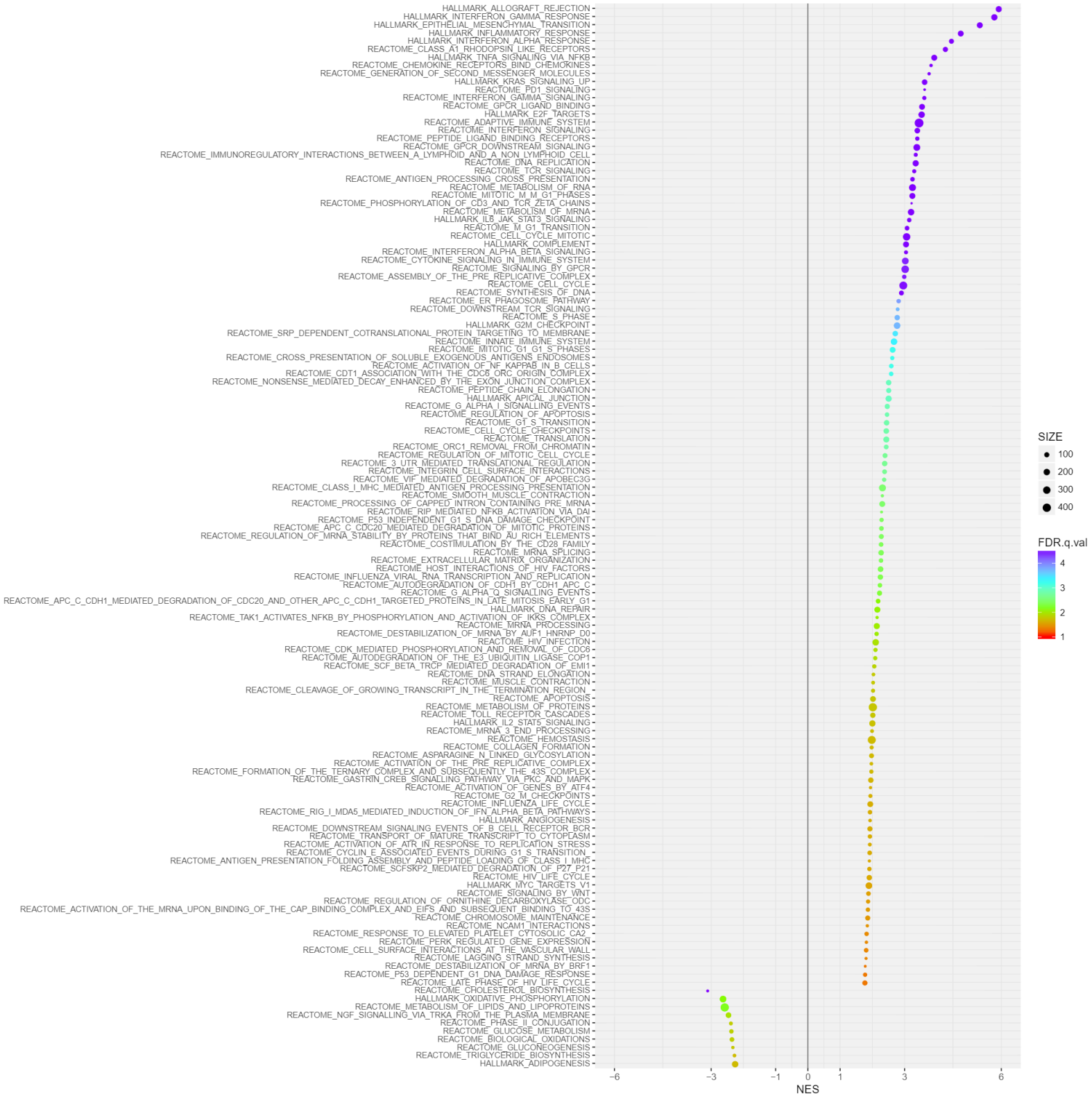

Supplementary Figure 5: GSEA enrichment plots for RAC1-WT (amplification) vs RAC1-P29S in the TCGA-SKCM cohort. A total of 323 Reactome and Hallmarks gene sets were identified with an FDR.q.Value<5%.

6) Mitochondrial Respiration – Effects of RAC1-P29S on Oxidative Phosphorylation.

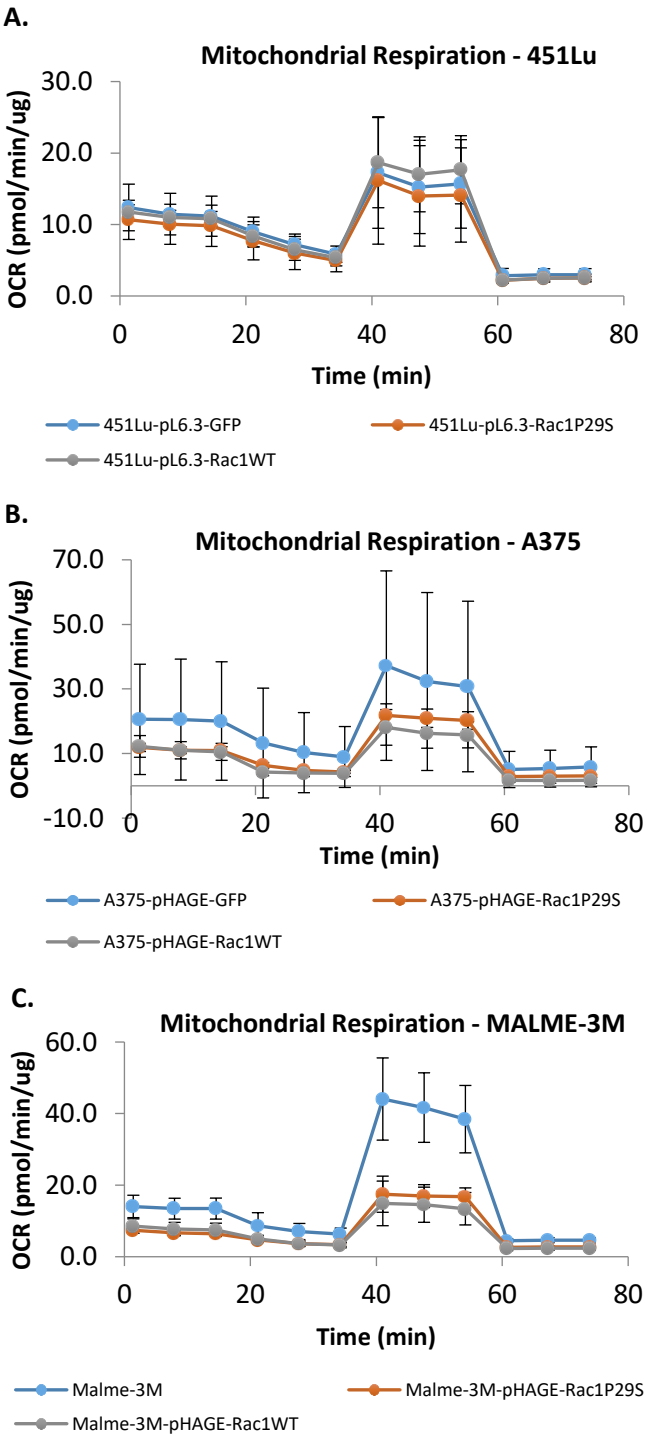

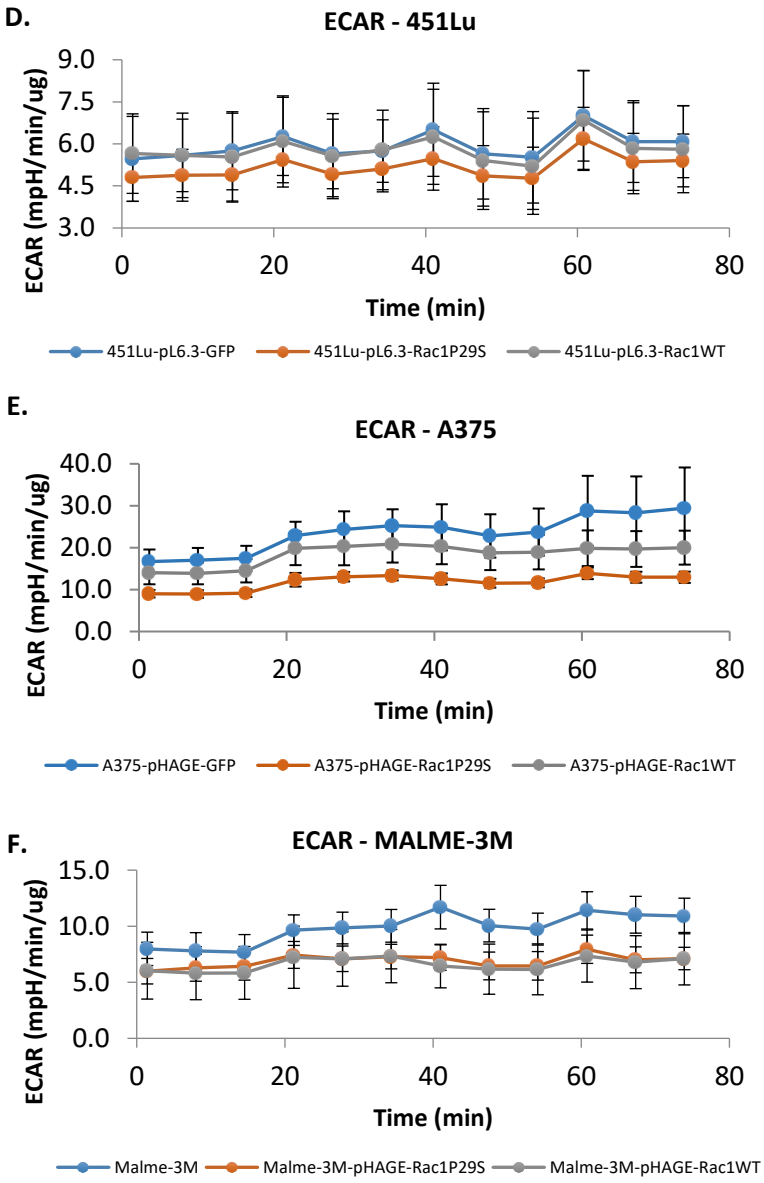

Supplementary Figure 6: A-C) Normalized measurements of Oxygen Consumption Rate (OCR) for 451Lu, A75 and MALME-3M melanoma cell lines that stably overexpress RAC1 (WT & P29S) and GFP. **D-F)** Normalized measurements of extracellular acidification rate (ECAR) for 451Lu, A75 and MALME-3M melanoma cell lines that stably overexpress RAC1 (WT & P29S) and GFP.

Measurements for all graphs (**A-F**) were done by Seahorse Bioscience Extracellular Flux Analyzer and analyzed by the Wave 2.4 software.

7) RAC1-P29S Interactome Characterization through Public Databases.

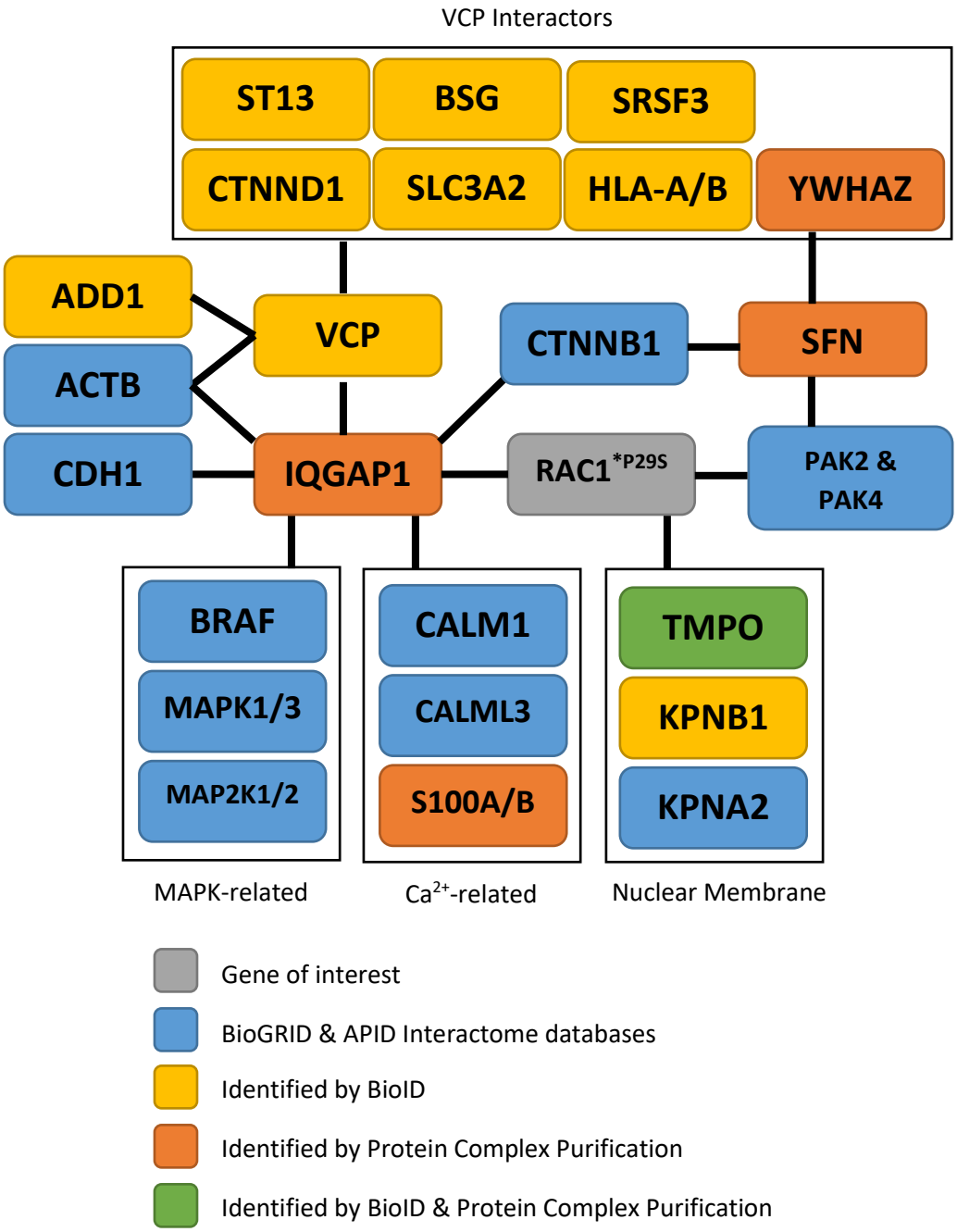

Supplementary Figure 7: Schematic of the direct interactions between proteins that were identified through BioID and protein complex affinity purification. The gene names are displayed in this schematic. The Cytoscape 3.5 software was used to verify protein interactions, by using public BioGRID and APID Interactome databases as references.

9. References

1. Hodis, E., et al., *A landscape of driver mutations in melanoma.* Cell, 2012. **150**.
2. Krauthammer, M., et al., *Exome sequencing identifies recurrent somatic RAC1 mutations in melanoma.* Nat Genet, 2012. **44**.
3. Watson, I.R., et al., *The RAC1 P29S hotspot mutation in melanoma confers resistance to pharmacological inhibition of RAF.* Cancer research, 2014. **74**(17): p. 4845-4852.
4. Kawazu, M., et al., *Transforming mutations of RAC guanosine triphosphatases in human cancers.* Proc Natl Acad Sci U S A, 2013. **110**(8): p. 3029-34.
5. Bastian, B.C., *The molecular pathology of melanoma: an integrated taxonomy of melanocytic neoplasia.* Annual Review of Pathology: Mechanisms of Disease, 2014. **9**: p. 239-271.
6. Balch, C.M., et al., *Final Version of 2009 AJCC Melanoma Staging and Classification.* Journal of Clinical Oncology, 2009. **27**(36): p. 6199-6206.
7. Linos, E., et al., *Increasing Burden of Melanoma in the United States.* Journal of Investigative Dermatology, 2009. **129**(7): p. 1666-1674.
8. Garibyan, L. and D.E. Fisher, *How Sunlight Causes Melanoma.* Current Oncology Reports, 2010. **12**(5): p. 319-326.
9. Taylor, J.S., *Biomolecules. The dark side of sunlight and melanoma.* Science, 2015. **347**(6224): p. 824.
10. Brash, D.E., *UV signature mutations.* Photochem Photobiol, 2015. **91**(1): p. 15-26.
11. Whiteman, D.C., et al., *Melanocytic nevi, solar keratoses, and divergent pathways to cutaneous melanoma.* J Natl Cancer Inst, 2003. **95**(11): p. 806-12.
12. Girotti, M.R., et al., *No longer an untreatable disease: How targeted and immunotherapies have changed the management of melanoma patients.* Molecular Oncology, 2014. **8**(6): p. 1140-1158.
13. Hodis, E., et al., *A Landscape of Driver Mutations in Melanoma.* Cell, 2012. **150**(2): p. 251-263.
14. Krauthammer, M., et al., *Exome sequencing identifies recurrent somatic RAC1 mutations in melanoma.* Nat Genet, 2012. **44**(9): p. 1006-1014.
15. Davis, M.J., et al., *RAC1P29S is a spontaneously activating cancer-associated GTPase.* Proc Natl Acad Sci U S A, 2013. **110**(3): p. 912-7.
16. Didsbury, J., et al., *rac, a novel ras-related family of proteins that are botulinum toxin substrates.* J Biol Chem, 1989. **264**(28): p. 16378-82.

17. Haataja, L., J. Groffen, and N. Heisterkamp, *Characterization of RAC3, a novel member of the Rho family.* J Biol Chem, 1997. **272**(33): p. 20384-8.
18. Knaus, U.G., et al., *Purification and characterization of Rac 2. A cytosolic GTP-binding protein that regulates human neutrophil NADPH oxidase.* J Biol Chem, 1992. **267**(33): p. 23575-82.
19. Haeusler, L.C., et al., *Purification and biochemical properties of Rac1, 2, 3 and the splice variant Rac1b.* Methods Enzymol, 2006. **406**: p. 1-11.
20. Haeusler, L.C., et al., *Comparative functional analysis of the Rac GTPases.* FEBS Lett, 2003. **555**(3): p. 556-60.
21. Grizot, S., et al., *Crystal structure of the Rac1-RhoGDI complex involved in nadph oxidase activation.* Biochemistry, 2001. **40**(34): p. 10007-13.
22. Hirshberg, M., et al., *The crystal structure of human rac1, a member of the rho-family complexed with a GTP analogue.* Nat Struct Biol, 1997. **4**(2): p. 147-52.
23. Hall, A. and A.J. Self, *The effect of Mg2+ on the guanine nucleotide exchange rate of p21N-ras.* J Biol Chem, 1986. **261**(24): p. 10963-5.
24. Zhang, B., et al., *The role of Mg2+ cofactor in the guanine nucleotide exchange and GTP hydrolysis reactions of Rho family GTP-binding proteins.* J Biol Chem, 2000. **275**(33): p. 25299-307.
25. Zhang, F.L. and P.J. Casey, *Protein prenylation: molecular mechanisms and functional consequences.* Annu Rev Biochem, 1996. **65**: p. 241-69.
26. Michaelson, D., et al., *Differential localization of Rho GTPases in live cells: regulation by hypervariable regions and RhoGDI binding.* J Cell Biol, 2001. **152**(1): p. 111-26.
27. Bustelo, X.R., V. Sauzeau, and I.M. Berenjeno, *GTP-binding proteins of the Rho/Rac family: regulation, effectors and functions in vivo.* Bioessays, 2007. **29**(4): p. 356-70.
28. ten Klooster, J.P., et al., *Targeting and activation of Rac1 are mediated by the exchange factor beta-Pix.* J Cell Biol, 2006. **172**(5): p. 759-69.
29. Matos, P., et al., *Small GTPase Rac1: structure, localization, and expression of the human gene.* Biochem Biophys Res Commun, 2000. **277**(3): p. 741-51.
30. Schnelzer, A., et al., *Rac1 in human breast cancer: overexpression, mutation analysis, and characterization of a new isoform, Rac1b.* Oncogene, 2000. **19**(26): p. 3013-20.
31. Fiegen, D., et al., *Alternative splicing of Rac1 generates Rac1b, a self-activating GTPase.* J Biol Chem, 2004. **279**(6): p. 4743-9.

32. Matos, P., J.G. Collard, and P. Jordan, *Tumor-related alternatively spliced Rac1b is not regulated by Rho-GDP dissociation inhibitors and exhibits selective downstream signaling.* J Biol Chem, 2003. **278**(50): p. 50442-8.

33. Lozano, E., et al., *PAK is required for the disruption of E-cadherin adhesion by the small GTPase Rac.* J Cell Sci, 2008. **121**(Pt 7): p. 933-8.

34. Kumar, A., et al., *Molecular dynamic simulation reveals damaging impact of RAC1 F28L mutation in the switch I region.* PLoS One, 2013. **8**(10): p. e77453.

35. Zheng, Y., et al., *Biochemical comparisons of the Saccharomyces cerevisiae Bem2 and Bem3 proteins. Delineation of a limit Cdc42 GTPase-activating protein domain.* J Biol Chem, 1993. **268**(33): p. 24629-34.

36. Musacchio, A., L.C. Cantley, and S.C. Harrison, *Crystal structure of the breakpoint cluster region-homology domain from phosphoinositide 3-kinase p85 alpha subunit.* Proc Natl Acad Sci U S A, 1996. **93**(25): p. 14373-8.

37. Rittinger, K., et al., *Crystal structure of a small G protein in complex with the GTPase-activating protein rhoGAP.* Nature, 1997. **388**(6643): p. 693-7.

38. Bos, J.L., H. Rehmann, and A. Wittinghofer, *GEFs and GAPs: critical elements in the control of small G proteins.* Cell, 2007. **129**(5): p. 865-77.

39. Zhang, B., J. Chernoff, and Y. Zheng, *Interaction of Rac1 with GTPase-activating proteins and putative effectors. A comparison with Cdc42 and RhoA.* J Biol Chem, 1998. **273**(15): p. 8776-82.

40. Marei, H. and A. Malliri, *GEFs: Dual regulation of Rac1 signaling.* Small GTPases, 2017. **8**(2): p. 90-99.

41. Laurin, M. and J.F. Cote, *Insights into the biological functions of Dock family guanine nucleotide exchange factors.* Genes Dev, 2014. **28**(6): p. 533-47.

42. Quilliam, L.A., et al., *Guanine nucleotide exchange factors: activators of the Ras superfamily of proteins.* Bioessays, 1995. **17**(5): p. 395-404.

43. Liu, X., et al., *NMR structure and mutagenesis of the N-terminal Dbl homology domain of the nucleotide exchange factor Trio.* Cell, 1998. **95**(2): p. 269-77.

44. Worthylake, D.K., K.L. Rossman, and J. Sondek, *Crystal structure of Rac1 in complex with the guanine nucleotide exchange region of Tiam1.* Nature, 2000. **408**(6813): p. 682-8.

45. Moshfegh, Y., et al., *A Trio-Rac1-Pak1 signalling axis drives invadopodia disassembly.* Nat Cell Biol, 2014. **16**(6): p. 574-86.

46. Coppola, J., et al., *Mechanism of activation of the vav protooncogene.* Cell Growth Differ, 1991. **2**(2): p. 95-105.
47. Kaminuma, O., et al., *Vav-Rac1-mediated activation of the c-Jun N-terminal kinase/c-Jun/AP-1 pathway plays a major role in stimulation of the distal NFAT site in the interleukin-2 gene promoter.* Mol Cell Biol, 2001. **21**(9): p. 3126-36.
48. Han, J., et al., *Role of substrates and products of PI 3-kinase in regulating activation of Rac-related guanosine triphosphatases by Vav.* Science, 1998. **279**(5350): p. 558-60.
49. Manser, E., et al., *PAK kinases are directly coupled to the PIX family of nucleotide exchange factors.* Mol Cell, 1998. **1**(2): p. 183-92.
50. Marei, H., et al., *Proteomic analysis of Rac1 signaling regulation by guanine nucleotide exchange factors.* Cell Cycle, 2016. **15**(15): p. 1961-74.
51. Uhlenbrock, K., et al., *The RacGEF Tiam1 inhibits migration and invasion of metastatic melanoma via a novel adhesive mechanism.* J Cell Sci, 2004. **117**(Pt 20): p. 4863-71.
52. Marei, H., et al., *Differential Rac1 signalling by guanine nucleotide exchange factors implicates FLII in regulating Rac1-driven cell migration.* Nat Commun, 2016. **7**: p. 10664.
53. Chuang, T.H., et al., *Abr and Bcr are multifunctional regulators of the Rho GTP-binding protein family.* Proc Natl Acad Sci U S A, 1995. **92**(22): p. 10282-6.
54. Price, L.S., et al., *Calcium signaling regulates translocation and activation of Rac.* J Biol Chem, 2003. **278**(41): p. 39413-21.
55. Kwon, T., et al., *Akt protein kinase inhibits Rac1-GTP binding through phosphorylation at serine 71 of Rac1.* J Biol Chem, 2000. **275**(1): p. 423-8.
56. del Pozo, M.A., et al., *Integrins regulate Rac targeting by internalization of membrane domains.* Science, 2004. **303**(5659): p. 839-42.
57. Kumar, R., et al., *Structure, biochemistry, and biology of PAK kinases.* Gene, 2017. **605**: p. 20-31.
58. Edwards, D.C., et al., *Activation of LIM-kinase by Pak1 couples Rac/Cdc42 GTPase signalling to actin cytoskeletal dynamics.* Nat Cell Biol, 1999. **1**(5): p. 253-9.
59. Yang, N., et al., *Cofilin phosphorylation by LIM-kinase 1 and its role in Rac-mediated actin reorganization.* Nature, 1998. **393**(6687): p. 809-12.
60. Eden, S., et al., *Mechanism of regulation of WAVE1-induced actin nucleation by Rac1 and Nck.* Nature, 2002. **418**(6899): p. 790-3.
61. White, C.D., H.H. Erdemir, and D.B. Sacks, *IQGAP1 and its binding proteins control diverse biological functions.* Cell Signal, 2012. **24**(4): p. 826-34.

62. Wu, Y. and Y.C. Chen, *Structure and function of IQ-domain GTPase-activating protein 1 and its association with tumor progression (Review).* Biomed Rep, 2014. **2**(1): p. 3-6.
63. Owen, D., et al., *The IQGAP1-Rac1 and IQGAP1-Cdc42 interactions: interfaces differ between the complexes.* J Biol Chem, 2008. **283**(3): p. 1692-704.
64. Brandt, D.T. and R. Grosse, *Get to grips: steering local actin dynamics with IQGAPs.* EMBO Rep, 2007. **8**(11): p. 1019-23.
65. Sanz-Moreno, V., et al., *Rac activation and inactivation control plasticity of tumor cell movement.* Cell, 2008. **135**(3): p. 510-23.
66. Doanes, A.M., et al., *A requirement for rac1 in the PDGF-stimulated migration of fibroblasts and vascular smooth cells.* Biochem Mol Biol Int, 1998. **45**(2): p. 279-87.
67. Braga, V.M., et al., *Regulation of cadherin function by Rho and Rac: modulation by junction maturation and cellular context.* Mol Biol Cell, 1999. **10**(1): p. 9-22.
68. Stockton, R.A., E. Schaefer, and M.A. Schwartz, *p21-activated kinase regulates endothelial permeability through modulation of contractility.* J Biol Chem, 2004. **279**(45): p. 46621-30.
69. Olson, M.F., A. Ashworth, and A. Hall, *An essential role for Rho, Rac, and Cdc42 GTPases in cell cycle progression through G1.* Science, 1995. **269**(5228): p. 1270-2.
70. Karin, M., *The regulation of AP-1 activity by mitogen-activated protein kinases.* J Biol Chem, 1995. **270**(28): p. 16483-6.
71. Wu, X., et al., *Rac1 activation controls nuclear localization of beta-catenin during canonical Wnt signaling.* Cell, 2008. **133**(2): p. 340-53.
72. Murga, C., et al., *Rac1 and RhoG promote cell survival by the activation of PI3K and Akt, independently of their ability to stimulate JNK and NF-kappaB.* Oncogene, 2002. **21**(2): p. 207-16.
73. Chaigne-Delalande, B., et al., *Nonadherent cells switch to a Rac-mediated, SHIP regulated, Akt activation mode for survival.* Oncogene, 2008. **27**(13): p. 1876-85.
74. Friedland, J.C., et al., *alpha6beta4 integrin activates Rac-dependent p21-activated kinase 1 to drive NF-kappaB-dependent resistance to apoptosis in 3D mammary acini.* J Cell Sci, 2007. **120**(Pt 20): p. 3700-12.
75. Klein, E.A., et al., *NFkappaB-independent signaling to the cyclin D1 gene by Rac.* Cell Cycle, 2007. **6**(9): p. 1115-21.
76. Moore, K.A., et al., *Rac1 is required for cell proliferation and G2/M progression.* Biochem J, 1997. **326 (Pt 1)**: p. 17-20.

77. Qin, C., R. Liu, and H. Liu, *The conflicting role of Rac1 in inflammation.* Inflammation and Cell Signaling, 2015. **2**(3).
78. Kremer, K.N., et al., *TCR-CXCR4 signaling stabilizes cytokine mRNA transcripts via a PREX1-Rac1 pathway: implications for CTCL.* Blood, 2017. **130**(8): p. 982-994.
79. Heyworth, P.G., et al., *Regulation of NADPH oxidase activity by Rac GTPase activating protein(s).* Mol Biol Cell, 1993. **4**(11): p. 1217-23.
80. Li, J.M. and A.M. Shah, *ROS generation by nonphagocytic NADPH oxidase: potential relevance in diabetic nephropathy.* J Am Soc Nephrol, 2003. **14**(8 Suppl 3): p. S221-6.
81. Keyer, K., A.S. Gort, and J.A. Imlay, *Superoxide and the production of oxidative DNA damage.* J Bacteriol, 1995. **177**(23): p. 6782-90.
82. Chen, X.L., et al., *Rac1 and superoxide are required for the expression of cell adhesion molecules induced by tumor necrosis factor-alpha in endothelial cells.* J Pharmacol Exp Ther, 2003. **305**(2): p. 573-80.
83. Moldovan, L., et al., *The actin cytoskeleton reorganization induced by Rac1 requires the production of superoxide.* Antioxidants & redox signaling, 1999. **1**(1): p. 29-43.
84. Gastonguay, A., et al., *The role of Rac1 in the regulation of NF-kappaB activity, cell proliferation, and cell migration in non-small cell lung carcinoma.* Cancer Biol Ther, 2012. **13**(8): p. 647-56.
85. Madonna, G., et al., *NF-kB as potential target in the treatment of melanoma.* J Transl Med, 2012. **10**: p. 53.
86. Reuther-Madrid, J.Y., et al., *The p65/RelA subunit of NF-kappaB suppresses the sustained, antiapoptotic activity of Jun kinase induced by tumor necrosis factor.* Mol Cell Biol, 2002. **22**(23): p. 8175-83.
87. Anrather, J., G. Racchumi, and C. Iadecola, *NF-kappaB regulates phagocytic NADPH oxidase by inducing the expression of gp91phox.* J Biol Chem, 2006. **281**(9): p. 5657-67.
88. Morgan, M.J. and Z.G. Liu, *Crosstalk of reactive oxygen species and NF-kappaB signaling.* Cell Res, 2011. **21**(1): p. 103-15.
89. Lanning, C.C., et al., *The Rac1 C-terminal polybasic region regulates the nuclear localization and protein degradation of Rac1.* J Biol Chem, 2004. **279**(42): p. 44197-210.
90. Sandrock, K., et al., *The nuclear import of the small GTPase Rac1 is mediated by the direct interaction with karyopherin α2.* Traffic, 2010. **11**(2): p. 198-209.

91. Piazzi, M., et al., *Phosphoinositide-specific phospholipase C beta 1b (PI-PLCbeta1b) interactome: affinity purification-mass spectrometry analysis of PI-PLCbeta1b with nuclear protein.* Mol Cell Proteomics, 2013. **12**(8): p. 2220-35.
92. Simon, A.R., et al., *Regulation of STAT3 by direct binding to the Rac1 GTPase.* Science, 2000. **290**(5489): p. 144-7.
93. Kawashima, T., et al., *Rac1 and a GTPase-activating protein, MgcRacGAP, are required for nuclear translocation of STAT transcription factors.* J Cell Biol, 2006. **175**(6): p. 937-46.
94. Michaelson, D., et al., *Rac1 accumulates in the nucleus during the G2 phase of the cell cycle and promotes cell division.* J Cell Biol, 2008. **181**(3): p. 485-96.
95. Lin, Y. and Y. Zheng, *Approaches of targeting Rho GTPases in cancer drug discovery.* Expert Opin Drug Discov, 2015. **10**(9): p. 991-1010.
96. Arnst, J.L., et al., *Discovery and characterization of small molecule Rac1 inhibitors.* Oncotarget, 2017. **8**(21): p. 34586-34600.
97. Sussman, M.A., et al., *Altered focal adhesion regulation correlates with cardiomyopathy in mice expressing constitutively active rac1.* J Clin Invest, 2000. **105**(7): p. 875-86.
98. Talukder, M.A., et al., *Cardiomyocyte-specific overexpression of an active form of Rac predisposes the heart to increased myocardial stunning and ischemia-reperfusion injury.* Am J Physiol Heart Circ Physiol, 2013. **304**(2): p. H294-302.
99. Satoh, M., et al., *Requirement of Rac1 in the development of cardiac hypertrophy.* Proc Natl Acad Sci U S A, 2006. **103**(19): p. 7432-7.
100. Aikawa, R., et al., *Reactive oxygen species in mechanical stress-induced cardiac hypertrophy.* Biochem Biophys Res Commun, 2001. **289**(4): p. 901-7.
101. Barry-Lane, P.A., et al., *p47phox is required for atherosclerotic lesion progression in ApoE(-/-) mice.* J Clin Invest, 2001. **108**(10): p. 1513-22.
102. Judkins, C.P., et al., *Direct evidence of a role for Nox2 in superoxide production, reduced nitric oxide bioavailability, and early atherosclerotic plaque formation in ApoE-/- mice.* Am J Physiol Heart Circ Physiol, 2010. **298**(1): p. H24-32.
103. Orr, A.W., et al., *Matrix-specific p21-activated kinase activation regulates vascular permeability in atherogenesis.* J Cell Biol, 2007. **176**(5): p. 719-27.
104. Rectenwald, J.E., et al., *Direct evidence for cytokine involvement in neointimal hyperplasia.* Circulation, 2000. **102**(14): p. 1697-702.

105. Worthylake, R.A. and K. Burridge, *Leukocyte transendothelial migration: orchestrating the underlying molecular machinery.* Curr Opin Cell Biol, 2001. **13**(5): p. 569-77.

106. de Curtis, I., *Functions of Rac GTPases during neuronal development.* Dev Neurosci, 2008. **30**(1-3): p. 47-58.

107. MacLeod, D., et al., *The familial Parkinsonism gene LRRK2 regulates neurite process morphology.* Neuron, 2006. **52**(4): p. 587-93.

108. Chan, D., et al., *Rac1 protein rescues neurite retraction caused by G2019S leucine-rich repeat kinase 2 (LRRK2).* J Biol Chem, 2011. **286**(18): p. 16140-9.

109. Barth, B.M., S. Stewart-Smeets, and T.B. Kuhn, *Proinflammatory cytokines provoke oxidative damage to actin in neuronal cells mediated by Rac1 and NADPH oxidase.* Mol Cell Neurosci, 2009. **41**(2): p. 274-85.

110. Harraz, M.M., et al., *SOD1 mutations disrupt redox-sensitive Rac regulation of NADPH oxidase in a familial ALS model.* J Clin Invest, 2008. **118**(2): p. 659-70.

111. Glenner, G.G. and C.W. Wong, *Alzheimer's disease: initial report of the purification and characterization of a novel cerebrovascular amyloid protein.* Biochem Biophys Res Commun, 1984. **120**(3): p. 885-90.

112. Bloom, G.S., *Amyloid-beta and tau: the trigger and bullet in Alzheimer disease pathogenesis.* JAMA Neurol, 2014. **71**(4): p. 505-8.

113. Wang, P.L., et al., *Rac1 inhibition negatively regulates transcriptional activity of the amyloid precursor protein gene.* J Neurosci Res, 2009. **87**(9): p. 2105-14.

114. Sylow, L., et al., *Akt and Rac1 signaling are jointly required for insulin-stimulated glucose uptake in skeletal muscle and downregulated in insulin resistance.* Cell Signal, 2014. **26**(2): p. 323-31.

115. Sylow, L., et al., *Rac1 signaling is required for insulin-stimulated glucose uptake and is dysregulated in insulin-resistant murine and human skeletal muscle.* Diabetes, 2013. **62**(6): p. 1865-75.

116. Chiu, T.T., et al., *Arp2/3- and cofilin-coordinated actin dynamics is required for insulin-mediated GLUT4 translocation to the surface of muscle cells.* Mol Biol Cell, 2010. **21**(20): p. 3529-39.

117. Chiu, T.T., et al., *Rac1 signalling towards GLUT4/glucose uptake in skeletal muscle.* Cell Signal, 2011. **23**(10): p. 1546-54.

118. Long, D.L., J.S. Willey, and R.F. Loeser, *Rac1 is required for matrix metalloproteinase 13 production by chondrocytes in response to fibronectin fragments.* Arthritis Rheum, 2013. **65**(6): p. 1561-8.

119. Goldring, M.B. and K.B. Marcu, *Cartilage homeostasis in health and rheumatic diseases.* Arthritis Res Ther, 2009. **11**(3): p. 224.

120. Zhu, S., et al., *Inhibition of Rac1 activity by controlled release of NSC23766 from chitosan microspheres effectively ameliorates osteoarthritis development in vivo.* Ann Rheum Dis, 2015. **74**(1): p. 285-93.

121. Chan, A., et al., *The GTPase Rac regulates the proliferation and invasion of fibroblast-like synoviocytes from rheumatoid arthritis patients.* Mol Med, 2007. **13**(5-6): p. 297-304.

122. Muise, A.M., et al., *Single nucleotide polymorphisms that increase expression of the guanosine triphosphatase RAC1 are associated with ulcerative colitis.* Gastroenterology, 2011. **141**(2): p. 633-41.

123. Winge, M.C., et al., *RAC1 activation drives pathologic interactions between the epidermis and immune cells.* J Clin Invest, 2016. **126**(7): p. 2661-77.

124. Hanahan, D. and R.A. Weinberg, *Hallmarks of cancer: the next generation.* Cell, 2011. **144**(5): p. 646-74.

125. Zbytek, B., et al., *Current concepts of metastasis in melanoma.* Expert Rev Dermatol, 2008. **3**(5): p. 569-585.

126. Khosravi-Far, R., et al., *Activation of Rac1, RhoA, and mitogen-activated protein kinases is required for Ras transformation.* Mol Cell Biol, 1995. **15**(11): p. 6443-53.

127. Qiu, R.G., et al., *An essential role for Rac in Ras transformation.* Nature, 1995. **374**(6521): p. 457-9.

128. Kissil, J.L., et al., *Requirement for Rac1 in a K-ras induced lung cancer in the mouse.* Cancer Res, 2007. **67**(17): p. 8089-94.

129. Wang, Z., et al., *Rac1 is crucial for Ras-dependent skin tumor formation by controlling Pak1-Mek-Erk hyperactivation and hyperproliferation in vivo.* Oncogene, 2010. **29**(23): p. 3362-73.

130. Senger, D.L., et al., *Suppression of Rac activity induces apoptosis of human glioma cells but not normal human astrocytes.* Cancer Res, 2002. **62**(7): p. 2131-40.

131. Forbes, S.A., et al., *The Catalogue of Somatic Mutations in Cancer (COSMIC).* Curr Protoc Hum Genet, 2008. **Chapter 10**: p. Unit 10 11.

132. Zehir, A., et al., *Mutational landscape of metastatic cancer revealed from prospective clinical sequencing of 10,000 patients.* Nat Med, 2017. **23**(6): p. 703-713.

133. Cerami, E., et al., *The cBio cancer genomics portal: an open platform for exploring multidimensional cancer genomics data.* Cancer Discov, 2012. **2**(5): p. 401-4.

134. Gao, J., et al., *Integrative analysis of complex cancer genomics and clinical profiles using the cBioPortal.* Sci Signal, 2013. **6**(269): p. pl1.

135. Kumar, R. and D.Q. Li, *PAKs in Human Cancer Progression: From Inception to Cancer Therapeutic to Future Oncobiology.* Adv Cancer Res, 2016. **130**: p. 137-209.

136. Radu, M., et al., *PAK signalling during the development and progression of cancer.* Nat Rev Cancer, 2014. **14**(1): p. 13-25.

137. Adam, L., et al., *Heregulin regulates cytoskeletal reorganization and cell migration through the p21-activated kinase-1 via phosphatidylinositol-3 kinase.* J Biol Chem, 1998. **273**(43): p. 28238-46.

138. Adam, L., et al., *Regulation of microfilament reorganization and invasiveness of breast cancer cells by kinase dead p21-activated kinase-1.* J Biol Chem, 2000. **275**(16): p. 12041-50.

139. Vadlamudi, R.K., et al., *Regulatable expression of p21-activated kinase-1 promotes anchorage-independent growth and abnormal organization of mitotic spindles in human epithelial breast cancer cells.* J Biol Chem, 2000. **275**(46): p. 36238-44.

140. Scott, R.W., et al., *LIM kinases are required for invasive path generation by tumor and tumor-associated stromal cells.* J Cell Biol, 2010. **191**(1): p. 169-85.

141. Tyagi, N., et al., *p-21 activated kinase 4 promotes proliferation and survival of pancreatic cancer cells through AKT- and ERK-dependent activation of NF-kappaB pathway.* Oncotarget, 2014. **5**(18): p. 8778-89.

142. Gong, W., et al., *P21-activated kinase 5 is overexpressed during colorectal cancer progression and regulates colorectal carcinoma cell adhesion and migration.* Int J Cancer, 2009. **125**(3): p. 548-55.

143. Porter, A.P., A. Papaioannou, and A. Malliri, *Deregulation of Rho GTPases in cancer.* Small GTPases, 2016. **7**(3): p. 123-38.

144. Patel, V., et al., *Persistent activation of Rac1 in squamous carcinomas of the head and neck: evidence for an EGFR/Vav2 signaling axis involved in cell invasion.* Carcinogenesis, 2007. **28**(6): p. 1145-52.

145. Chan, A.Y., et al., *Roles of the Rac1 and Rac3 GTPases in human tumor cell invasion.* Oncogene, 2005. **24**(53): p. 7821-9.

146. Innocenti, M., et al., *Mechanisms through which Sos-1 coordinates the activation of Ras and Rac.* J Cell Biol, 2002. **156**(1): p. 125-36.

147. Wertheimer, E., et al., *Rac signaling in breast cancer: a tale of GEFs and GAPs.* Cell Signal, 2012. **24**(2): p. 353-62.

148. Kuroda, S., et al., *Regulation of cell-cell adhesion of MDCK cells by Cdc42 and Rac1 small GTPases.* Biochem Biophys Res Commun, 1997. **240**(2): p. 430-5.

149. Ehrlich, J.S., M.D. Hansen, and W.J. Nelson, *Spatio-temporal regulation of Rac1 localization and lamellipodia dynamics during epithelial cell-cell adhesion.* Dev Cell, 2002. **3**(2): p. 259-70.

150. Parri, M. and P. Chiarugi, *Rac and Rho GTPases in cancer cell motility control.* Cell Commun Signal, 2010. **8**: p. 23.

151. Burridge, K. and M. Chrzanowska-Wodnicka, *Focal adhesions, contractility, and signaling.* Annu Rev Cell Dev Biol, 1996. **12**: p. 463-518.

152. Rottner, K., A. Hall, and J.V. Small, *Interplay between Rac and Rho in the control of substrate contact dynamics.* Curr Biol, 1999. **9**(12): p. 640-8.

153. Linder, S., C. Wiesner, and M. Himmel, *Degrading devices: invadosomes in proteolytic cell invasion.* Annu Rev Cell Dev Biol, 2011. **27**: p. 185-211.

154. Kheradmand, F., et al., *Role of Rac1 and oxygen radicals in collagenase-1 expression induced by cell shape change.* Science, 1998. **280**(5365): p. 898-902.

155. Westermarck, J. and V.M. Kahari, *Regulation of matrix metalloproteinase expression in tumor invasion.* FASEB J, 1999. **13**(8): p. 781-92.

156. Engers, R., et al., *Rac affects invasion of human renal cell carcinomas by up-regulating tissue inhibitor of metalloproteinases (TIMP)-1 and TIMP-2 expression.* J Biol Chem, 2001. **276**(45): p. 41889-97.

157. Bid, H.K., et al., *RAC1: an emerging therapeutic option for targeting cancer angiogenesis and metastasis.* Mol Cancer Ther, 2013. **12**(10): p. 1925-34.

158. Vader, P., et al., *Examining the role of Rac1 in tumor angiogenesis and growth: a clinically relevant RNAi-mediated approach.* Angiogenesis, 2011. **14**(4): p. 457-66.

159. Ridley, A.J., et al., *The small GTP-binding protein rac regulates growth factor-induced membrane ruffling.* Cell, 1992. **70**(3): p. 401-10.

160. Jiang, Y., et al., *Inhibition of anchorage-independent growth and lung metastasis of A549 lung carcinoma cells by IkappaBbeta.* Oncogene, 2001. **20**(18): p. 2254-63.

161. Yang, Y., et al., *Activation of Rac1-PI3K/Akt is required for epidermal growth factor-induced PAK1 activation and cell migration in MDA-MB-231 breast cancer cells.* J Biomed Res, 2011. **25**(4): p. 237-45.

162. Weber, D.S., et al., *Phosphoinositide-dependent kinase 1 and p21-activated protein kinase mediate reactive oxygen species-dependent regulation of platelet-derived growth factor-induced smooth muscle cell migration.* Circ Res, 2004. **94**(9): p. 1219-26.

163. Liu, L.Z., et al., *Reactive oxygen species regulate epidermal growth factor-induced vascular endothelial growth factor and hypoxia-inducible factor-1alpha expression through activation of AKT and P70S6K1 in human ovarian cancer cells.* Free Radic Biol Med, 2006. **41**(10): p. 1521-33.

164. Saci, A., L.C. Cantley, and C.L. Carpenter, *Rac1 regulates the activity of mTORC1 and mTORC2 and controls cellular size.* Mol Cell, 2011. **42**(1): p. 50-61.

165. Bosco, E.E., et al., *NF2-deficient cells depend on the Rac1-canonical Wnt signaling pathway to promote the loss of contact inhibition of proliferation.* Oncogene, 2010. **29**(17): p. 2540-9.

166. Wang, S.E., et al., *Oncogenic mutations regulate tumor microenvironment through induction of growth factors and angiogenic mediators.* Oncogene, 2010. **29**(23): p. 3335-48.

167. Zhou, C., et al., *The Rac1 splice form Rac1b promotes K-ras-induced lung tumorigenesis.* Oncogene, 2013. **32**(7): p. 903-9.

168. Singh, A., et al., *Rac1b, a tumor associated, constitutively active Rac1 splice variant, promotes cellular transformation.* Oncogene, 2004. **23**(58): p. 9369-80.

169. Jordan, P., et al., *Cloning of a novel human Rac1b splice variant with increased expression in colorectal tumors.* Oncogene, 1999. **18**(48): p. 6835-9.

170. Stallings-Mann, M.L., et al., *Matrix metalloproteinase induction of Rac1b, a key effector of lung cancer progression.* Sci Transl Med, 2012. **4**(142): p. 142ra95.

171. Mehner, C., et al., *Tumor cell-derived MMP3 orchestrates Rac1b and tissue alterations that promote pancreatic adenocarcinoma.* Mol Cancer Res, 2014. **12**(10): p. 1430-9.

172. Matos, P. and P. Jordan, *Increased Rac1b expression sustains colorectal tumor cell survival.* Mol Cancer Res, 2008. **6**(7): p. 1178-84.

173. Faria, M., et al., *Extending the Impact of RAC1b Overexpression to Follicular Thyroid Carcinomas.* Int J Endocrinol, 2016. **2016**: p. 1972367.

174. Akbani, R., et al., *Genomic Classification of Cutaneous Melanoma.* Cell, 2015. **161**(7): p. 1681-1696.

175. Garraway, L.A., et al., *Integrative genomic analyses identify MITF as a lineage survival oncogene amplified in malignant melanoma.* Nature, 2005. **436**(7047): p. 117-22.

176. Beroukhim, R., et al., *Assessing the significance of chromosomal aberrations in cancer: methodology and application to glioma.* Proc Natl Acad Sci U S A, 2007. **104**(50): p. 20007-12.

177. Orchansky, P., et al., *Type I and Type II interferon receptors.* J Interferon Res, 1984. **4**(2): p. 275-82.

178. Jonasch, E. and F.G. Haluska, *Interferon in oncological practice: review of interferon biology, clinical applications, and toxicities.* Oncologist, 2001. **6**(1): p. 34-55.

179. Gowrishankar, K., et al., *Inducible but not constitutive expression of PD-L1 in human melanoma cells is dependent on activation of NF-kappaB.* PLoS One, 2015. **10**(4): p. e0123410.

180. Sharma, P. and J.P. Allison, *The future of immune checkpoint therapy.* Science, 2015. **348**(6230): p. 56-61.

181. Ott, P.A., F.S. Hodi, and C. Robert, *CTLA-4 and PD-1/PD-L1 blockade: new immunotherapeutic modalities with durable clinical benefit in melanoma patients.* Clinical Cancer Research, 2013. **19**(19): p. 5300-5309.

182. Vu, H.L., et al., *RAC1 P29S regulates PD-L1 expression in melanoma.* Pigment Cell & Melanoma Research, 2015. **28**(5): p. 590-598.

183. Roux, K.J., et al., *A promiscuous biotin ligase fusion protein identifies proximal and interacting proteins in mammalian cells.* J Cell Biol, 2012. **196**(6): p. 801-10.

184. Kim, D.I., et al., *Probing nuclear pore complex architecture with proximity-dependent biotinylation.* Proc Natl Acad Sci U S A, 2014. **111**(24): p. E2453-61.

185. Ling, M., et al., *The human mitochondrial elongation factor tu (EF-Tu) gene: cDNA sequence, genomic localization, genomic structure, and identification of a pseudogene.* Gene, 1997. **197**(1-2): p. 325-36.

186. Mu, X., et al., *HIV-1 Exploits the Host Factor RuvB-like 2 to Balance Viral Protein Expression.* Cell Host Microbe, 2015. **18**(2): p. 233-42.

187. Bernard, G., et al., *CD99 (E2) up-regulates alpha4beta1-dependent T cell adhesion to inflamed vascular endothelium under flow conditions.* Eur J Immunol, 2000. **30**(10): p. 3061-5.

188. Skvortsov, S., et al., *Rac1 as a potential therapeutic target for chemo-radioresistant head and neck squamous cell carcinomas (HNSCC).* Br J Cancer, 2014. **110**(11): p. 2677-87.

189. Wetterskog, D., et al., *Identification of novel determinants of resistance to lapatinib in ERBB2-amplified cancers.* Oncogene, 2014. **33**(8): p. 966-76.

190. Warburg, O., *On respiratory impairment in cancer cells.* Science, 1956. **124**(3215): p. 269-70.

191. Scott, D.A., et al., *Comparative metabolic flux profiling of melanoma cell lines: beyond the Warburg effect.* J Biol Chem, 2011. **286**(49): p. 42626-34.

192. Hall, A., et al., *Dysfunctional oxidative phosphorylation makes malignant melanoma cells addicted to glycolysis driven by the (V600E)BRAF oncogene.* Oncotarget, 2013. **4**(4): p. 584-99.
193. Barbi de Moura, M., et al., *Mitochondrial respiration--an important therapeutic target in melanoma.* PLoS One, 2012. **7**(8): p. e40690.
194. Ferretta, A., et al., *New insight into the role of metabolic reprogramming in melanoma cells harboring BRAF mutations.* Biochim Biophys Acta, 2016. **1863**(11): p. 2710-2718.
195. Ratnikov, B.I., et al., *Metabolic rewiring in melanoma.* Oncogene, 2017. **36**(2): p. 147-157.
196. Corazao-Rozas, P., et al., *Mitochondrial oxidative stress is the Achille's heel of melanoma cells resistant to Braf-mutant inhibitor.* Oncotarget, 2013. **4**(11): p. 1986-98.
197. Abildgaard, C. and P. Guldberg, *Molecular drivers of cellular metabolic reprogramming in melanoma.* Trends Mol Med, 2015. **21**(3): p. 164-71.
198. Müller, J., et al., *Low MITF/AXL ratio predicts early resistance to multiple targeted drugs in melanoma.* Nat Commun, 2014. **5**.
199. Haq, R., et al., *Oncogenic BRAF regulates oxidative metabolism via PGC1alpha and MITF.* Cancer Cell, 2013. **23**(3): p. 302-15.
200. Carreira, S., et al., *Mitf regulation of Dia1 controls melanoma proliferation and invasiveness.* Genes Dev, 2006. **20**(24): p. 3426-39.
201. Cheli, Y., et al., *Mitf is the key molecular switch between mouse or human melanoma initiating cells and their differentiated progeny.* Oncogene, 2011. **30**(20): p. 2307-18.
202. Bianchi-Smiraglia, A., et al., *Microphthalmia-associated transcription factor suppresses invasion by reducing intracellular GTP pools.* Oncogene, 2017. **36**(1): p. 84-96.
203. Wawrzyniak, J.A., et al., *A purine nucleotide biosynthesis enzyme guanosine monophosphate reductase is a suppressor of melanoma invasion.* Cell Rep, 2013. **5**(2): p. 493-507.
204. Ivashkiv, L.B. and L.T. Donlin, *Regulation of type I interferon responses.* Nat Rev Immunol, 2014. **14**(1): p. 36-49.
205. Huang, S., et al., *Level of interleukin-8 expression by metastatic human melanoma cells directly correlates with constitutive NF-kappaB activity.* Cytokines Cell Mol Ther, 2000. **6**(1): p. 9-17.
206. Payne, A.S. and L.A. Cornelius, *The role of chemokines in melanoma tumor growth and metastasis.* J Invest Dermatol, 2002. **118**(6): p. 915-22.
207. Murakami, T., et al., *Immune evasion by murine melanoma mediated through CC chemokine receptor-10.* J Exp Med, 2003. **198**(9): p. 1337-47.

208. Shain, A.H., et al., *Exome sequencing of desmoplastic melanoma identifies recurrent NFKBIE promoter mutations and diverse activating mutations in the MAPK pathway.* Nature genetics, 2015. **47**(10): p. 1194-1199.

209. Park, E.J., et al., *Rac1 contributes to maximal activation of STAT1 and STAT3 in IFN-gamma-stimulated rat astrocytes.* J Immunol, 2004. **173**(9): p. 5697-703.

210. Li, F.Z., et al., *Phenotype switching in melanoma: implications for progression and therapy.* Front Oncol, 2015. **5**: p. 31.

211. Alonso, S.R., et al., *A high-throughput study in melanoma identifies epithelial-mesenchymal transition as a major determinant of metastasis.* Cancer Res, 2007. **67**(7): p. 3450-60.

212. Vandamme, N. and G. Berx, *Melanoma cells revive an embryonic transcriptional network to dictate phenotypic heterogeneity.* Front Oncol, 2014. **4**: p. 352.

213. Caramel, J., et al., *A switch in the expression of embryonic EMT-inducers drives the development of malignant melanoma.* Cancer Cell, 2013. **24**(4): p. 466-80.

214. Denecker, G., et al., *Identification of a ZEB2-MITF-ZEB1 transcriptional network that controls melanogenesis and melanoma progression.* Cell Death Differ, 2014. **21**(8): p. 1250-61.

215. Babagana, M., et al., *P21-activated kinase 1 regulates resistance to BRAF inhibition in human cancer cells.* Mol Carcinog, 2017. **56**(5): p. 1515-1525.

216. Lu, H., et al., *PAK signalling drives acquired drug resistance to MAPK inhibitors in BRAF-mutant melanomas.* Nature, 2017. **550**(7674): p. 133-136.

217. Araiza-Olivera, D., et al., *Suppression of RAC1-driven malignant melanoma by group A PAK inhibitors.* Oncogene, 2017.

218. Ryan, M.B., et al., *ERK/MAPK Signaling Drives Overexpression of the Rac-GEF, PREX1, in BRAF- and NRAS-Mutant Melanoma.* Mol Cancer Res, 2016. **14**(10): p. 1009-1018.

219. Berger, M.F., et al., *Melanoma genome sequencing reveals frequent PREX2 mutations.* Nature, 2012. **485**(7399): p. 502-6.

220. Lissanu Deribe, Y., et al., *Truncating PREX2 mutations activate its GEF activity and alter gene expression regulation in NRAS-mutant melanoma.* Proc Natl Acad Sci U S A, 2016. **113**(9): p. E1296-305.

221. Tomino, T., et al., *DOCK1 inhibition suppresses cancer cell invasion and macropinocytosis induced by self-activating Rac1(P29S) mutation.* Biochem Biophys Res Commun, 2018. **497**(1): p. 298-304.

222. Johnson, M., M. Sharma, and B.R. Henderson, *IQGAP1 regulation and roles in cancer.* Cell Signal, 2009. **21**(10): p. 1471-8.

223. Clark, E.A., et al., *Genomic analysis of metastasis reveals an essential role for RhoC.* Nature, 2000. **406**(6795): p. 532-5.

224. Usatyuk, P.V., et al., *Phospholipase D-mediated activation of IQGAP1 through Rac1 regulates hyperoxia-induced p47phox translocation and reactive oxygen species generation in lung endothelial cells.* J Biol Chem, 2009. **284**(22): p. 15339-52.

225. Kaur, R., et al., *Increased PAK6 expression in prostate cancer and identification of PAK6 associated proteins.* Prostate, 2008. **68**(14): p. 1510-6.

226. Roy, M., Z. Li, and D.B. Sacks, *IQGAP1 binds ERK2 and modulates its activity.* J Biol Chem, 2004. **279**(17): p. 17329-37.

227. Roy, M., Z. Li, and D.B. Sacks, *IQGAP1 is a scaffold for mitogen-activated protein kinase signaling.* Mol Cell Biol, 2005. **25**(18): p. 7940-52.

228. Ren, J.G., Z. Li, and D.B. Sacks, *IQGAP1 modulates activation of B-Raf.* Proc Natl Acad Sci U S A, 2007. **104**(25): p. 10465-9.

229. Jameson, K.L., et al., *IQGAP1 scaffold-kinase interaction blockade selectively targets RAS-MAP kinase-driven tumors.* Nat Med, 2013. **19**(5): p. 626-630.

230. Lee, B.H., et al., *IQGAP1 is an oncogenic target in canine melanoma.* PLoS One, 2017. **12**(4): p. e0176370.

231. Harris, C.A., et al., *Structure and mapping of the human thymopoietin (TMPO) gene and relationship of human TMPO beta to rat lamin-associated polypeptide 2.* Genomics, 1995. **28**(2): p. 198-205.

232. Dechat, T., et al., *Lamina-associated polypeptide 2alpha binds intranuclear A-type lamins.* J Cell Sci, 2000. **113 Pt 19**: p. 3473-84.

233. Gotzmann, J. and R. Foisner, *Lamins and lamin-binding proteins in functional chromatin organization.* Crit Rev Eukaryot Gene Expr, 1999. **9**(3-4): p. 257-65.

234. Navarro-Lerida, I., et al., *Rac1 nucleocytoplasmic shuttling drives nuclear shape changes and tumor invasion.* Dev Cell, 2015. **32**(3): p. 318-34.

235. Mbele, G.O., et al., *The zinc- and calcium-binding S100B interacts and co-localizes with IQGAP1 during dynamic rearrangement of cell membranes.* J Biol Chem, 2002. **277**(51): p. 49998-50007.

236. Donato, R., *Functional roles of S100 proteins, calcium-binding proteins of the EF-hand type.* Biochim Biophys Acta, 1999. **1450**(3): p. 191-231.

237. Cochran, A.J., et al., *S-100 protein remains a practical marker for melanocytic and other tumours.* Melanoma Res, 1993. **3**(5): p. 325-30.

238. Marks, A., et al., *S100 protein expression in human melanoma cells: comparison of levels of expression among different cell lines and individual cells in different phases of the cell cycle.* Exp Cell Res, 1990. **187**(1): p. 59-64.

239. Joyal, J.L., et al., *Calmodulin modulates the interaction between IQGAP1 and Cdc42. Identification of IQGAP1 by nanoelectrospray tandem mass spectrometry.* J Biol Chem, 1997. **272**(24): p. 15419-25.

240. Jang, D.J., B. Ban, and J.A. Lee, *Characterization of novel calmodulin binding domains within IQ motifs of IQGAP1.* Mol Cells, 2011. **32**(6): p. 511-8.

241. Sun, B.K., et al., *CALML5 is a ZNF750- and TINCR-induced protein that binds stratifin to regulate epidermal differentiation.* Genes Dev, 2015. **29**(21): p. 2225-30.

242. Riker, A.I., et al., *The gene expression profiles of primary and metastatic melanoma yields a transition point of tumor progression and metastasis.* BMC Med Genomics, 2008. **1**: p. 13.

243. Huttlin, E., et al., *High-Throughput Proteomic Mapping of Protein Interaction Networks: Toward a Global View of the Human Interactome*. Vol. 13. 2014. S43-S43.

244. Meek, S.E., W.S. Lane, and H. Piwnica-Worms, *Comprehensive proteomic analysis of interphase and mitotic 14-3-3-binding proteins.* J Biol Chem, 2004. **279**(31): p. 32046-54.

245. Itoh, N., et al., *Valosin-containing protein (VCP) is a novel IQ motif-containing GTPase activating protein 1 (IQGAP1)-interacting protein.* Biochem Biophys Res Commun, 2017. **493**(4): p. 1384-1389.

246. Meyer, H., M. Bug, and S. Bremer, *Emerging functions of the VCP/p97 AAA-ATPase in the ubiquitin system.* Nat Cell Biol, 2012. **14**(2): p. 117-23.

247. Dantuma, N.P., K. Acs, and M.S. Luijsterburg, *Should I stay or should I go: VCP/p97-mediated chromatin extraction in the DNA damage response.* Exp Cell Res, 2014. **329**(1): p. 9-17.

248. Yu, C.C., et al., *VCP phosphorylation-dependent interaction partners prevent apoptosis in Helicobacter pylori-infected gastric epithelial cells.* PLoS One, 2013. **8**(1): p. e55724.

249. Raskin, L., et al., *Transcriptome profiling identifies HMGA2 as a biomarker of melanoma progression and prognosis.* J Invest Dermatol, 2013. **133**(11): p. 2585-2592.

250. Matos, P., et al., *B-Raf(V600E) cooperates with alternative spliced Rac1b to sustain colorectal cancer cell survival.* Gastroenterology, 2008. **135**(3): p. 899-906.